

การสกัดสารต้านมะเร็งแอมนาแคนซ์จากรากของต้นข่อย โดยน้ำกึ่งวิกฤต



นางสาว จุติพร เอนกพันธ์กุล

สถาบันวิทยบริการ

จุฬาลงกรณ์มหาวิทยาลัย

วิทยานิพนธ์นี้เป็นส่วนหนึ่งของการศึกษาตามหลักสูตรปริญญาวิทยาศาสตรมหาบัณฑิต

สาขาวิชาวิศวกรรมเคมี ภาควิชาวิศวกรรมเคมี

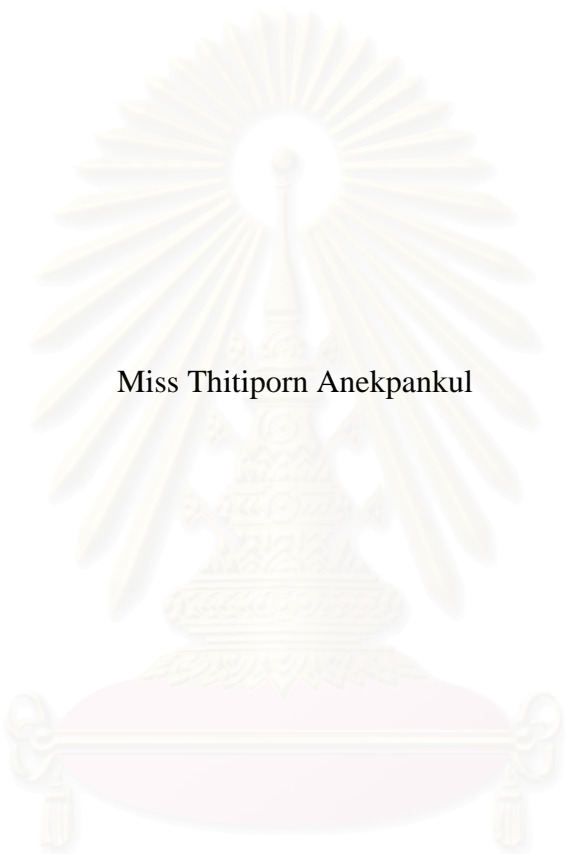
คณะวิศวกรรมศาสตร์ จุฬาลงกรณ์มหาวิทยาลัย

ปีการศึกษา 2548

ISBN 974-17-3472-7

ลิขสิทธิ์ของจุฬาลงกรณ์มหาวิทยาลัย

EXTRACTION OF ANTI-CANCER DAMNACANTHAL FROM ROOTS OF
MORINDA CITRIFOLIA BY SUBCRITICAL WATER



Miss Thitiporn Anekpankul

สถาบันวิทยบริการ
A Thesis Submitted in Partial Fulfillment of the Requirements
for the Degree of Master of Engineering Program in Chemical Engineering

Department of Chemical Engineering
Faculty of Engineering
Chulalongkorn University
Academic Year 2005

ISBN 974-17-3472-7

Thesis Title	EXTRACTION OF ANTI-CANCER DAMNACANTHAL FROM ROOTS OF <i>MORINDA CITRIFOLIA</i> BY SUBCRITICAL WATER
By	Miss Thitiporn Anekpankul
Field of study	Chemical Engineering
Thesis Advisor	Assistant Professor Artiwan Shotipruk, Ph.D.
Thesis Co-advisor	Jarupan Kuldiloke, Dr.-Ing

Accepted by the Faculty of Engineering, Chulalongkorn University in Partial
Fulfillment of the Requirements for the Master's Degree

DL Lavansiri
.....Dean of the Faculty of Engineering
(Professor Direk Lavansiri, Ph.D.)

THESIS COMMITTEE

Muel Phis
.....Chairman
(Assistant Professor Muenduen Phisalaphong, Ph.D.)

artiwant shotipruk
.....Thesis Advisor
(Assistant Professor Artiwan Shotipruk, Ph.D.)

J. Kul.
.....Thesis Co-advisor
(Jarupan Kuldiloke, Dr.-Ing)

Prasert Pavasant
.....Member
(Associate Professor Prasert Pavasant, Ph.D.)

Bunjerd Jongsomjit
.....Member
(Assistant Professor Bunjerd Jongsomjit, Ph.D.)

จูติพร เอนกพันธุ์กุล: การสกัดสารต้านมะเร็งแรมนาแคนธัลจากรากของต้นข่อย โดยน้ำกึ่งวิกฤต. (EXTRACTION OF ANTI-CANCER DAMNACANTHAL FROM ROOTS OF *MORINDA CITRIFOLIA* BY SUBCRITICAL WATER) อ. ที่ปรึกษา: ผศ. ดร. อาทิวรรณ โชติพฤษณ์, อ. ที่ปรึกษาร่วม: ดร. จารุพรรณ กุลดิลก หน้า 119. ISBN 974-17-3472-7.

งานวิจัยนี้ได้ศึกษาการสกัดสารแรมนาแคนธัลที่มีคุณสมบัติต่อต้านมะเร็งจากรากของต้นข่อย โดยใช้ตัวทำละลายคือน้ำที่สภาวะกึ่งวิกฤต หรือเรียกอีกชื่อว่า น้ำร้อนที่สภาวะความดันสูง ในการทดลองได้ทำการสกัดสารที่สภาวะต่างๆ ดังนี้คือ ที่อุณหภูมิ 150 170 200 และ 220 องศาเซลเซียส และอัตราการไหล 2 3 4 และ 5 มิลลิลิตรต่อนาที โดยใช้ความดันคงที่ที่ 4 เมกกะปาสกาล ในขั้นตอนการวิเคราะห์หาปริมาณสารแรมนาแคนธัลจะใช้วิธีโครมาโทกราฟีของเหลวสมรรถนะสูง ซึ่งจะต้องเพิ่มค่าความเข้มข้นของสารแรมนาแคนธัลที่สกัดออกมาให้มีค่าความเข้มข้นเพิ่มขึ้น โดยนำสารที่สกัดออกมาเข้าสู่กระบวนการระเหยภายใต้ความดันสุญญากาศเพื่อระเหยน้ำออกจนสารสกัดแห้ง และนำน้ำกลั่นเดิมลงในสารสกัดแห้ง ซึ่งผลที่ได้จะออกมา 2 ส่วน คือ ส่วนที่ละลายในน้ำ และตะกอนของสารสกัด ซึ่งในส่วนของตะกอนจะทำการเติมสารละลายไดเมททิวซันฟอกไซด์ หลังจากนั้นจึงนำทั้ง 2 ส่วน ไปวิเคราะห์ด้วยเครื่องโครมาโทกราฟีของเหลวสมรรถนะสูง ผลการวิเคราะห์แสดงให้เห็นว่า สารแรมนาแคนธัลจะพบอยู่ในทั้ง 2 ส่วน คือ ส่วนที่ละลายในน้ำ และตะกอนที่ละลายในสารละลายไดเมททิวซันฟอกไซด์ จากผลการทดลองแสดงให้เห็นว่าความสามารถในการสกัดสูงขึ้นเมื่ออุณหภูมิเพิ่มขึ้น จนถึง 170 องศาเซลเซียส แต่ที่อุณหภูมิ 200 และ 220 องศาเซลเซียส ปริมาณสารที่สกัดออกมาได้จะมีสารแรมนาแคนธัลลดลง เนื่องจากสารแรมนาแคนธัลถูกทำลายที่อุณหภูมิสูง นอกจากนี้ได้ทำการศึกษาหาสมการแบบจำลองทางคณิตศาสตร์ที่อัตราการไหลต่างๆ เพื่อใช้ทำนายการสกัดสารแรมนาแคนธัลจากรากของต้นข่อย โดยน้ำกึ่งวิกฤตเพื่อหาสภาวะที่เหมาะสมสำหรับการสกัดนี้ ซึ่งพบว่ากลไกการสกัดนี้จะมีอิทธิพลจากสมดุลการกระจายตัวของตัวถูกละลาย และการถ่ายเทมวลสารภายนอกสู่ชั้นฟิล์มของของเหลว ถึงแม้ว่าแบบจำลองการคายของสารนั้น จะสามารถอธิบายการสกัดนี้ได้ก็อัตราการไหลที่ความเร็วสูง

ภาควิชา.....วิศวกรรมเคมี.....ลายมือชื่อนิสิต..... จูติพร เอนกพันธุ์กุล
สาขาวิชา.....วิศวกรรมเคมี.....ลายมือชื่ออาจารย์ที่ปรึกษา..... อาทิวรรณ โชติพฤษณ์
ปีการศึกษา.....2548.....ลายมือชื่ออาจารย์ที่ปรึกษาร่วม..... จารุพรรณ กุลดิลก

4770276121 : MAJOR CHEMICAL ENGINEERING

KEY WORD: SUBCRITICAL WATER / *MORINDA CITRIFOLIA* / DAMNACANTHAL / MATHEMATIC MODELING

THITIPORN ANEKPANKUL: EXTRACTION OF ANTI-CANCER DAMNACANTHAL FROM ROOTS OF *MORINDA CITRIFOLIA* BY SUBCRITICAL WATER. THESIS ADVISOR: ASST. PROF. ARTIWAN SHOTIPRUK, Ph.D., THESIS COADVISOR: JARUPAN KULDILOKE, Dr.-Ing., 119 pp. ISBN 974-17-3472-7.

A technique of solvent-free extraction of anti-cancer damnacanthal, from roots of *Morinda citrifolia* was proposed. The technique utilizes subcritical water, or sometimes called pressurize hot water (PHW) as extraction medium. A series of extraction experiments were carried out at different conditions, i.e., temperatures of 150, 170, 200, and 220°C and flow rates of 2, 3, 4, and 5 ml/min, while the pressure remained fixed at 4 MPa. The quantitative analysis of damnacanthal was performed with reverse phase-high performance liquid chromatography (RP-HPLC). Prior to the analysis, a sample preparation step was required to concentrate the damnacanthal product. This was achieved by evaporating off water from the extract under vacuum, and the distilled water was added to the dried extract. This resulted in two parts, the aqueous solution and the precipitate. The aqueous solution was analyzed for the amount of damnacanthal by RP-HPLC, while the precipitate was re-dissolved into dimethylsulfoxide (DMSO), and then analyzed with RP-HPLC. The total amount of damnacanthal extracted was the sum of the amounts in the two fractions. The results of the study revealed that the extraction yield increased as the temperature increased. However, at the temperature of 200 and 220°C, decomposition of damnacanthal occurred. In addition to the effect of temperatures, extractions were conducted at various flow rates and the data were fitted with mathematic models to determine the extraction mechanism. The results suggested that the overall extraction mechanism was influenced by solute partitioning equilibrium and external mass transfer through liquid film, although the desorption model could describe the subcritical extraction behavior of *Morinda citrifolia* reasonably at high flow rates.

Department....Chemical Engineering.....Student's signature...*Thitiporn Anekpankul*
 Field of study..Chemical Engineering.....Advisor's signature.....*Artawan Shotipruk*
 Academic year....2005.....Co-advisor's signature.....*Jarupan Kuldiroke*

ACKNOWLEDGMENTS

The work presented in this thesis was meticulously conducted with the help and encouragements from many people who make such work possible. I would like to take this opportunity to thank the following people for their contributions to this work.

Firstly, I would like to express my sincere gratitude to my advisor Asst. Prof. Artiwan Shotipruk for her encouragement and guidance throughout the entire course of this work, and thanks to my co-advisor Dr. Jarupan Kuldiloke and all my thesis committee, Assoc. Prof. Prasert Pavasant, and Asst. Prof. Bunjerd Jongsomjit, and the Chairperson, Asst. Prof. Muenduen Phisalaphong, for giving critical reviews of this work and for their advice on my thesis. Their comments are important and have added a great deal of quality to this work.

Special thanks for Prof. Motonobu Goto, and Assoc. Prof. Mitsuru Sasaki for their suggestions, supports, and the impressive experiences at Kumamoto University, Japan.

I would like to thank to Mr.Kijchai Kanjanapaparkul and Ms. Sunun Rangseekansong for their assistance in analytical work and sincere thanks are made to all members of the Biochemical Engineering Research Laboratory, especially Mr. Prachanart Kittikaiwan, Mr. Jesada Pititphanapong Mr. Surasak Hemwimol, Mr. Boonchai Pongnaravane, and Mr. Narupon Jomtip for their any assistance and warm collaborations.

Thanks to Thai-Japan Technology Transfer Program “TJTTP” and Faculty of Engineering, Chulalongkorn University for financial supports.

Finally, I would like to express the highest gratitude to my parents, everyone in my family, and all of my friends for their help, their unfailing understanding and affectionate encouragements.

2.5 Solubility.....	30
Literature review.....	31
III.MATERIALS AND METHODS.....	41
3.1 Material.....	41
3.1.1 Chemicals.....	41
3.1.2 Plant material preparation.....	41
3.2 Methodology.....	42
3.2.1 Subcritical water extraction.....	42
3.2.2 Sample preparation for RP-HPLC.....	44
3.2.3 Analysis RP-HPLC procedure.....	44
IV.RESULT AND DISSCUSSION.....	45
4.1 Evaluation of extraction protocols.....	46
4.2 Effect of subcritical water temperature.....	49
4.3 Effect of flow rate.....	50
4.4 Modeling of extraction behavior.....	53
4.4.1 Partitioning coefficient (K_D).....	53
4.4.2 One-site kinetic desorption model.....	57
4.4.3 Two-site kinetic desorption model.....	61
4.4.4 External mass transfer model.....	62
4.5 Comparison of extraction models	65
V.CONCLUSIONS AND RECOMMENDATIONS.....	67
5.1 Conclusions.....	67
5.2 Recommendations.....	68
REFERENCES.....	69
APPENDICES.....	74
APPENDIX A.....	75
APPENDIX B.....	82
APPENDIX C.....	100

	Page
APPENDIX D.....	104
APPENDIX E.....	111
VITA.....	119



สถาบันวิทยบริการ
จุฬาลงกรณ์มหาวิทยาลัย

LIST OF TABLES

	Page
Table 2.1 Properties of damnacantal	6
Table 2.2 Review on investigation of subcritical water extraction of Pollutants from soil	33
Table 2.3 Review on Investigation of subcritical water extraction of Natural Product	36
Table 3.1 Parameter condition in experiment.....	43
Table 4.1 K_D values of partitioning coefficient model for different flow rate.....	57
Table 4.2 k values for one-site kinetic desorption model for different flow rate...	61
Table 4.3 k_1 and k_2 values for two-site kinetic desorption model for different flow rate ($F = 0.76$).....	62
Table 4.4 Parameters K_D and k_{ea_p} for external mass transfer model.....	65
Table 4.5 Mean percent absolute errors between experimental data and extraction model results.....	66
Table A-1.1 Standard calibration curve data.....	75
Table A.2.1 Particle size result of <i>Morinda citrifolia</i> roots.....	76
Table A.2.2 Density results of <i>Morinda citrifolia</i> roots.....	77
Table A-3.1 Subcritical water extraction of temperature 150°C and pressure 4 MPa for flow rate 5 ml/min.....	77
Table A-3.2 Subcritical water extraction of temperature 170°C and pressure 4 MPa for flow rate ml/min.....	78
Table A-3.3 Subcritical water extraction of temperature 200°C and pressure 4 MPa for flow rate 5 ml/min.....	78
Table A-3.4 Subcritical water extraction of temperature 220°C and pressure 4 MPa for flow rate 5 ml/min.....	79
Table A-3.5 Subcritical water extraction of temperature 170°C and pressure 4 MPa for flow rate 2 ml/min.....	79
Table A-3.6 Subcritical water extraction of temperature 170°C and pressure 4 MPa for flow rate 3 ml/min.....	80

Table A-3.7	Subcritical water extraction of temperature 170°C and pressure 4 MPa for flow rate 4 ml/min.....	80
Table A-3.8	Subcritical water extraction of temperature 170°C and pressure 4 MPa for flow rate 5 ml/min.....	81
Table B-1.1	Value of %extracted ($\%S_d/S_0$) with flow rate 2 ml/min, at temperature 170°C and pressure 4 MPa.....	83
Table B-1.2	Value of %extracted ($\%S_d/S_0$) with flow rate 3 ml/min, at temperature 170°C and pressure 4 MPa	83
Table B-1.3	Value of %extracted ($\%S_d/S_0$) with flow rate 4 ml/min, at temperature 170°C and pressure 4 MPa	84
Table B-1.4	Value of %extracted ($\%S_d/S_0$) with flow rate 5 ml/min, at temperature 170°C and pressure 4 MPa.....	84
Table B-1.5	Value of %extracted ($\%S_d/S_0$) with flow rate 3 ml/min, at temperature 170°C and pressure 4 MPa.....	85
Table B-1.6	Value of %extracted ($\%S_d/S_0$) with flow rate 4 ml/min, at temperature 170°C and pressure 4 MPa.....	85
Table B-1.7	Value of %extracted ($\%S_d/S_0$) with flow rate 5 ml/min, at temperature 170°C and pressure 4 MPa.....	86
Table B-2.1	Value of $\ln(S_r/S_0)$ with flow rate 2 ml/min, at temperature 170°C and pressure 4 MPa	87
Table B-2.2	Value of $\ln(S_r/S_0)$ with flow rate 3 ml/min, at temperature 170°C and pressure 4 MPa.....	87
Table B-2.3	Value of $\ln(S_r/S_0)$ with flow rate 4 ml/min, at temperature 170°C and pressure 4 MPa	88
Table B-2.4	Value of $\ln(S_r/S_0)$ with flow rate 5 ml/min, at temperature 170°C and pressure 4 MPa.....	88
Table B-2.5	Value of %extracted ($\%S_r/S_0$) with flow rate 2 ml/min, at temperature 170°C and pressure 4 MPa	89
Table B-2.6	Value of %extracted ($\%S_r/S_0$) with flow rate 3 ml/min, at temperature 170°C and pressure 4 MPa	90

Table B-2.7	Value of %extracted ($\%S_t/S_0$) with flow rate 4 ml/min, at temperature 170°C and pressure 4 MPa	90
Table B-2.8	Value of %extracted ($\%S_t/S_0$) with flow rate 5 ml/min at temperature 170°C and pressure 4 MPa	91
Table B-2.9	Value of %extracted ($\%S_t/S_0$) with flow rate 2 ml/min, at temperature 170°C and pressure 4 MPa	91
Table B-2.10	Value of %extracted ($\%S_t/S_0$) with flow rate 3 ml/min, at temperature 170°C and pressure 4 MPa	92
Table B-2.11	Value of %extracted ($\%S_t/S_0$) with flow rate 4 ml/min, at temperature 170°C and pressure 4 MPa	92
Table B-3.1	Value of %extracted ($\%S_t/S_0$) with flow rate 2 ml/min, at temperature 170°C and pressure 4 MPa	93
Table B-3.2	Value of %extracted ($\%S_t/S_0$) with flow rate 3 ml/min, at temperature 170°C and pressure 4 MPa	94
Table B-3.3	Value of %extracted ($\%S_t/S_0$) with flow rate 4 ml/min, at temperature 170°C and pressure 4 MPa	94
Table B-3.4	Value of %extracted ($\%S_t/S_0$) with flow rate 5 ml/min, at temperature 170°C and pressure 4 MPa.....	95
Table B-3.5	Value of %extracted ($\%S_t/S_0$) with flow rate 2 ml/min, at temperature 170°C and pressure 4 MPa	95
Table B-3.6	Value of %extracted ($\%S_t/S_0$) with flow rate 3 ml/min, at temperature 170°C and pressure 4 MPa	96
Table B-3.7	Value of %extracted ($\%S_t/S_0$) with flow rate 4 ml/min, at temperature 170°C and pressure 4 MPa.....	96
Table B-4.1	Value of %extracted ($\%S_t/S_0$) with flow rate 2 ml/min, at temperature 170°C and pressure 4 MPa.....	97
Table B-4.2	Value of %extracted ($\%S_t/S_0$) with flow rate 3 ml/min, at temperature 170°C and pressure 4 MPa.....	98
Table B-4.3	Value of %extracted ($\%S_t/S_0$) with flow rate 4 ml/min, at temperature 170°C and pressure 4 MPa.....	98
Table B-4.4	Value of %extracted ($\%S_t/S_0$) with flow rate 5 ml/min, at temperature 170°C and pressure 4 MPa.....	99

LIST OF FIGURES

	Page
Figure 2.1 <i>Morinda citrifolia</i> plant.....	5
Figure 2.2a Basic structures of anthraquinones.....	5
Figure 2.2b 3-Hydroxy-1-methoxyanthraquinone-2-aldehyde (damnacanthal).....	6
Figure 2.2c 1,2-dihydroxyanthraquinone (alizarin).....	6
Figure 2.2d 3-hydroxy-2-hydroxymethylantraquinone (lucidin).....	6
Figure 2.3 Theoretical Pressure – Temperature phase diagram for pure compound.....	7
Figure 2.4 Relative permittivity (dielectric constant) of liquid water along the saturation line.....	8
Figure 2.5 Equilibrium curve.....	21
Figure 2.6 Theoretical curve for the hot-ball model.....	27
Figure 3.1 <i>Morinda citrifolia</i> plant (Experimental).....	41
Figure 3.2 Dried roots and ground roots of <i>Morinda citrifolia</i>	42
Figure 3.3 Diagram of experimental setup subcritical water extraction.....	44
Figure 4.1 Comparison of anthraquinone extracted with water, subcritical water and ethanol.....	46
Figure 4.2 HPLC chromatogram of damnacanthal (retention time, $t_R = 12.44$ min) in (a) standard, (b-c) noni roots extracts obtained from subcritical water extraction.....	48
Figure 4.3 Effect of water temperature on yield of damnacanthal (Flow rate 5 ml/min at 4 MPa).....	50
Figure 4.4 a)Percent extracted versus extraction time, b) Percent extract versus volume of water for subcritical water extraction at 170°C.....	52
Figure 4.5 Theoretical curve calculate for extractions controlled by thermodynamic partitioning as a flow of 2 ml/min.....	55

Figure 4.6	Theoretical extraction curves for K_D values of a) 50 and b) 1000 for extractions controlled by thermodynamic partitioning.....	56
Figure 4.7	Comparison of the K_D model fit with experimental data for subcritical water extraction of damnacanthal at various of flow rate (Symbols represent the experimental data and the lines are calculate based on the K_D 55.60).....	56
Figure 4.8	Damnacanthal extract with subcritical curve for the hot ball model at flow rate 2 and 4 ml/min.....	60
Figure 4.9	The one-site model fit of subcritical water extraction data (Symbols represent the experimental data, and the solid lines based on curve fitting the experimental data).....	60
Figure 4.10	Volumetric mass transfer coefficient ($k_e a_p$) versus flow rate (W).....	64
Figure 4.11	External mass transfer model fit of subcritical water extraction data (Symbols represent the experimental data, and the lines are based on curve fitting the experimental data).....	64
Figure A-1.2	Standard calibration curve of damnacanthal (average).....	75
Figure A-2.1	Particle size distribution of <i>Morinda citrifolia</i>	76
Figure C.1	Path independence thermodynamic properties.....	100

NOMENCLATURES

a	interfacial area per unit volume of bed (m^2/m^3)
a_p	interfacial area per unit volume of particle (m^2/m^3)
A	mass of easily accessible solute (kg)
B	mass of inaccessible solute inside the solid phase particles (kg)
c	fluid phase concentration (mol/m^3)
c^*	fluid phase interface concentration, in equilibrium with the solid phase (mol/m^3)
c_{equi}	equilibrium concentration of solubility (mol/m^3)
c_p	concentration in pores at the particle (mol/m^3)
c_s	solid phase concentration (mol/m^3)
c_s^*	solid phase interface concentration in equilibrium with the fluid phase concentration (mol/m^3)
\bar{c}_s	average value of solid-phase concentration (mol/m^3)
c_{s0}	initial solid-phase concentration (mol/m^3)
C_o	constant depending on pore geometry and form of rate equation
d_p	particle diameter (mm)
D	diffusion coefficient of the compound in the material of the sphere (m^2/s)
D_a	axial dispersion coefficient (m^2/s)
D_e	effective diffusion coefficient (m^2/s)
D_{macp}	macropore diffusion coefficient (m^2/s)
D_{micp}	micropore diffusion coefficient (m^2/s)
D_{12}	binary diffusion coefficient (m^2/s)
f	initial fraction solute in broken cell to total solute in the ground particle
F	fraction of the analyte released quickly.
g	acceleration due to gravity (m^2/s)
Gr	Grashof number ($gd_p^3\rho\Delta\rho/\mu^2$)
k_e	external mass transfer resistance (m/s)
k_i	internal mass transfer resistance (m/s)
k_1	first-order rate constant describing the quickly released fraction (min^{-1})

k_2	first-order rate constant describing the slowly released fraction (min^{-1})
K	equilibrium constant concentration (mol/m^3)
K_D	thermodynamics distribution coefficient
m_0	quantity of sample matrix loaded in the extractor (g)
n	an integer
N	mass of the solute-free solid phase (kg)
O	mass of the solute contained initially in the solid phase (kg)
Pe	Peclet number ($d_p u / D_a a$)
Q	solvent flow rate (g/s)
u	superficial velocity (m/s)
r	radial position in particle (m)
r_c	radius of unleached core (m)
R	particle radius (m)
S_0	initial total mass of analyte in the matrix (mg/g)
S_a	cumulate mass of the analyte extracted after volume V_a (mg/g)
$\frac{S_a}{S_0}$	cumulative fractions of the analyte extracted by the extraction fluid of the volume V_a
S_b	cumulate mass of the analyte extracted after volume V_b (mg/g)
$\frac{S_b}{S_0}$	cumulative fractions of the analyte extracted by the extraction fluid of the volume V_b
S_{fluid}	mass of solute extracted into the fluid of the volume $V_b - V_a$ (mg/g)
S_r	mass of extractable compound that remains in the matrix sphere after extraction for time (mg/g)
S_t	mass of the analyte removed by the extraction fluid after time t (mg/g)
$\frac{S_t}{S_0}$	fraction of the analyte extracted after time t
Sc	Schmidt number ($\mu / \rho D_{12}$)
Sh	Shearwood number ($k_e d_p / D_{12}$)
t	time (min)
t_c	a characteristic time for the extraction (min)
T	temperature ($^{\circ}\text{C}$)

T_a	absolute temperature ($^{\circ}\text{C}$)
T_m	normal melting temperature ($^{\circ}\text{C}$)
T_0	ambient temperature ($^{\circ}\text{C}$)
W	Flow rate (ml/min)
x	solid phase concentration (kg solute/kg insoluble solid)
x_a	solute inside the solid phase concentration (kg solute/kg insoluble solid)
x_b	inaccessible solute in the solid phase concentration (kg solute/kg insoluble solid)
x_c	transition concentration (kg solute/kg insoluble solid)
x_i	solute fraction in untreated solute (kg solute/kg insoluble solid)
x_0	initial solid phase concentration (kg solute/kg insoluble solid)
x_1	concentration of solid phase in broken cells (kg solute/kg insoluble solid)
x_{10}	initial concentration of solid phase with broken cells (kg solute/kg insoluble solid)
x_2	concentration of solid phase in intact cells (kg solute/kg insoluble solid)
x_{20}	initial concentration of solid phase with intact cells (kg solute/kg insoluble solid)
y	fluid phase concentration (kg solute/kg solvent)
y_{equi}	equilibrium fluid phase concentration (kg solute/kg solvent)
y_s	concentration of solubility (kg solute/kg solvent)
y_0	initial concentration of fluid phase (kg solute/kg solvent)
Y	percent of extraction yield
z	bed height (m)
z_2	mole-fraction of organic compound of interest in water
Z	solubility parameter (mole fraction of the solute)
$1-F$	fraction of the analyte released slowly

Greek letter

β	particle porosity
ε	bed voidage
ρ_f	fluid density (kg/m^3)

ρ_s	solid density (kg/m ³)
$\Delta\rho$	difference between saturated and pure fluid density (kg/m ³)
$\Delta_{fus}S$	entropy of fusion
μ	viscosity (kg/ms)
κ	gas constant
γ	activity coefficient



สถาบันวิทยบริการ
จุฬาลงกรณ์มหาวิทยาลัย

CHAPTER I

INTRODUCTION

1.1 Rationale

For centuries, scientists and medical professionals have been investigating chemical constituents in *Morinda citrifolia* (Noni or Yor). Whole parts of this plant, which include fruits, flowers, leaves, bark, stem, and roots have been shown to contain various biological activities (Yang et al., 2002). The roots of noni plants contain medicinally active components, namely anthraquinones, which show several therapeutic effects. These include anti-bacterial, anti-viral, and anti-cancer activities as well as analgesic effects, which make the roots potentially useful in several medical applications (Hiramatsu et al., 1993; Asahina et al., 1994). Of the anthraquinones present in the plant, damnacanthal is the most important and has been reported to be one of the most effective anti-cancer agents. Therefore, it is of interest to investigate effective means for extraction of this compound.

Conventionally, anthraquinones can be extracted with ethanol. This method is simple but it requires long extraction time and solvent residue may be left in the extract. Nowadays, the desire to reduce the use of the organic solvent in food and medicine processing has led to new extraction methods including supercritical fluid extraction (SFE) and subcritical water extraction (SWE). Supercritical carbon dioxide is commonly used in extraction of non-polar compound and the process has been commercialized for a variety of natural products. However, anthraquinones are slightly polar compound, thus the solubility in supercritical carbon dioxide is low.

Water is another preferred solvent, however at ambient condition it is a poor solvent for most organic compounds. Water at subcritical condition, which refers to liquid water whose temperature lies between boiling (100°C) and critical temperature (374°C), has a unique property. At such condition, water polarity, thus dielectric constant decreases due to the breakdown of intermolecular hydrogen bonds. The decrease in water polarity makes it an effective solvent for several medicinal

compounds. Examples of plants that have been extracted by subcritical water are such as berberine from *coptidis rhizoma*, glycyrrhizin from *radix glycyrrhizae*/liquorice and baicalein from *scutellariae radix* (Ong and Len, 2003). Due to high operating temperature however, thermal degradation may occur. Rogalinski et al., 2002 reported that at the operating temperature above 150°C, degradation of some compounds in *Peumus boldus M.* took place.

In our preliminary study, we have shown the feasibility of extracting anthraquinones from noni roots with subcritical water (Shotipruk et al., 2004). The subsequent study on antioxidant activity of the root extracts showed that subcritical water extraction yields the extract with the highest antioxidant activity compared to that obtained by conventional solvent extraction techniques (Pongnaravane, 2005). In this study also, the solubility of anthraquinones in subcritical water was determined at various temperatures. However, the method of quantitative analysis employed in these studies was spectrophotometry, with alizarin as a reference compound. Spectrophotometric analysis allowed quick determination of the amount of anthraquinones. However, the quantity measured was the “total” anthraquinones, which included all other anthraquinones beside damnacanthal. In this work we propose to more accurately measure the amount of this target anti-cancer compound, damnacanthal, using reversed-phase high performance liquid chromatography (RP-HPLC) and determine the effects of various factors such as temperature and flow rate on extraction efficiency. In addition, the data for extraction efficiency at various flow rates were fitted with simple thermodynamic partition, equilibrium with external mass transfer resistant and desorption models to describe the behavior of subcritical water extraction of this compound. This will provide useful information for the initial sizing and the economic evaluation of the system in a commercial scale.

1.2 Objectives

- 1.2.1 To find the suitable conditions for subcritical water extraction of damnacanthal from *Morinda citrifolia* roots.
- 1.2.2 To establish appropriate protocol for the analysis of damnacanthal extracted with subcritical water using reversed-phase high performance liquid chromatography.

- 1.2.3 To propose a mathematical model that describes the behavior of subcritical water extraction.

1.3 Working scopes

- 1.3.1 Investigation of anthraquinones (damnacanthal) extraction by subcritical water extraction at the various temperatures of 150 - 220°C and various flow rate 2-5 ml/min.
- 1.3.2 Establishment of an appropriate method for the analysis of damnacanthal with reversed-phase high performance liquid chromatography.

1.4 Expected benefits

- 1.4.1 Provide a new and efficient alternative for extraction of plant derived medicinal compounds.
- 1.4.2 Provide fundamental information useful for industrial scale-up of an extraction process.

CHAPTER II

BACKGROUND AND LITERATURE REVIEWS

Background

2.1 *Morinda citrifolia*

Morinda citrifolia, sometimes known as Noni, Indian Mulberry, Ba Ji Tian, Nono or Nonu, Cheese Fruit, Nhau, or in Thai, Ton Yor or Yor (Figure 2.1) is a plant in the Rubiaceae family, that is found widely in tropical areas, including parts of Asia. The plant is a small evergreen shrub or tree that grows from three to six metres. The plant has a straight trunk, large elliptical leaves, white tubular flowers and ovoid yellow fruits of up to 12 cm in diameter.

The roots, stems, bark, leaves, flowers, and fruits of the noni plant are all involved in various combinations in almost 40 known herbal remedies. For example, ripe noni fruits are reported to have a broad range of health benefits such as prevention and suppression of cancer, infection, arthritis, diabetes, asthma, hypertension, and pain. The leaves are used to treat eye problems; heated leaves are used to relieve coughs, nausea, colic; juice of the leaves can be taken for treatment of arthritis; and the roots are used to produce yellow dye as well as to relieve chronic diseases such as cancer, diabetes, and cardiovascular diseases. One of the most important constituents responsible for these therapeutic properties is anthraquinones. The compounds can be found in the leaves, barks, and roots, but the highest amount of anthraquinones are found in the roots of *Morinda citrifolia* (Yang et al., 2002).



Figure 2.1 *Morinda citrifolia* plant (Greig, 2005).

2.2 Anthraquinones

Anthraquinones are the main constituent in the root of *Morinda citrifolia*, consisting of several derivatives, differing in the R groups at five positions as show Figure 2.2 a). Examples of these compounds are damnacanthal, alizarin, and lucidin whose structures are shown in Figure 2.2 b), c), and d).

Of all the anthraquinones, damnacanthal is the most important in terms of medicinal values. It has been shown to be more effective than over 500 other botanical isolates in changing cancer cells back into normal cells. It is thus effective for fighting cancer, preventing the growth of pre-cancerous cells, and stimulating T cell activity (Hiramatsu et al., 1993). Physical and chemical properties of damnacanthal are summarized in Table 2.1.

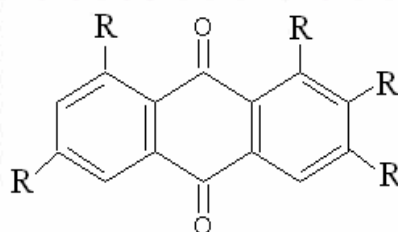


Figure 2.2a) Basic structure of anthraquinones.

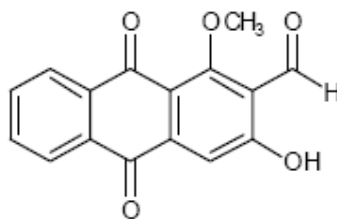


Figure 2.2b) 3-hydroxy-1-methoxyanthraquinone-2-carboxaldehyde (damnacanthal).

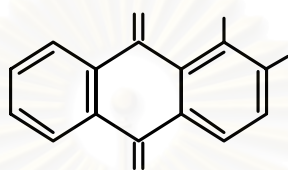


Figure 2.2c) 1,2-dihydroxyanthraquinone (alizarin).

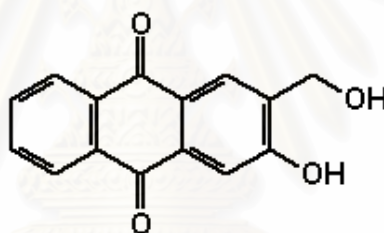


Figure 2.2d) 3-hydroxy-2-hydroxymethylantraquinone (lucidin).

Table: 2.1 Properties of damnacanthal (Biomol Research Laboratory Inc., 2005).

Name	3-hydroxy-1-methoxyanthraquinone-2-carboxaldehyde
Formula	C ₁₆ H ₁₀ O ₅
Molecular weight	282.3
Solubility at 25 °C (M)	Soluble in DMSO (25 mg/ml)

2.3 Sub and supercritical technology and natural product extraction

Sub and supercritical fluid technology is currently expanding into a wide range of applications. Supercritical fluids are defined as fluid at the temperatures and pressures above the critical values. These fluids can no longer be classified as a liquid or a gas (Figure 2.3). The most often used supercritical fluid is CO₂, particularly for analytical and process-scale extractions of natural products. CO₂ has low critical temperature, thus the operating temperature is desirably low. Furthermore, the process leaves no toxic residues in the final products. Pure supercritical CO₂ can be used to extract a wide variety of low-polarity solutes from natural materials, however, in many cases, the polarity of pure CO₂ is too low to quantitatively remove polar analytes without the need to add polar organic modifiers or to increase the extraction temperature.

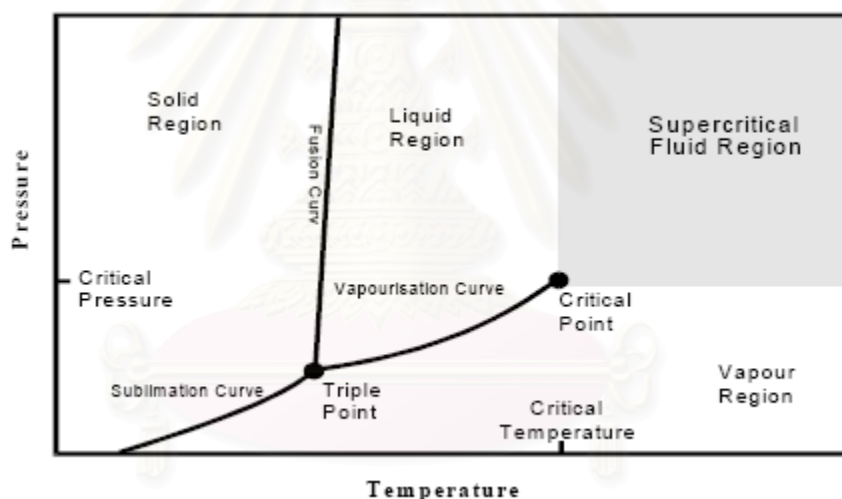


Figure 2.3 Theoretical Pressure – Temperature phase diagram for pure compound.

Another “environment-friendly solvent” is water, which has additional advantages of being readily available, at low cost. However, water in its “natural” state is not a good solvent for most organics. When water temperature rises nevertheless, it can quantitatively extract a wide variety of organic solutes from many different matrixes. Water at elevated temperature (typically between its boiling point and its critical temperature (374°C) and at a pressure high enough to maintain the liquid state) is called “subcritical water” or “superheated water”, or “pressurized hot water”. The breakdown of the hydrogen-bonded structure

causes water dielectric constant to fall, making it possible to dissolve organic compound. For instance, pure water at ambient condition has a dielectric constant of 79, as is shown in the Figure 2.4. Increasing the temperature to 250°C at a pressure of 5 MPa (necessary to maintain the liquid state) yields a significant reduction of this value to about 27. At this condition water has the polarity similar to that of ethanol at 25°C and 0.1 MPa (Clifford et al., 2002; Smith, 2002).

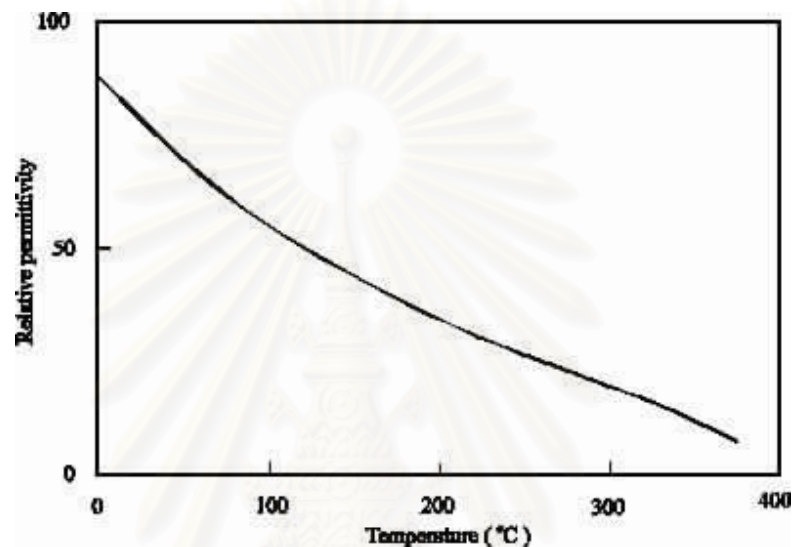


Figure 2.4 Relative permittivity (dielectric constant) of liquid water along the saturation line (Critical Process Ltd, 2005).

2.4 Mathematical modeling of extraction process

Extraction of natural materials consists of releasing solutes from porous or cellular matrix into solvent and transferring these solutes in the solution to the bulk fluid. In fact, a series of sequential steps comprises diffusion of solvent into the pores, adsorption of solvent on the solid surface, formation of an external liquid film around the solid particles, dissolution and convective transport of the solute in the bulk fluid phase, desorption of the solute to fluid phase in the pores, diffusion through the pores, and finally transport to the bulk solvent. The rate-limiting process for the extraction of these materials may be different from one material to another. Generally speaking, the extraction behavior is controlled by either one of the following; solute-solid interaction (adsorption), solute-fluid interaction (solubility), or mass transfer. Mathematical modeling of the extraction of natural materials is an activity of

increasing importance due to the economic potentials it offers. It is important to develop models for an extraction process if the process is to be scaled up and optimized. A number of mathematical models have been developed for various extraction processes. Generally, they differ in the description of phase equilibrium, mass transfer in the solid phase, and flow pattern (Sovava, 2005).

Phase equilibrium depends on the extraction pressure and temperature and on the composition of solute, solvent, and matrix. It generally controls the first period when the fluid phase leaving the extractor either is in equilibrium with solid phase at the extractor outlet or it is not far from the equilibrium. Thus, the first part of extraction curve contains information on the type of equilibrium between the solid and fluid phase. When the solute concentration in solid phase is high, the fluid phase equilibrium concentration is independent of matrix and equal to solubility. When the initial solute concentration in the plant is only a few percent or less, the equilibrium is usually controlled by solute-matrix interaction and the fluid-phase concentration is much lower than the solubility.

Mass transfer: Particles of different shapes, sizes, and surface areas are formed as a result of plant pre-treatment by grinding, milling, cutting or other method of disintegration. During extraction, solute diffuses to particle surface; the internal diffusion is modeled using either effective diffusion coefficient or solid-phase mass transfer coefficient. Relations of these coefficients were published for various particle shapes such as spheres, cylinders, and slabs.

Flow pattern affects the local driving force and through it particularly the extraction rate of easily accessible solute. The ideal flow pattern is that of plug flow in which axial dispersion is negligible. In a real extractor, axial dispersion exists and it becomes more pronounced the lower the length-to-diameter ratio of extraction bed. Furthermore, channeling may occur in tightly packed beds especially when particle size is less than 0.4 mm or when the extractor diameter is large; it is connected with a dramatic decrease in extractor performance.

2.4.1 Extraction models

Generally, mathematical models of any extraction process consist of mass balance equations for the solute in the solid phase as well as that in the fluid phase. In a packed bed, solvent and solid materials content change with time and distance along the axis of the bed. In most modeling procedures for fixed bed extraction, the following assumptions are made: constant pressure, constant temperature, solute free entering fluid, and homogeneous solid bed with respect to both particle size and solid phase solute concentration at initial state. Generally, the following properties and characteristics are considered to be known: bed voidage, solubility data, and thermodynamic properties of the fluid at the required conditions.

The governing partial differential equation for the fluid phase derived from different mass balance as a function of bed height, z , and time, t , is as follows:

$$\varepsilon \frac{\partial c}{\partial t} = D_a \frac{\partial^2 c}{\partial z^2} - u \frac{\partial c}{\partial z} + j(c_s, c) \quad (2.1)$$

The governing differential equation for the solid phase as a function of time is as follows:

$$(1 - \varepsilon) \frac{\partial c_s}{\partial t} = -j(c_s, c) \quad (2.2)$$

where c = fluid phase concentration (mol/m³)

c_s = solid phase concentration (mol/m³)

ε = bed voidage

D_a = axial dispersion coefficient (m²/s)

u = superficial velocity (m/s)

The concentration of dissolved solute, c_p , in the pore of an assumed spherical particle, depends on solid phase concentration and time, and its variation is given by:

$$\beta \frac{\partial c_p}{\partial t} = \frac{D_e}{r^2} \frac{\partial}{\partial r} \left(r^2 \frac{\partial c_p}{\partial r} \right) - (1 - \beta) \frac{\partial c_s}{\partial t} \quad (2.3)$$

where β = particle porosity

D_e = effective diffusion coefficient (m²/s)

r = radial position in particle (m)

The function $j(c_s, c)$ varies with the model proposed, taking into account the equilibrium relationship and the mass transfer phenomena.

The above partial differential equations can be solved when $j(c_s, c)$ is specified and the initial conditions on c and c_s and the boundary conditions on c are given.

Danckwerts' boundary conditions at the inlet and at the outlet of the column are given by

$$\text{B.C. at } z = 0; \quad \frac{u}{\varepsilon} c - D_a \frac{\partial c}{\partial z} = 0 \quad (2.4)$$

$$\text{B.C. at } z = L; \quad \frac{\partial c}{\partial z} = 0 \quad (2.5)$$

If axial dispersion is neglected only one boundary condition is required:

$$\text{B.C. at } z = 0: \quad c = 0 \quad (2.6)$$

By integration of these different equations, with appropriate equilibrium relationship and appropriate boundary and initial conditions, time-dependent concentration profiles in both liquid phase, $c(t, z)$, and solid phase, $c_s(t, z)$ are obtained and the extraction curve can be calculated from fluid-phase concentration at the extractor outlet by the following equation:

$$Y(t) = \frac{Q \int_0^t c(s, L) ds}{m_0} \cdot 100 \quad (2.7)$$

where Y = percent of extraction yield

- Q = solvent flow rate (g/s)
 m_0 = quantity of sample loaded in the extractor (g)

In an extraction process in which mass transfer resistances are negligible, equilibrium model is employed.

2.4.1.1 Equilibrium model (Reverchon et al, 1997)

There are two cases for equilibrium model. In the first case where solute has no affinity with the solid matrix, it is possible to describe the process through the physical solubility in the fluid phase. For a bed of solid material, the solubility isotherm can be expressed as

$$c = c_{equi} \quad \text{where } c_s > 0 \quad (2.8)$$

$$c = 0 \quad \text{where } c_s = 0 \quad (2.9)$$

where c_{equi} = equilibrium concentration of solubility (mol/m^3)

If we suppose, instead, that the solute interacts with the solid; i.e. it is adsorbed on the solid phase, a linear relationship can be used:

$$c_s = Kc \quad (2.10)$$

where K = the equilibrium constant

If mass transfer resistance are limiting factor in the extraction process, it must be considered in the model.

2.4.1.2 Resistance models (Reverchon et al., 1997)

If we suppose that only the mass transfer resistance inside the solid phase has to be considered, $j(c_s, c)$ can be written as

$$j(c_s, c) = k_i a (c_s - c_s^*) = k_i a (c_s - Kc) \quad (2.11)$$

where c_s^* = solid phase interface concentration in equilibrium with the fluid phase concentration (mol/m³)

k_i = internal mass transfer resistance (m/s)

a = interfacial area per unit volume of bed (m²/m³)

K = equilibrium constant

If we suppose, instead, that only the fluid phase mass transfer controls the mass transfer process,

$$j(c_s, c) = k_e a (c^* - c) = k_e a [(c_s / K) - c] \quad (2.12)$$

where c^* = fluid phase interface concentration, in equilibrium with the solid phase concentration (mol/m³)

k_e = external mass transfer resistance (m/s)

The area, a , is effective surface area per unit volume of bed, which is conveniently expressed as a fraction l of the physical surface area (a_p) of the particles contained in that volume. a_p can be estimated from the mean diameter of the spherical particles and the bed voidage as follows:

$$a_p = \frac{6(1 - \varepsilon)}{d_p} \quad (2.13)$$

Then,

$$a = la_p \quad (2.14)$$

Amongst the simplest resistance models used in natural product extraction are the Shrinking Core Model (SCM), used by Roy et al., 1997, and Akgun et al., 2002 and the Broken and Intact Model (BICM), used by Sovova, 1994, 1996, Marrone et al., 1998, and Reverchon et al., 2000. In the SCM, there is irreversible separation of material extracted from a boundary of a shrinking core inside the particle. The extracted solute then diffuses to the particle surface through the pores. Throughout the extraction process, the solute concentration is assumed to be constant

at the shrinking core boundary. In the BICM, two regions are distinguished in the particle. Close to surface there is a region of broken cells whose walls have been damaged by mechanical pre-treatment and particle core contains intact cells. Mass transfer resistance of cell walls is high and therefore there is a large difference in diffusion rates from both regions; the initial fast extraction from broken cells is followed by much slower extraction from intact cells. An example of this type of model is Sovova's model. The detailed development of each model is described as follows.

- *Shrinking core model* (Goto et al., 1996)

This model describes the situation of the irreversible desorption followed by diffusion in the porous solid through the pores. When mass transfer rate of the solute in the nonextracted inner part is much slower than that in the outer part where most of the solute has been extracted, or the solute concentration is much higher than the solubility of the solute in the solvent phase, a sharp boundary may exit between the outer and the inner region. A core of inner region shrinks with the progress of the extraction. These situations can be modeled by the shrinking core model. An example of these situations is the supercritical fluid extraction of vegetable oils

For this model, the factor $j(c_s, c)$ in Equation. 2.1 and 2.2 is then expressed as

$$j(c_s, c) = k_e a [c_p(R) - c] \quad (2.15)$$

where $c_p(R)$ = concentration in pores at the particle surface at $r = R$, the particle radius (mol/m^3).

Substituting Equation 2.13 and 2.14 with $l = 1$ into Equation 2.15, the following equation results:

$$j(c_s, c) = \frac{3(1-\varepsilon)k_e}{R} [c_p(R) - c] \quad (2.16)$$

The time dependence of the average concentration of solute in solid phase is obtained by equating the rate of diffusion of the solute through the surface film surrounding the particle to the rate at which the total solute content of the particle fall with time. Equation 2.2 can be rearranged to give:

$$(1 - \varepsilon) \frac{\partial \bar{c}_s}{\partial t} = -j(c_s, c) \quad (2.17)$$

where \bar{c}_s = average value of solid-phase concentration (mol/m³)

The radial dependence of the concentration of dissolved solute in the pore, c_p , is obtained from Equation 2.3, for the outer region of the particle, Equation 2.3 becomes:

$$\frac{D_e}{r^2} \frac{\partial}{\partial r} \left(r^2 \frac{\partial c_p}{\partial r} \right) = 0 \quad (2.18)$$

where D_e = effective diffusion coefficient of the compound in the material of the sphere (m²/s)

The above results are general for mass transfer from a spherical pellet and do not presuppose a specific distribution of solute within the pellet. The consequences of the shrinking core model are now examined. According to this model the solute-rich phase (liquid oil in the present example) is concentrated within a core, the radius (r_c) of which gradually diminishes with time.

Because of the low solubility in systems of interest and the fact that the extractant phase will normally be less dense than the solute-rich phase, virtually all the solute contained within the particles will be present in the solute-rich phase, i.e. within the core, outside the core therefore $c_s \approx 0$.

The average solid phase concentration is equal to the initial solid phase concentration multiplied by the ratio of the core volume to the particle volume.

$$\bar{c}_s = c_{s0} \left(\frac{r_c}{R} \right)^3 \quad (2.19)$$

where c_{s0} = initial solid-phase concentration (mol/m³)
 r_c = radius of unleached core (m)
 R = particle radius (m)

Boundary conditions are given as follows. At the core boundary, the concentration in the fluid phase is at its saturation value (solubility).

$$c_p = c_{equi} \quad \text{at } r = r_c \quad (2.20)$$

Diffusion flux at the outer surface of a particle is equal to the mass transfer through the external film.

$$\left(D_e \frac{\partial c_p}{\partial r} \right)_{r=R} = k_e [c - c_p(R)] \quad (2.21)$$

Initial conditions are given as follows:

$$r_c = R \quad \text{at } t = 0 \quad (2.22)$$

$$c = 0 \quad \text{at } t = 0 \quad (2.23)$$

These boundary and initial conditions, long with the Danckwert's boundary conditions (Equation 2.4-2.6), could be used to solve the above equations to obtain the concentration of the extract at the exit of the bed.

- **Broken and intact cells model (BICM)**

The broken and intact cells model (BICM) was introduced by Sovova 1994, 2005 to describe extraction behavior of vegetable seed oil. The advantage of this model is that it gives reasonably realistic description of the biological material structure. In this model, the structure of biological material is divided to two regions: broken cells and intact cells. Mass transfer resistance of broken cells is high and that of the intact cell is low, therefore there is a large difference in diffusion rates between

the two regions. In this model, the factor $j(c_s, c)$ is expressed in terms of solute free solid base y and y^* is equivalent to c^* .

Like the previous models described, BIC model describes a situation when solvent flows axially with superficial velocity u through a bed of milled plant material in a cylinder reactor. The solvent is solute-free at the entrance of the extractor, and the temperature and pressure are regarded as constants. The solid bed is homogenous with respect to both the particle size and the initial distribution of the solute. In this model, the solute is taken to be deposited in plant cells and protected by cell walls. However, a part of the walls has been broken open by milling, so that a part of the solute is directly exposed to the solvent. Both the models developed by Sovova in 1994 and 2005 used the above mentioned assumptions. However, there are slight differences in the Sovova BIC models which will be described here.

a) Sovova, 1994

In this model, extraction is divided into step; the initial fast extraction from broken cells is followed by much slower extraction from intact cells. The mass of the solute contained initially in the solid phase, O , consists of the mass of easily accessible solute, A , and the mass of inaccessible solute inside the solid phase particles, B

$$O = A + B \quad (2.24)$$

Mass of the solute-free solid phase, N , remains constant during the extraction. Amounts of solute are related to this quantity so that the initial concentration are

$$x(t=0) = x_0 = O/N = x_a + x_b = A/N + B/N \quad (2.25)$$

where x = solid phase concentration (kg solute/kg insoluble solid)
 x_0 = initial solid phase concentration (kg solute/kg insoluble solid)
 x_a = solute inside the solid phase concentration (kg solute/kg insoluble solid)

x_b = inaccessible solute in the solid phase concentration (kg solute/kg insoluble solid)

From Equation 2.1-2.2, the material balances for fluid and solid phase in the bed are given by

$$\rho_f \varepsilon \frac{\partial y}{\partial t} = D_a \frac{\partial^2 y}{\partial z^2} - \rho_f u \frac{\partial y}{\partial z} + j(x, y) \quad (2.26)$$

$$\rho_s (1 - \varepsilon) \frac{\partial x}{\partial t} = -j(x, y) \quad (2.27)$$

where ρ_f = fluid density (kg/m³)

ρ_s = solid density (kg/m³)

y = fluid phase concentration (kg solute/kg solvent)

If the solvent is solute-free at the entrance of the extractor and if all particles have the same initial solute content x_0 the boundary conditions are

$$x(z, t = 0) = x_0 \quad (2.28)$$

$$y(z = 0, t) = 0 \quad (2.29)$$

The easily accessible solute which surmounts only the diffusion resistance in the solvent is extracted first. When the solid-phase concentration decreases to x_b , mass transfer is retarded by the diffusion in the solid phase:

$$j(x > x_b, y) > j(x \leq x_b, y) \quad (2.30)$$

As the plant tissue is torn during the grinding, part of the solute is released. Concentration of this easily accessible solute in the solid phase is x_b at the beginning of extraction. In other words, mass transfer from broken cells to the solvent is characterized by fluid phase mass transfer coefficient (k_e)

$$j(x, y) = k_e a \rho_f (y_s - y) \quad \text{for } x > x_b \quad (2.31)$$

where y_s = concentration of solubility (kg solute/kg solvent)

The second period of extraction starts when the easily accessible solute has been removed. The rate of extraction depended on the diffusion of solute from the interior of the plant tissue to the surface.

$$j(x, y) = k_i a \rho_s (x - x^*) \quad \text{for } x \leq x_b \quad (2.32)$$

In this period, k_i is much smaller than k_e , the interfacial concentration x^* could be neglected a comparison with the concentration inside particle x , thus $x - x^* \approx 0$. It also holds in the second period that the fluid phase concentration (y) is much smaller than the solubility (y_s), then Equation 2.32 can be rearranged as:

$$j(x, y) = k_i a \rho_s x (1 - y / y_s) \quad \text{for } x \leq x_b \quad (2.33)$$

b) Sovova, 2005

In recent publication, *Sovova* proposed a slight variation of BICM. Again, mass transfer from broken cells to the solvent is characterized by fluid phase mass transfer coefficient (k_e) that is by several orders of magnitude larger than the solid phase mass transfer coefficient (k_i) related to the diffusion, j_s , from intact cells to broken cells. In this model, the accessible solute from broken cells is transferred directly to the fluid phase, while the solute from intact cells diffuses first to broken cells and then to the fluid phase.

In this model, the volumetric fraction of broken cells in the particles, f , is defined where $0 < f < 1$. The initial proportions of the solute in the solid matrix in the broken and in the intact cells are determined by

$$\begin{aligned} x_0 &= x_1(t=0) + x_2(t=0) \\ x_1(t=0) &= f x_0 \\ x_2(t=0) &= (1 - f) x_0 \end{aligned} \quad (2.34)$$

- where x_0 = initial solute in solid matrix (kg solute/kg insoluble solid)
- x_1 = concentration of solid phase in broken cells (kg solute/kg insoluble solid)
- x_2 = concentration of solid phase in intact cells (kg solute/kg insoluble solid)
- f = initial fraction solute in broken cell to total solute in the ground particle

Mass balance per unit volume of extraction bed for plug flow, Equation 2.1 and 2.2 can then be rearranged as:

For fluid phase:

$$\rho_f \varepsilon \frac{\partial y}{\partial t} = D_a \frac{\partial^2 y}{\partial z^2} - \rho_f u \frac{\partial y}{\partial z} + j_f \quad (2.35)$$

For solid phase

- broken cells

$$f \rho_s (1 - \varepsilon) \frac{\partial x_1}{\partial t} = j_s - j_f \quad (2.36)$$

- intact cells

$$(1 - f) \rho_s (1 - \varepsilon) \frac{\partial x_2}{\partial t} = -j_s \quad (2.37)$$

The factor j_f is then expressed as

$$j_f = k_e a \rho_f (y_{equi} - y) \quad (2.38)$$

Whereas, the factor j_s is expressed as

$$j_s = k_i a \rho_s (x_2 - x_1) \quad (2.39)$$

- where y_0 = initial concentration of fluid phase (kg solute/kg solvent)
- y_{equi} = equilibrium fluid phase concentration (kg solute/kg solvent)

The initial and boundary conditions are

$$\begin{aligned}
 y|_{t=0} &= y_0 = y_{equi} & x_1|_{t=0} &= x_{10}; \\
 x_2|_{t=0} &= x_{20} = x_i; & y|_{z=0} &= 0; \\
 \frac{dy}{dz}|_{z=L} &= 0
 \end{aligned} \tag{2.40}$$

where x_i = solute fraction in untreated solute (kg solute/kg insoluble solid)
 x_{10} = initial concentration of solid phase with broken cells (kg solute/kg insoluble solid)
 x_{20} = initial concentration of solid phase with intact cells (kg solute/kg insoluble solid)

Phase equilibrium between the fluid phase and the solid phase with broken cells is given by the discontinuous equilibrium function depicted in Figure 2.5 which is proposed by Perrut et al., 1997. The discontinuity occurs at transition concentration, x_c , which is equal to matrix capacity for interaction with the solute (kg solute/kg insoluble solid). At solid phase concentration lower than x_c , all solute interacts with matrix and phase equilibrium is determined by partition coefficient, K . At the concentration higher than x_c , the solid phase contains also free solute whose equilibrium fluid phase concentration is equal to the solubility, y_s .

$$y_{equi} = y_s \quad \text{for } x_1 > x_c; \tag{2.41}$$

$$y_{equi} = Kx_1 \quad \text{for } x_1 \leq x_c, \text{ where } Kx_c < y_s \tag{2.42}$$

where y_s = solubility concentration (kg solute/kg solvent)

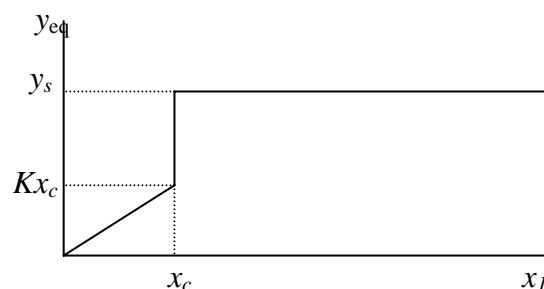


Figure 2.5 Equilibrium curve (Perrut et al., 1997).

2.4.1.3 Parameter

The parameters involved in the model are the mass transfer coefficient to the bulk phase, the axial dispersion coefficient in the fluid phase, the effective pore diffusivity in the particles and the solubility. These were evaluated using existing correlations, experiment data and available data.

- **Film transfer coefficient** (King et al.,1993)

The film transfer coefficient k_e is a measure of the resistance to mass transfer in the fluid phase. The coefficient is a function of the superficial velocity u , density ρ , viscosity μ and binary diffusion coefficient D_{12} . The coefficient is usually predicted from correlations using dimensionless numbers that have been developed from mass transfer studies using gases and liquids at near-ambient conditions. The correlations are of the form

$$Sh = f(Re, Sc, Gr, \varepsilon) \quad (2.43)$$

where $Sh = \text{Shearwood number} = k_e d_p / D_{12} \quad (2.44)$

$$Sc = \text{Schmidt number} = \mu / \rho D_{12} \quad (2.45)$$

$$Gr = \text{Grashof number} = g d_p^3 \rho \Delta \rho / \mu^2 \quad (2.46)$$

$$k_e = \text{external mass transfer resistance (m/s)}$$

$$g = \text{acceleration due to gravity (m}^2\text{/s)}$$

$$\rho_f = \text{fluid density (kg /m}^3\text{)}$$

$$\Delta \rho = \text{difference between saturated and pure fluid density (kg/m}^3\text{)}$$

$$d_p = \text{particle diameter (m)}$$

$$\mu = \text{viscosity (kg /m s)}$$

$$D_{12} = \text{binary diffusion coefficient (m}^2\text{/s)}$$

The prediction of k_e at near-critical conditions required an accurate value of the binary diffusion coefficient at the same temperature and pressure.

- ***Axial dispersion coefficients*** (King et al.,1993)

The axial dispersion coefficient is a measure of the extent of back-mixing as the fluid traverses the packed bed. The dispersion coefficient is in the range zero to infinity, where zero represents no mixing, or plug flow and infinity represents perfect mixing.

Dispersion coefficients are also predicted using dimensionless number correlations, which are generally of the form

$$Pe = f(Re, Sc) \quad (2.47)$$

Where Pe = Peclet number = $d_p u / D_a$

- ***Effective diffusivity*** (Kiriamiti et al., 2002, King et al.,1993)

The effective diffusivity on the form of the porous network and is then correlated as follows:

$$D_e = \beta^2 D_{12} \quad (2.48)$$

where D_{12} = binary diffusion coefficient (m^2 / s)

β = particle porosity

If the porous structure is bidisperse, the effective diffusivity D_e is obtained from

$$\frac{1}{D_e} = \frac{1}{D_{macp}} + \frac{C_0}{D_{micp}} \quad (2.49)$$

where D_{macp} = macropore diffusion coefficient (m^2/s)

D_{micp} = micropore diffusion coefficient (m^2 / s)

C_0 = constant depending on pore geometry and form of rate equation

2.4.2 Simple models

When consider extraction in continuous flow passing short extraction vessels, it is not necessary to consider the concentration profile within the bed. The extraction models become simpler. In this case, two simple models have been used to describe the extraction curves depending on whether the extraction is controlled by diffusion out of the solid matrix or by equilibrium. If the solute concentration in the matrix phase is high the fluid phase equilibrium concentration is equal to solubility and simple saturation solubility calculations can be used to predict extraction curve. When the initial solute concentration in the plant is only a few percent or less, the equilibrium is usually controlled by partitioning of solute between matrix and solvent, and the fluid phase concentration is much lower than the solubility.

2.4.2.1 Extraction controlled by partitioning of solute between matrix and solvent (Kubátová et al., 2002)

This model is based on a single thermodynamics partitioning coefficient (K_D) defined as

$$K_D = \frac{\text{Concentration of analyte in the matrix}}{\text{Concentration of analyte in the extraction fluid}}; \text{ at equilibrium}$$

For this model, it is assumed that the initial desorption step does not significantly affect the extraction rate. In addition the subsequent fluid-matrix partitioning is assumed to be rapid. Essentially, the mass of analyte in each unit mass of extraction fluid and the mass of analyte remaining in the matrix at that period in the extraction time is calculated for the entire extraction time based on the K_D value determined for each compound. Therefore, if the K_D model applies to a certain extraction, the shape of an extraction curve would be defined by:

$$\frac{S_b}{S_0} = \frac{\left(1 - \frac{S_a}{S_0}\right)}{\left(\frac{K_D m}{(V_b - V_a)\rho} + 1\right)} + \frac{S_a}{S_0} \quad (2.50)$$

where S_a = cumulate mass of the analyte extracted after volume V_a (mg/g)

S_b = cumulate mass of the analyte extracted after volume V_b (mg/g)

S_0 = initial total mass of analyte in the matrix (mg/g)

$\frac{S_a}{S_0}$ = cumulative fractions of the analyte extracted by the extraction fluid
of the volume V_a

$\frac{S_b}{S_0}$ = cumulative fractions of the analyte extracted by the extraction fluid
of the volume V_b

K_D = thermodynamic partitioning coefficient

ρ = density of extraction fluid at given conditions (mg/ml)

m = mass of the extracted sample (mg).

The derivation of the above equation can be found in Appendix D. Note that K_D model does not include extraction time, but only relies on the volume of extractant fluid used (assuming a constant sample size). Therefore, doubling the extraction fluid flow rate should double the extraction rate versus time if the extraction is described by K_D (and if all other extraction parameters remain the same).

2.4.2.2 Extraction controlled by diffusion out of the matrix

When the flow of fluid is fast enough for the concentration of a particular solute to be well below its solubility limit, the rate-determining process is the rate of diffusion out of the matrix.

We assume an effective diffusion coefficient, D_e , and a spherical geometry for the matrix and solve the appropriate differential equation with assumed boundary conditions. These conditions are that the compound is initially uniformly distributed within the matrix, and that as soon as extraction begins, the concentration of compound at the matrix surfaces is zero (corresponding to no solubility limitation), the solution is described as the hot-ball model because of the analogy of the mathematical solutions with those for a hot spherical object being dropped into cold water, given by Carlslaw and Jaeger's equation (Westwood et al., 1959). As shown in Appendix D, the ratio of the mass of diffusing substance leaving the sample to the initial mass of solute in the sample, S_t/S_0 is given by

$$S_t / S_0 = 1 - \frac{6}{\pi^2} \sum_{n=1}^{\infty} \frac{1}{n^2} \exp(-D_e n^2 \pi^2 t / r^2)$$

where n = an integer

D_e = effective diffusion coefficient of the compound in the material of the sphere (m^2/s).

The adaptation of this solution leads to the following equation for the ratio of the mass, S_r , of extractable compound that remains in the matrix sphere after extraction for time, t , to that of the initial mass of extractable compound, S_0

$$S_r / S_0 = \frac{6}{\pi^2} \sum_{n=1}^{\infty} \frac{1}{n^2} \exp(-D_e n^2 \pi^2 t / r^2) \quad (2.51)$$

Equation 2.51 above may be simplified using a quantity t_c defined as:

$$t_c = r^2 / \pi^2 D_e \quad (2.52)$$

This is a characteristic time for the extraction (t_c), to give, after expanding the summation, the solution becomes:

$$S_r / S_0 = \frac{6}{\pi^2} [\exp(-t/t_c) + (1/4)\exp(-4t/t_c) + (1/9)\exp(-9t/t_c) + \dots] \quad (2.53)$$

The solution is thus a sum of exponential decays, in which at longer times, the later (more rapidly decaying) terms decreases in importance and the first exponential term in the square brackets becomes dominant. This can be seen again if the natural logarithm of this equation is taken, after factorizing the term $\exp(-t/t_c)$ from the square bracket, to obtain

$$\ln(S_r / S_0) = \ln \frac{6}{\pi^2} - t/t_c + \ln[1 + (1/4)\exp(-3t/t_c) + (1/9)\exp(-8t/t_c) + \dots] \quad (2.54)$$

The term $\ln(6/\pi^2)$ equals -0.4977, the final term in this equation equals +0.4977 at $t = 0$ and so, as required, at $t = 0$ $\ln(S_r / S_0)$ is also equal to zero. A plot of

$\ln(S_r / S_0)$ versus time therefore tends to become linear at longer times, when the last term in the above equation tends to zero, and $\ln(S_r / S_0)$ is given approximately by

$$\ln(S_r / S_0) = -0.4977 - t/t_c \quad (2.55)$$

This has the form after taking exponentials of

$$S_r = K \exp(-t/t_c) \quad (2.56)$$

where K is a constant for a particular extraction equal to $S_0 \exp(-0.4977)$ for a sphere.

If the mass of solute in the matrix is S_0 initially and S_r after a given time, a plot of $\ln(S_r / S_0)$ versus time has the form given in Figure 2.6. It is characterized by a relatively rapid fall on to a linear portion, which corresponds to an extraction “tail”. The physical explanation of the form of the curve is that the initial portion is extraction, principally out of the outer parts of the sphere, which establishes a smooth concentration profile across each particle, peaking at the center and falling to zero at the surface. When this has happened, the extraction becomes an exponential decay.

The curve is characterized by two parameters: a characteristic time, t_c , and the intercept of the linear portion, $-I$, which has the value -0.5 (actually -0.4977) for the sphere. The slope of the linear portion is $-1/t_c$ and the linear portion appears to begin at approximately $0.5t_c$. As mentioned, t_c is theoretically related to the effective diffusion out of the matrix, D_e , and the radius of the sphere, r by Equation 2.52.

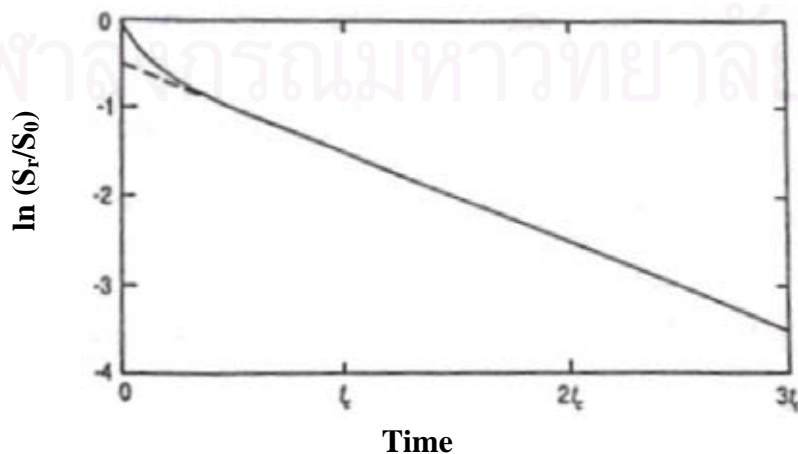


Figure 2.6 Theoretical curve for the hot-ball model (Westwood, 1959).

The value of the D_e will usually not be known, although its order of magnitude may be commented on. Most measurements published for D_e are for true diffusion and for small molecules in relatively mobile solvents and D_e is of the order of 10^{-5} . For system of interest, D_e will be between 1 (for oils) and 4 (for solids) orders of magnitude below this value. Equation 2.52 shows a squared dependence on r and rationalizes the commonsense rule that for rapid extraction, matrix particles must be small. This may be achieved for solids by crushing or grinding and for liquids by coating on a finely divided substrate, spraying or mechanical agitation. For solid matrix particles with r of the order of 0.1 mm, typical values of t_c are between 10 and 100 minutes.

In general, the value of I is thought to depend on the particle shape and size distribution (for the former in particular the surface to volume ratio) and also the distribution of solute within the matrix particles (i.e. whether the solute is primarily located near the surface or in the interior of the particle). For a model system of spheres of the same size, with uniform solute concentration, it is 0.5. For real system, values approximately 2 are common and it has been shown that the occurrence of an intercept below that of the theoretical value indicates either non-uniform distribution of extractable compound or irregular particle shape (Westwood, 1959). Although the non-uniformity could be factored into the model as a function of solid radius, a simpler account for this is to model the diffusion controlled by two site model described below. Equation 2.55 when written as the amount extracted at time t , becomes:

$$\frac{S_t}{S_0} = 1 - \frac{S_r}{S_0} = 1 - e^{-kt} \quad (2.57)$$

where S_t = mass of the analyte removed by the extraction fluid after time t
(mg/g)

S_0 = total initial mass of analyte in the matrix (mg/g)

$\frac{S_t}{S_0}$ = fraction of the analyte extracted after time t

k = a first order rate constant describing the extraction

This equation is sometimes called kinetic desorption model. In the case where the solute is uniformly distributed within the matrix, the first order rate constant describing the extraction, k , is equal to $-0.4977t_c$.

- *Two-site kinetic desorption model* (Kubátová et al., 2002)

This model is a modification of the kinetic desorption model described in the previous section. The two-site kinetic desorption model requires two steps to define an extraction curve, i.e. a certain fraction (F) of the analyte desorbs t a fast rate defined by k_1 , and the remaining fraction ($1-F$) desorbs by a slower rate defined by k_2 . The simple two-site kinetic model consists of two first order extractions:

$$\frac{S_t}{S_0} = 1 - [F e^{-k_1 t}] - [(1-F) e^{-k_2 t}] \quad (2.58)$$

where S_t = mass of the analyte removed by the extraction fluid after time t (mg/g)
 S_0 = total initial mass of analyte in the matrix (mg/g)
 $\frac{S_t}{S_0}$ = fraction of the analyte extracted after time t
 F = fraction of the analyte released quickly
 $1-F$ = fraction of the analyte released slowly
 k_1 = first-order rate constant describing the quickly released fraction (min^{-1})
 k_2 = first-order rate constant describing the slowly released fraction (min^{-1})

Note that the kinetic model includes no factor describing extraction flow rate, but relies solely on time. Therefore, doubling the extractant flow-rate should have little effect on the extraction efficiency per unit time if the extraction efficiency is controlled by the kinetics of the initial desorption (matrix-fluid

partitioning/diffusion out of fluid) step (assuming the other extraction parameters remain constant).

While it is possible that both a kinetic desorption (diffusion out of fluid) model and a K_D model could yield similar fits to extraction curve data, the dependence of the K_D model on extraction fluid volume (not time) and the dependence of kinetic models on extraction time (not volume of fluid) yields a simple method to determine the major factor controlling a particular extraction.

2.5 Solubility

As can be seen from the development of the mathematical models in previous section, solubility plays a key role in the efficiency of extraction process. Solubility is a measure of solute concentration that is in equilibrium with the solvent at a given temperature. The similar substances are soluble in each other and the most appropriate extraction solvents or mixtures of solvents should have nearly the same polarities as those of the solutes. Solubility of an organic substance can be derived from thermodynamics relations and expressed as:

$$\ln Z^{SAT} = \frac{\Delta_{fus}S}{\kappa} \left(1 - \frac{T_m}{T_a} \right) - \ln \gamma^{SAT} \quad (2.59)$$

where the superscript SAT = represent the values at equilibrium or saturation,

Z = solubility parameter (mole fraction of the solute)

$\Delta_{fus}S$ = entropy of fusion

T_m = normal melting temperature

T_a = absolute temperature

κ = gas constant

γ = activity coefficient

The detailed derivation of this equation can be found in Appendix C. This equation demonstrates that the solute solubility depends on temperature and intermolecular forces between solute and solvent as represented by the activity coefficient. For an ideal solution, the activity coefficient is equal to 1. For non-ideal

solution, activities coefficient is not equal to 1. Many solubility estimation methods such as Robbins chart, UNIFAC model, Hansen solubility parameter, and Margules equation can be used to estimate of the value of activity coefficient, and thus solubility (Prausnitz et al., 1999).

A specific mathematical model has been proposed for solubility of anthraquinones in subcritical water (Pongnaravane, 2005). The model takes a very simple form as follows:

$$\ln z_2(T) \approx (T_0/T) \ln z_2(T_0) \quad (2.60)$$

where z_2 = mole-fraction of organic compound of interest in water

T = temperature

T_0 = ambient temperature

This equation indeed can be derived from Equation 2.59, assuming that γ is equal to 1 and that the entropy does not change with temperature in the range studied.

A slight modification of Equation 2.61 is also proposed as an alternative model for solubility of anthraquinones in subcritical water. The model contains an additional term whose parameters were derived from the best fit of experimental results.

$$\ln z_2(T) \approx (T_0/T) \ln z_2(T_0) - 1.624[(T/T_0) - 1]^3 \quad (2.61)$$

Literature review

Recent reports have demonstrated the ability of “subcritical” water (water heated to any temperature up to its critical temperature with enough pressure to maintain its liquid state) to quantitatively remove a variety of polar and non-polar organics from many matrixes. Subcritical water extraction is initially used for the extraction of organic and inorganic metal pollutants such as the extraction of

polycyclic aromatic hydrocarbons (PAHs) from railroad bed soil, urban air particulate matter, petroleum waste sludge; phenols from petroleum waste sludge; alkyl benzenes from industrial soils and petroleum waste sludge; anilines from industrial soil (Hawthorne et al., 1994; Yang et al., 1997); and the extraction of polychlorinated biphenyls (PCBs) from soil and river sediment. (Yang et al., 1995; Hartonen et al., 1997). Because subcritical water extraction is nontoxic and thus it leaves no harmful residue. This technique is now more frequently used for isolation of natural product for the production of fragrances, flavors, and pharmaceuticals. Successful cases have been reported for essential oils from majoram (Jiménez-Carmona et al., 2002), savory and peppermint (Kubátová et al., 2001), and oregano (Ayala, et al., 2001). Other than essential oils, other bioactive compounds have been extracted by this technique. They are hypericin and pseudohypericin from St. John's wort (Mannila et al., 2002), iridoid glycosides from *Veronica lonifolia* (Suomi et al., 2000), kava lactones from kava root (Kubátová et al., 2001), and anthraquinones from roots of *Morinda citrifolia* (Shotipruk et al., 2004). Review of subcritical water extraction of environmental samples and natural product are summarized in Table 2.2 to 2.3. In comparison with conventional method, most study reports the same agreement of this technique as environmental friendly, inexpensive, and short extraction time at the same yields.

Our previous work also demonstrated that the activity of the root extracts from subcritical water extraction gave the highest antioxidant activity compared to that obtained by conventional solvent extraction techniques (Pongnaravane, 2005). In addition, the solubility of anthraquinones in subcritical water was determined at various temperatures and was found to increase with increasing temperature. Nevertheless, the method of quantitative analysis employed in these studies was spectrophotometry, with alizarin as a reference compound. In this work we propose to more accurately measure the amount of the target anti-cancer compound, damnacanthal, using reversed-phase high performance liquid chromatography (RP-HPLC) and to model the subcritical water extraction behavior of this compound.

Table 2.2: Reviews on investigation of subcritical water extraction of pollutants from soil.

<i>Author</i>	<i>Contaminant</i>	<i>Condition</i>	<i>Analysis</i>	<i>Objective</i>
1. Miller et al., 1998	Polycyclic aromatic hydrocarbons (PAHs)	Flow rate 0.1 ml/ min Temperature 25-225°C Pressure 30-60 bar Time 30 min	GC-MS	To screen for PAH and pesticide by SWE in compost.
2. Hawthorne et al., 2000	Polycyclic aromatic hydrocarbons (PAHs)	Flow rate 1 ml/ min Temperature 250, 300°C Pressure 50 bar Time 30,60 min	GC-FID GC-MS	To compare soxhlet extraction, PLE, SFE, and SWE in extraction of PAH from ore.
3. Krieger et al., 2000	Cloransulam-methyl	Flow rate 0.4 to 3.5 ml/ min Temperature 50, 100, 150°C Pressure 65, 135, 500 atm Time 30 min	HPLC	To report the results of SWE of triazolopyrimidine sulfonanilide herbicides from soil.

<i>Author</i>	<i>Contaminant</i>	<i>Condition</i>	<i>Analysis</i>	<i>Objective</i>
4. McGowin et al., 2001	PAHs & pesticide	Flow rate 1 ml/ min Temperature - PAH 110, 150, 250, 350°C - Pesticide 110, 130, 150, 250°C Time 20 min	N/A	To screen for PAH and pesticide by SWE in compost.
5. Dadkhah et al., 2002	PAHs	Flow rate 1 ml/ min Temperature 230, 250, 270°C Pressure 40 bar Time 45, 90 min	N/A	To report the results of small-scale batch extraction of soils polluted with PAHs by using SWE.
6. Kubátová et al., 2002	PAHs	Flow rate 0.25, 1,2 ml/ min Temperature 175°C Pressure 50 bar Time 60-120 min	GC-FID	To investigate the mechanism controlling the extraction rate achieved with subcritical water extraction.

<i>Author</i>	<i>Contaminant</i>	<i>Condition</i>	<i>Analysis</i>	<i>Objective</i>
7. Richter et al., 2003	Pesticides	Flow rate 2 ml/ min Temperature 50 to 300°C Pressure 1200 psi time 25 min	GC-MS	To evaluate efficiency of water at subcritical region to extract from soils a group of typical pesticides used in agriculture.
8. Hashimoto et al., 2004	Dioxins	Flow rate 2 ml/ min Temperature 125, 150, 300, 350°C Pressure 0.2 MPa time 30 min	GC	To understand of behavior of dioxins during SWE and optimize their efficiency.

Table 2.3: Reviews on investigation of subcritical water extraction of natural product.

<i>Author</i>	<i>Plants</i>	<i>Product</i>	<i>Condition</i>	<i>Analysis</i>	<i>Objective</i>
1. Basile et al., 1998	<i>Rosmarinus officinalis</i>	α -Pinene ,Camphor Camphene, Borneol, Limonene, Verbenone, 1, 8-Cineole, Isobornyl acetate	Flow rate 1, 2, 4 ml/ min Temperature 125-175°C Pressure 20 bar Time 200 min	GC-FID	To investigate the active principles extracted from the plant with superheat water.
2. Pawlowski et al., 1998	Agriculture commudities e.g. banana, lemon, etc.	Thiabendazole (TBZ), Carbendazim (MBC)	Flow rate 2-20 ml/ min Temperature 50, 75°C Pressure 50 atm Time 20 min	Ion- Paring HPLC	-To determine the feasibility of using water to extract TBZ and MBC from foods. -To study the experimental parameters which influence the extent of analyte recovery. -To determine the possibility of using pressurized hot water to extract more problematic matrixes such as citrus fruits.

<i>Author</i>	<i>Plants</i>	<i>Product</i>	<i>Condition</i>	<i>Analysis</i>	<i>Objective</i>
3. Clifford et al., 1999	<i>Syzygium aromaticum</i>	Eugenol, Eugenyl acetate, Caryophyllene	Flow rate 2 ml/ min Temperature 150°C Pressure N/A Time 100 min	GC-FID	To compare the extraction of the buds of cloves with supercritical carbon dioxide and superheated water.
4. Jiménez-Carmona et al., 1999	<i>Thymus mastichina</i>	α -Pinene, β -Pinene Linalool, Geraniol	Flow rate 2 ml/ min Temperature 150°C Pressure N/A Time 100 min	GC-FID GC-MS	To develop a rapid, efficient and inexpensive method for the extraction of the sample.
5. Miller et al., 2000	N/A	<i>d</i> -Limonene, Eugenol, Nerol 1,8-Cineolel	Flow rate 0.1 ml/ min Temperature 25 to 200°C Pressure 70 bar	GC-FID	To determine the solubility of liquid hydrophobic organic compound such as flavor and fragrance compound in subcritical water.

<i>Author</i>	<i>Plants</i>	<i>Product</i>	<i>Condition</i>	<i>Analysis</i>	<i>Objective</i>
6. Fernández-Perez et al., 2000	<i>Laurel</i>	1, 8 Cineole1, α -Phellandrene, β -Pinene	Flow rate 2 ml/ min Temperature 150°C Pressure 50 bar Time 30 min	GC	To develop an approach for the static-dynamic subcritical water extraction.
7. Gámiz-Gracia et al., 2000	<i>Foeniculum vulgare</i>	α Pinene, Limonene β Pinene, Comphor β Mircene, Linalyl propanoate	Flow rate 0.5-3.0 ml/ min Temperature 150°C Pressure 50 bar Time 50 min	GC-FID	To develop a method for the continuous subcritical water extraction of medicinal essential oils, and compare the results with those obtained by conventional techniques, in order to introduce this advantageous alternative in the pharmaceutical field.
8 Kubátová et al., 2001	Satureja hortensis and Menthe piperita	Cymene, Thymol , Borneol, Linalool	Flow rate 1 ml/ min Temperature 100, 150,175°C Pressure 65 bar Time 30 min	GC-FID GC-MS	To compare the use of subcritical water at several temperatures to conventional hydrodistillation and SFE for the extraction of flavours from samples.

<i>Author</i>	<i>Plants</i>	<i>Product</i>	<i>Condition</i>	<i>Analysis</i>	<i>Objective</i>
9. Kubátová et al., 2001	<i>Piper</i> <i>methysticum</i>	Dihydrokawain, Kawain, Yangonin	Flow rate 1 ml/ min Temperature 175°C Pressure 60 bar Time 20 min	GC	To compare of kava lactone extraction efficiencies using tradition water extraction and organic solvent extraction, as well as the new technique of subcritical water extraction.
10. Ayala et al., 2001	<i>Lippia</i> <i>graveolens</i>	1, 3-Cyclohexadien, α -Phellandrene, 3-Carene	Flow rate 1-4 ml/ min Temperature 100-175°C Pressure 1.0-5.1 MPa Time 24 min	GC-FID	To develop a method for the continuous SWE of samples and compare the results with those obtain by hydrodistillation.
11. Ollanketo et al., 2002	<i>Salvia</i> <i>officinalis</i>	Rosmarinic acid, Carnosal, Carnosic acid, Methyl carnosate	Flow rate 1 ml/ min Temperature 70, 100, 150°C Pressure 100 kg/cm ² Time 60 min	RP-HPLC	To examine in detail the effectiveness of PHWE for extraction of the sample.

<i>Author</i>	<i>Plants</i>	<i>Product</i>	<i>Condition</i>	<i>Analysis</i>	<i>Objective</i>
12. Eng Shi Ong et al., 2003	<i>Coptidis, Glycyrrhizae and Scutellariae radix</i>	Glycyrrhizin, Baicalein	Flow rate 1 ml/ min Temperature 95-140 °C Pressure 10-20 bar Time 40 min	HPLC	To develop a simple system using PHW for the extraction of thermally labile and reasonably polar components from medicinal plant.
13. Ozel et al., 2003	<i>Thymbra spicata</i>	Carvacrol ,p-Cymene, Thymol, Caryophyllene, E-3-carene-2-ol	Flow rate 2 ml/ min Temperature 100, 125, 150, 175°C Pressure 20, 60, 90 bar Time 40 min	GC, TOF/ MS	-To determine the optimum conditions for the continuous SWE of the sample. -To investigate the effect of temperature on the composition of extracted sample.
14. Shotipruk et al., 2004	<i>Morinda citrifolia</i>	Anthraquinones (Alizarin)	Flow rate 2,4,6 ml/ min Temperature 110, 170,220°C Pressure 70 bar	Spectro photo-metric	To determine the effects of extraction temperature and water flow rate on extraction yield and rate of extraction.

CHAPTER III

MATERIALS AND METHODS

3.1 Materials

3.1.1 Chemicals

Standard damnacanthal was purchased from Merck, Germany. Ethyl alcohol was purchased from Fisher Scientific, UK and dimethyl sulfoxide (DMSO) was purchased from Merck, Germany

3.1.2 Plant material preparation

Figure 3.1 shows the *Morinda citrifolia* used in the experiment. The roots of this plant were harvested, washed, and then oven dried at 50°C for 2 days. The dried sample was then ground to small size using mortar and pestle with liquid nitrogen. The ground samples were oven dried in at 50°C for 1 day, and then stored in a dry place until use (Figure 3.2).



Figure 3.1 *Morinda citrifolia* plant (Experimental).



Figure 3.2 Dried roots and ground roots of *Morinda citrifolia*.

3.2 Methodology

3.2.1 Subcritical water extraction

Subcritical water extraction was performed using an apparatus shown in Figure 3.3. The extraction system consisted of two HPLC pumps (PU 980, JASCO, Japan) used for delivering water and solvent, a degassing instrument (ERC 3215, CE, Japan), an oven (D63450, HARAEUS, Germany), in which the extraction vessel (10 ml, Thar Design, USA) was mounted, a pressure gauge, and a back pressure regulator valve (AKICO, Japan). All connections are made with stainless steel capillaries (1/16 inch inside diameter).

Distilled water was passed through a degassing equipment to remove dissolved oxygen. The degassed water was then delivered, at a constant flow rate with the first HPLC pump, to a 3-m preheating section installed in the oven to heat it to the required temperature, which then passed through the extraction vessel, preloaded with 1 g of ground noni roots. The pressure of the system was adjusted to the desired condition (4 MPa) by using the back-pressure regulator valve at the outlet coil to ensure that water was in liquid state at the temperatures tested. Before heating the extraction system, all connections were checked for possible leakage. The oven was turned on and the temperature was set to the desired operating condition. When the temperature reached the set point, the extraction started. The second pump was then turned on to deliver ethanol at constant flow rate to wash off any residual product in the outlet line behind the extractor. The extract was cooled in a coil immersed in a

water bath to prevent possible product degradation, and was then collected in fractions.

Several extraction experiments were carried out to determine the effect of temperature, pressure, and water flow rates on the product yield and quality. The conditions tested are summarized in Table 3.1. Because anthraquinones in the extract may not be in soluble form in ambient water after it exited the extraction system, ethanol was therefore added to the extract to keep the compound dissolved in the solvent mixture. The flow rate ratio of 1:4 (ethanol:water) was determined to be appropriate as this is the amount of ethanol that was just sufficient to keep the extract soluble.

Table 3.1: Parameter condition in experiment.

Parameter	Condition
Temperature	150, 170, 200 and 220°C
Flow rate	2, 3, 4, and 5 ml/min
Pressure	4 MPa
Approximate roots size	0.37 mm

After each extraction, the amount of anthraquinones remained in the root residue was determined by solvent extraction with ethanol. The root residue was taken out of the extractor and placed into a 125 ml Erlenmeyer flask, containing 30 ml of ethyl alcohol. It was then allowed to release the products into the solvent overnight. The solution was then replaced with 20 ml of fresh ethanol daily until the extract was clear.

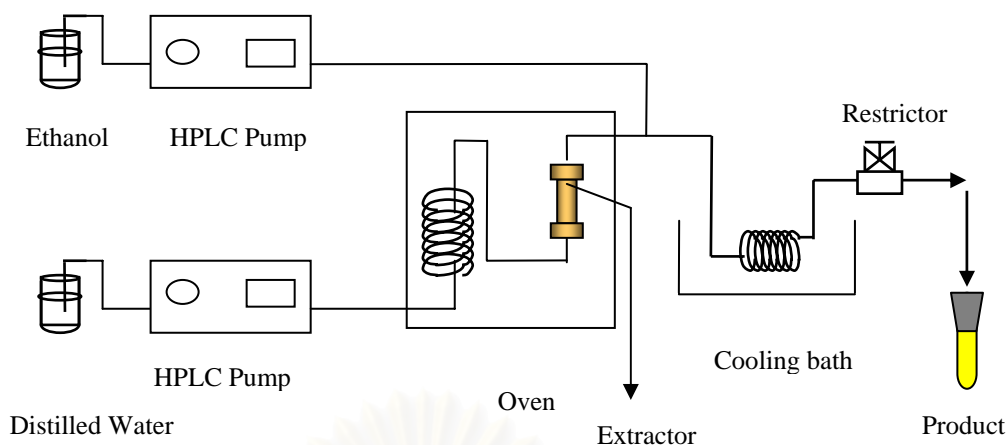


Figure 3.3 Diagram of experimental setup subcritical water extraction.

3.2.2 Sample preparation for RP-HPLC

Subcritical water extracts were evaporated under vacuum to dryness, and re-dissolved in distilled water. This resulted in two parts: solid precipitate and water soluble part which were centrifuged at 3000 rpm for 15 minutes to separate the supernatant from the precipitate. DMSO was added to the precipitate from the previous step, and the mixture was then sonicated for 15 minutes. Both supernatant and precipitate-DMSO fractions contain the active compound of interest. The supernatant and the precipitate-DMSO fraction were filtered through a membrane filter (0.45 μ m, Millipore, USA) before being subjected to HPLC analysis.

3.2.3 Analysis RP-HPLC procedure

The HPLC apparatus consisted of pump (Prostar 240, Varian, USA), equipped with photodiode array detector (Prostar 335, Varian, USA). The analysis was carried out at room temperature on a phenomenex Luna C18, 100 A pore size, 5 μ m particle size, 250mm \times 4.60 mm I.D. column. The mobile phase used was modified from that described by Dabiri et al., 2004, which consisted of a mixture of (70:30) acidic methanol (50 mM TFA)-buffer (50 mM KH_2PO_4 , pH = 3). The flow rate of the mobile phase was 1 ml/min and an injection volume of 50 μ L was used. The UV detection wavelength was 250 nm. Each analysis was carried out at ambient temperature. A standard calibration curve was made from a plot of peak areas versus concentrations for a series of standard solutions in DMSO.

CHAPTER IV

RESULTS AND DISCUSSION

The main purpose of this study is to investigate the extraction of an anticancer anthraquinone compound, damnacanthal, from the roots of *Morinda citrifolia*. In our previous study (Shotipruk et al., 2004), the feasibility of subcritical water extraction (SWE) was demonstrated for extraction of anthraquinones from roots of this plant. This result is qualitatively shown here in Figure 4.1 which shows that SW extract had yellow color of anthraquinones similar to the ethanol extract. In the previous study, the effects of water temperature on the yield and the antioxidant activity of the extract were also determined. The results indicated that SWE has high potential as an interesting alternative to replace organic solvent extraction. However, in such case, the analyte was measured as “total” anthraquinones by a spectrophotometer using alizarin as a reference. Although the spectroscopic method was simple, it did not provide quantitative information regarding the composition and the content of different anthraquinones in the extract. When special interest is placed on a specific constituent such as damnacanthal, a chromatographic analysis is more appropriate. We begin this study by evaluating the appropriate protocol for quantitative analysis of damnacanthal using reverse phase-high performance liquid chromatography (RP-HPLC). When the accurate determination of the compound could be achieved, the study on the effect of extraction temperature and flow rate on extraction efficiency would be determined. The effect of flow rate in particular provides basic understanding of the importance of thermodynamics mass transfer on extraction process which greatly helps the optimization of extraction conditions.

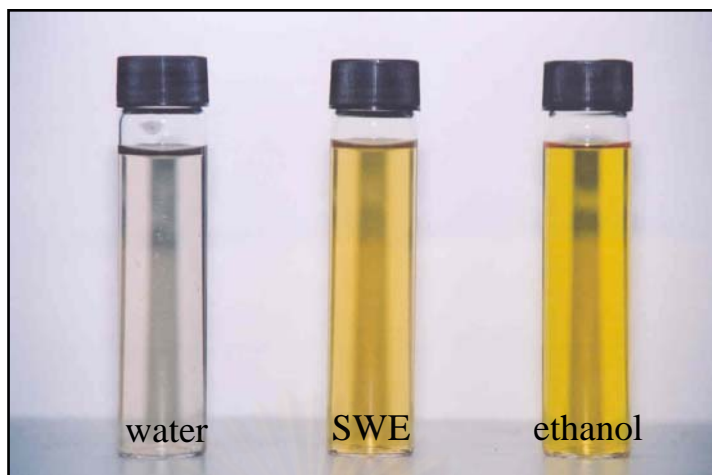


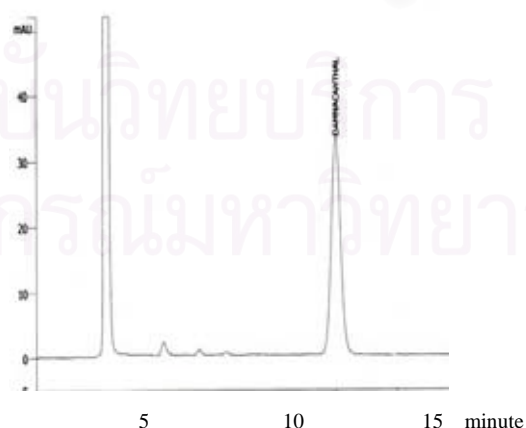
Figure 4.1 Comparison of anthraquinone extracted with water, subcritical water and ethanol.

4.1 Evaluation of RP-HPLC analysis protocols

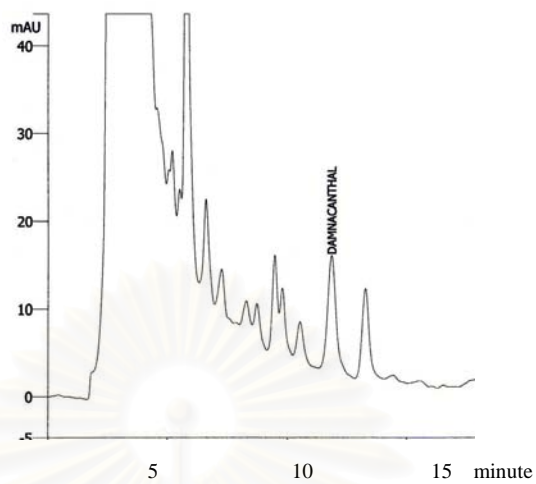
As mentioned, chromatography allows accurate determination of the amount of a compound of interest in plant extracts. It does this by first separating the compound of interest from other components. Typically, chromatography could be achieved either by using normal or reverse-phase chromatography. Normal phase chromatography employs a polar stationary phase, and less polar (usually non-aqueous) chromatographic eluents, such as hexane, heptane or halogenated hydrocarbons. Thus, a non-polar analyte elutes more quickly than polar analyte since they interact less strongly with the highly polar surface of the adsorbent particles. On the other hand reverse-phase chromatography uses a non-polar stationary phase, and more polar eluents. Thus, the more polar analyte elutes more quickly than a less polar analyte.

In this study RP-HPLC was chosen as a means to quantitatively determine the amount of damnacanthal target compound. However, the concentration of the compound of interest in the water extract is typically lower than the detection limit of the apparatus. Thus, a few steps are required to concentrate and to purify the extract prior to proper HPLC analysis. Concentration of the extract could be achieved by evaporating off water under vacuum to dryness, after which water at ambient

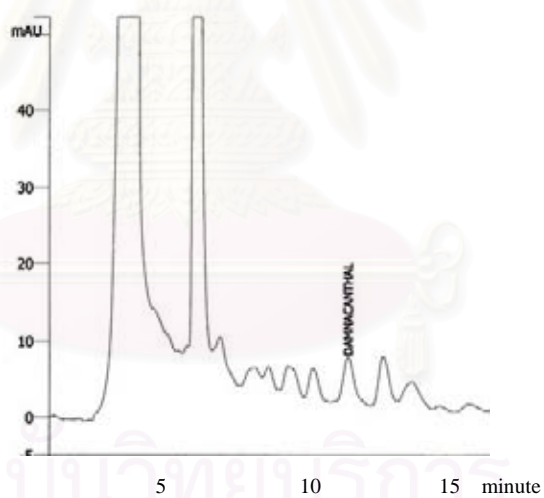
temperature was then added to re-dissolve the extract. In this step, two fractions were obtained, the aqueous solution, and the water insoluble precipitate, which were separated by centrifugation at 3000 rpm for 15 minutes. The water soluble part could be directly analyzed by HPLC while the water insoluble part must be re-dissolved in DMSO before an injection. As can be seen from the chromatograms in Figure 4.2, both the water and DMSO fractions contained damnacanthal, and the sum of the amounts of damnacanthal in the two fractions accounted for the total amount in the extract. The fact that damnacanthal are found in both fractions means that damnacanthal is soluble to a certain degree in water at ambient condition and in DMSO. It was indeed reported that damnacanthal is slightly soluble in water and very soluble in DMSO. Thus it seems at first that the dried extract could be re-dissolved only in DMSO in one step prior to RP-HPLC injection. However, the preliminary analysis showed that dissolving the dried extract with DMSO alone resulted in the sample that contained a large quantity of impurities, and thus resulted in unresolved HPLC peaks. Re-dissolving the dried extract first in water and then in DMSO, was proven to be necessary as water initially helped remove highly polar impurities which were eluted early as can be seen in Figure 4.2b) and 4.2c). Although the purification steps could be further improved so that damnacanthal is contained only in a single fraction, the method currently proposed could reasonably be used to quantify the amount of the compound extracted.



a)



b)



c)

Figure 4.2 HPLC chromatogram of damnacanthal (retention time, $t_R = 12.44$ min) in a) standard, b)-c) noni roots extracts obtained from subcritical water extraction (b = supernatant, c = precipitate dissolve into the DMSO).

4.2 Effect of subcritical water temperature

In subcritical water extraction (SWE), temperature is considered a key variable affecting the extraction process. In this study, the effect of SW temperature on the extraction yield was determined for the temperature range between 150 and 220°C and at the water flow rate of 5 ml/min. At 150°C, 0.659 mg of damnacanthol per g of dried roots was extracted and the amount extracted increased to 0.722 mg per g of dried roots when the temperature increased to 170°C (Figure 4.3). As described earlier, the increase in temperature decreases water polarity as a result of reduced polar forces and hydrogen bonding between water molecules, making it more suitable for extraction of organic compounds. Moreover, at elevated temperature, the water density and viscosity decrease, resulting in increased mass transfer of the solvent into the matrix of plant sample. However, at 200 and 220°C, the yields were only 0.227 and 0.197 mg per g of dried roots, which were 69 % and 73% lower than the yield at 170°C. Analysis of the sample residue showed that negligible amount of damnacanthol remained. This suggested that degradation of the product occurred during extraction at such high temperatures. This finding differed from that obtained from the previous study which showed the highest amount of total anthraquinones was extracted at the highest temperature of 220°C (Shotipruk et al., 2004). The result in this study demonstrated that the temperature has different effects on degradation of different though related compounds.

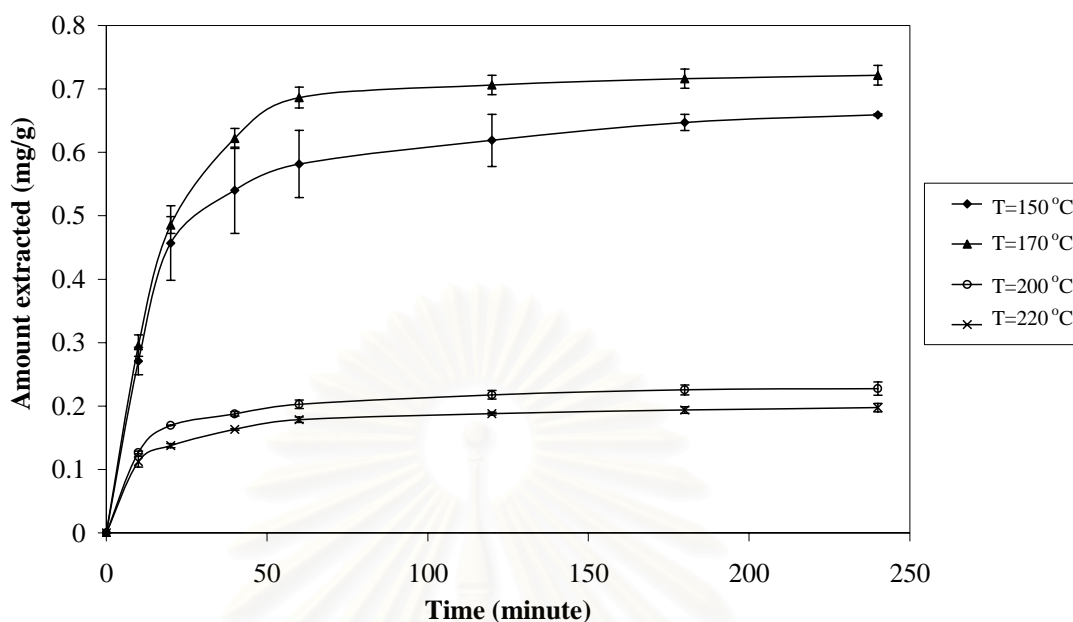


Figure 4.3 Effect of water temperature on yield of damnacanthal (Flow rate 5 ml/min at pressure of 4 MPa).

4.3 Effect of flow rate

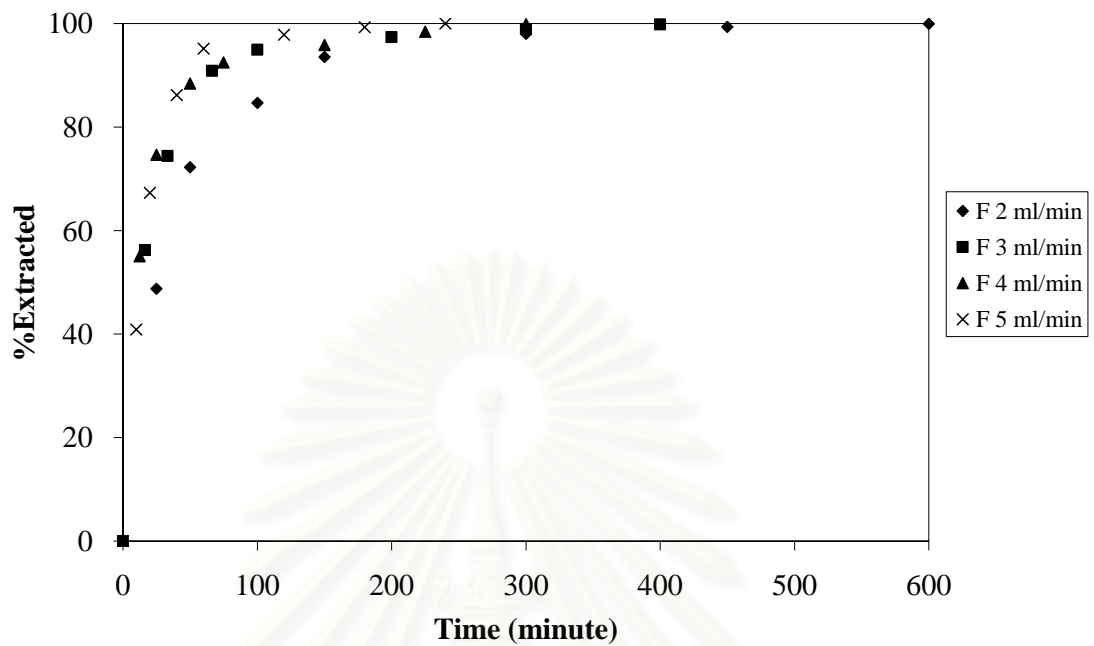
In general, the extraction of any compound from a solid matrix requires two steps. First, the compound must be desorbed from its original binding site in (or on) the sample matrix (generally modeled by rate process such as diffusion), then compound must be eluted from the sample in a manner analogous to frontal elution chromatography.

In systems where the extraction fluid is saturated, such as the extraction of fat or oil from oil seeds, simple saturation solubility calculations can be used to predict extraction rate. However, in systems where the bulk solubility of the analyte is sufficiently large, either kinetic desorption or elution step, or a combination of both steps may limit extraction rates. It can be difficult to determine the relative importance thermodynamic and mass transfer only by observing the shape of the extraction curve, since it is possible for kinetic desorption (or known as internal diffusion) or thermodynamic partitioning models to give good agreement with the

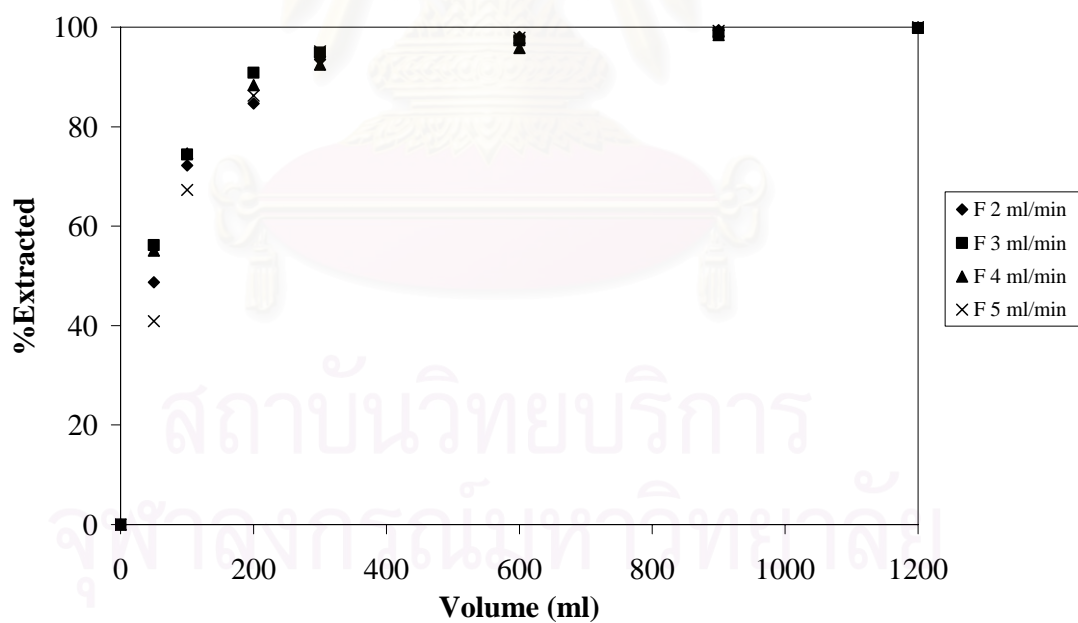
experimental data. However, observing the effect of extraction fluid flow rate on the extraction rates can be a simple approach to determine the relative importance of these steps. For example, if the rate of extraction is controlled by kinetic desorption, the increase in bulk fluid flow rate would have little effect on extraction rate. On the other hand, if the extraction rate is controlled by thermodynamic partitioning or external mass transfer diffusion, increasing the bulk fluid flow rate would increase the extraction rate. In extraction in which thermodynamic partitioning is controlling, the curves of extraction efficiency versus the volume of water passed for all flow rates would overlap.

In this study, the experimental extraction curves were obtained for the flow rate of 2, 3, 4, and 5 ml/min and for the temperatures of 170°C at the fixed pressure of 4 MPa. The results were plotted in Figure 4.4a), which shows that the rate of damnacanthol extracted increases when the volumetric flow rate increased from 2 to 3 ml/min and the difference in the rate of extraction is more apparent up to 200 minutes. After this, the effect was small possibly due to the depletion of the solute from the plant matrix. When the flow rate increases from 3 to 4 and 5 ml/min, there was little effect of flow rate on the extraction efficiency per unit time. The dependence of extraction efficiency on volumetric flow rate indicated that extraction could be controlled either by equilibrium partitioning or by external mass transfer, or the combination of the two. When the extraction yield was plotted against volume of water however, the data for all flow rates lied almost on the same curve. It seemed therefore that the extraction could be controlled by partitioning of the solute between the solid matrix and liquid water, particularly at the lower flow rates. At low flow rates, the contact time between the solvent and the plant materials is high enough for the system to reach partition equilibrium. In such case, the amount of the compound extracted would be directly proportional to the amount of water passed. Nevertheless, the experimental data shows that at high flow rates where there might not be enough contact time, extraction rate did not increase with increasing flow rate, in which case, extraction could be limited by intra-particle diffusion. This result demonstrates that extraction could be controlled by a combination of different processes, and that the mechanism controlling extraction behavior may change depending on the extraction flow rate conditions. A more quantitative account was given in the following section,

in which the data were fitted with the partition and the diffusion model to determine the mechanism of extraction behavior.



a)



b)

Figure 4.4 a) Percent extracted versus extraction time, b) Percent extracted versus volume of water (at temperature 170°C and pressure 4 MPa).

4.4 Modeling of extraction behavior

As mentioned, it is obvious that thermodynamic partitioning and mass transfer are key factors affecting extraction processes and both must be favorable to obtain faster extraction. To understand the relative importance of thermodynamic partitioning, external mass transfer, and kinetic desorption, the simple thermodynamic partitioning, kinetic desorption, and external mass diffusion models are employed to describe the data.

4.4.1 Partitioning coefficient (K_D) model

This model describes the extraction process in which the kinetics of the initial desorption step and the subsequent fluid-matrix partitioning is rapid, and thus do not significantly affect the extraction rate. If it is also assumed that the matrix has a uniform size, essentially, the mass of analyte in each unit mass of extraction fluid and the mass of analyte remaining in the matrix at that period in the extraction time can be calculated for the entire extraction time based on the K_D value determined for a plant compound of interest. In this case, the shape of an extraction curve would be defined by:

$$\frac{S_b}{S_0} = \frac{\left(1 - \frac{S_a}{S_0}\right)}{\left(\frac{K_D m}{(V_b - V_a)\rho} + 1\right)} + \frac{S_a}{S_0} \quad (4.1)$$

where S_a = cumulate mass of the analyte extracted after volume V_a (mg/g)

S_b = cumulate mass of the analyte extracted after volume V_b (mg/g)

S_0 = initial total mass of analyte in the matrix (mg/g)

$\frac{S_a}{S_0}$ = cumulative fractions of the analyte extracted by the extraction fluid

of the volume V_a

- $\frac{S_b}{S_0}$ = cumulative fractions of the analyte extracted by the extraction fluid
of the volume V_b
 K_D = thermodynamic partitioning coefficient
 ρ = density of extraction fluid at given conditions (mg/ml)
 m = mass of the extracted sample (mg).

The above model could be used to predict the effect of different values of the thermodynamic partitioning coefficient (K_D) on extraction rates (with flow rate of 5 ml /min) (shown in Figure 4.5). As expected, a higher K_D (stronger competition of matrix versus the fluid for the solute) yields slower extraction rates. In addition, it is reiterated here that K_D model does not include extraction time, but only relies on the volume of extractant fluid used (assuming a constant sample size). Doubling the extraction fluid flow rate should double the extraction volume passed for the same unit time, thus doubling the rate of extraction. The effect of flow rate on extraction curves for the representative $K_D = 50$ and $K_D = 1000$ are shown in Figure 4.6. It is important to note that the x-axis values are in units of time (not volume). If the same data were plotted in terms of volume, the theoretical curves from all flow rates would overlap completely, as is required by the K_D model since no time parameter is included in the calculations.

The model Equation 4.1 and the experimental data from all flow rate plots were used to determine the K_D value by minimizing the errors between the measured data and the K_D model using Microsoft EXCEL solver. The K_D values determined for different flow rates are summarized in Table 4.1 The calculated K_D values determined at 2 ml /min ($K_D = 55.60$), was used to calculate the model curves for all the other flow rates, which as shown in the Figure 4.7, the K_D model agreed reasonably with the experimental data. Nevertheless, if the extraction is strictly controlled by partitioning equilibrium, K_D values for all flow rates must be equal. This was not the case and the reason could be that some of the assumptions made were not valid. For instance, the assumption of rapid liquid-solid partitioning might need to be adjusted to include external film transfer resistance. This model will be discussed again in the section that follows.

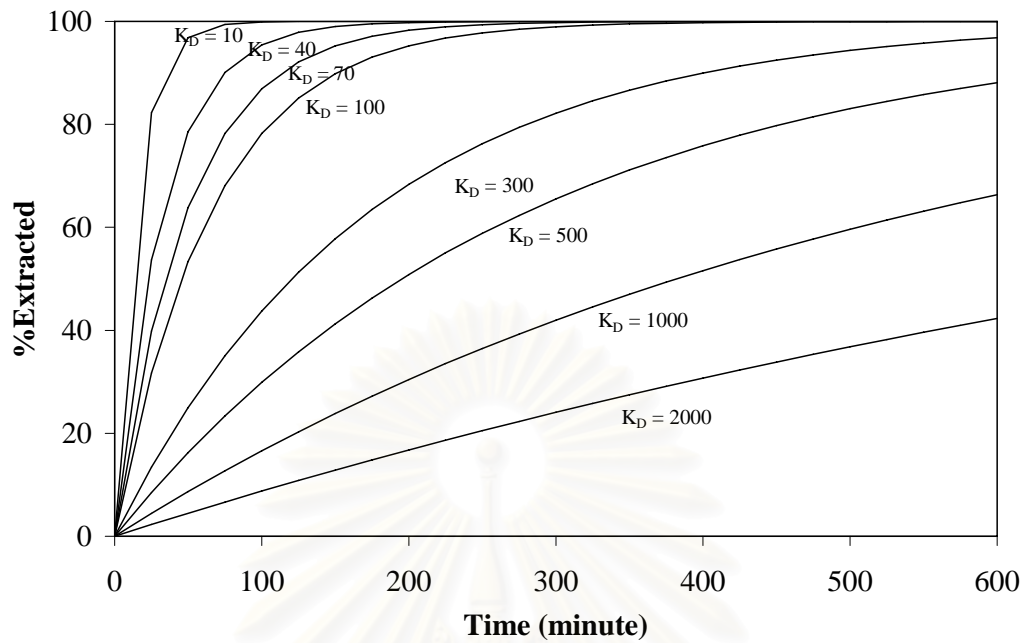
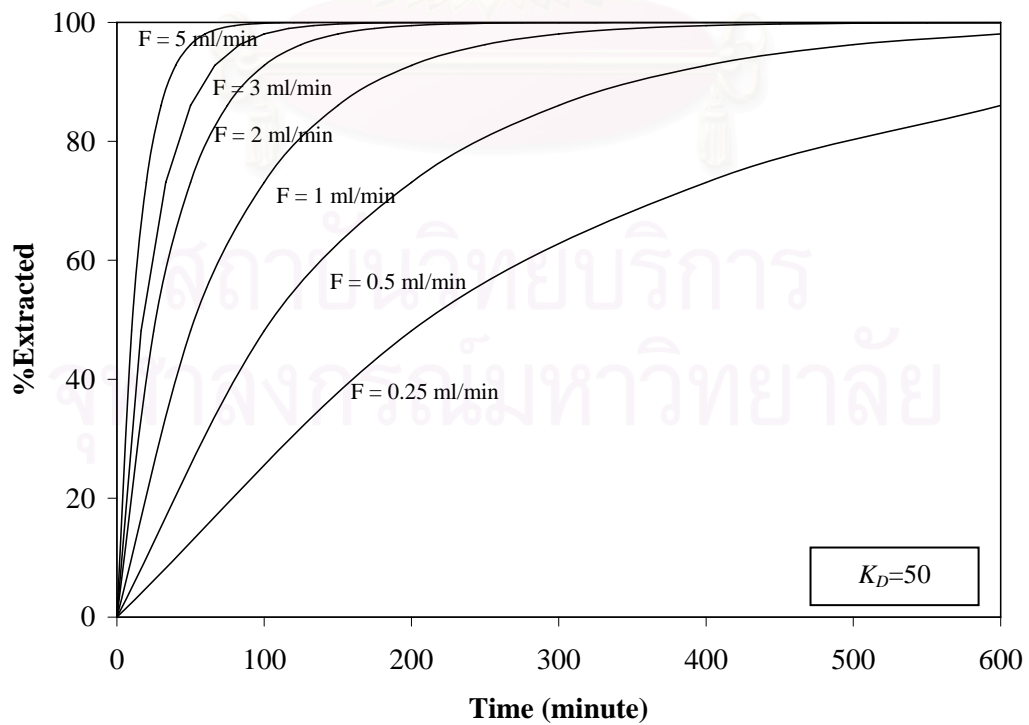


Figure 4.5 Theoretical curve calculate for extractions controlled by thermodynamic partitioning as a flow of 2 ml/min.



a)

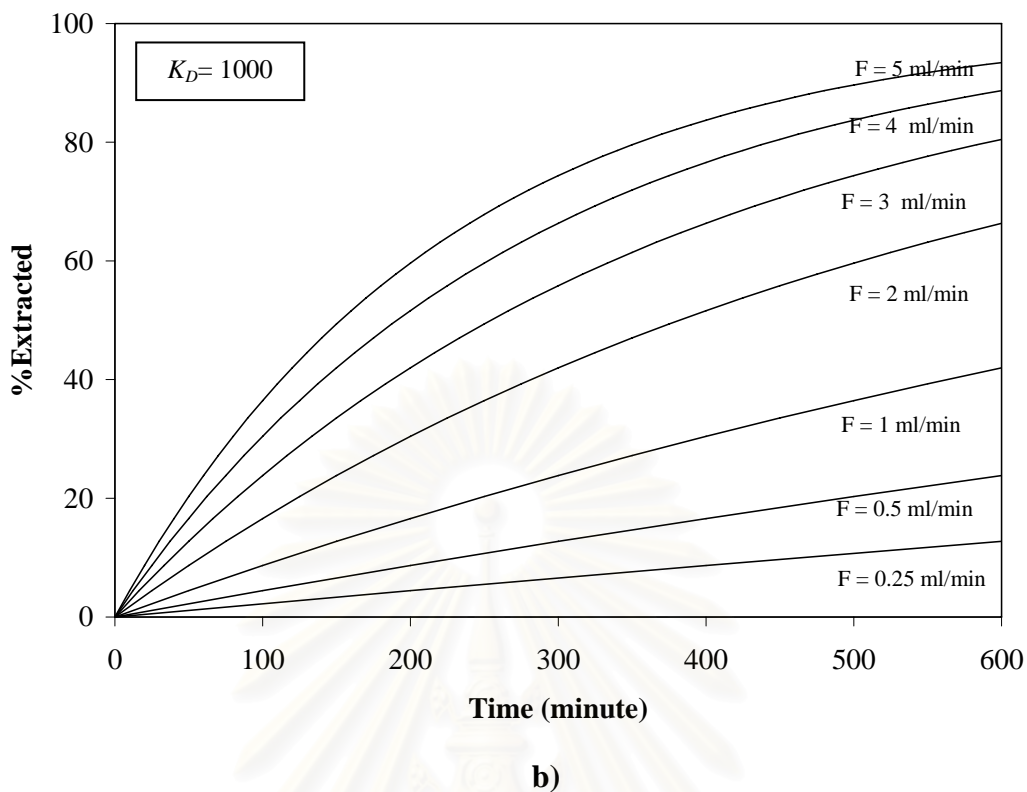


Figure 4.6 Theoretical extraction curves for K_D values of a) 50 and b) 1000 for extractions controlled by thermodynamic partitioning.

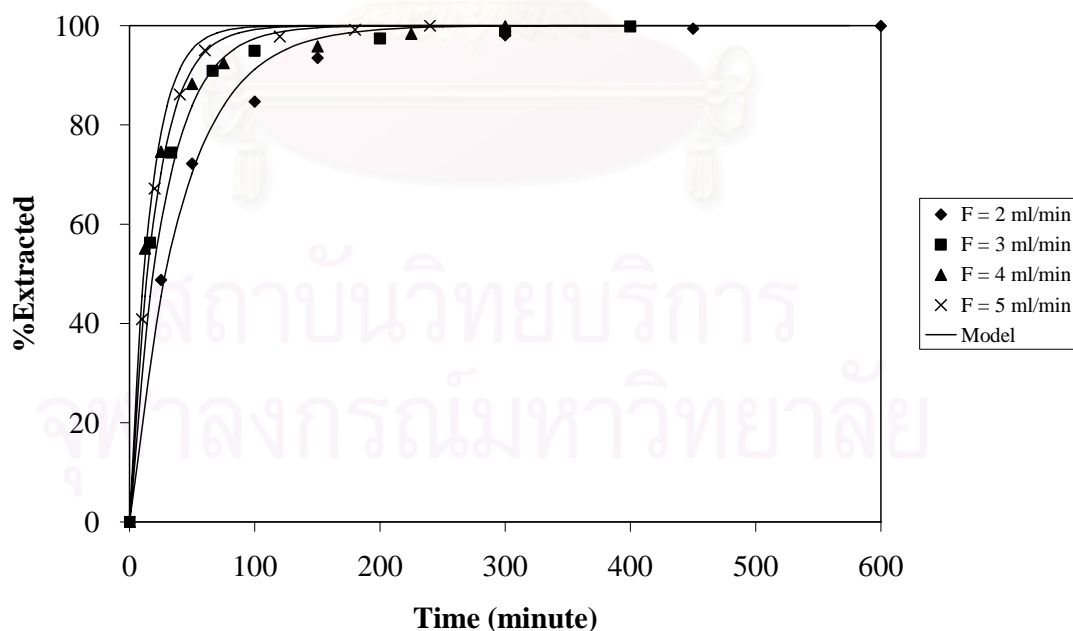


Figure 4.7 Comparison of the K_D model fit with experimental data for subcritical water extraction of damnacanthol at various of flow rate (Symbols represent the experimental data and the lines are calculate based on the $K_D = 55.60$).

Table 4.1: K_D values of partitioning coefficient model for different flow rate.

Parameter	Flow rate (ml/min)			
	2	3	4	5
K_D	55.60	43.27	45.68	66.46

4.4.2 One-site kinetic desorption model

In the last section, extraction data were fitted with a thermodynamic model in which equilibrium partitioning controlled the extraction. In this and the next section, kinetic models such as one-site and two-site models were considered, in which extractions were controlled by intra-particle diffusion. This occurs when the flow of fluid is fast enough for the concentration of a particular solute to be well below its solubility limit. The one-site kinetic model was derived based on the analogy with hot ball heat transfer model and with the assumptions that the compound was initially uniformly distributed within the matrix and that, as soon as extraction begins, the concentration of compound at the matrix surfaces is zero (corresponding to no solubility limitation). For spherical matrix of uniform size, the solution for the ratio of the mass, S_r , of the compound that remains in the matrix sphere after extraction for time, t , to that of the initial mass of extractable compound, S_0 are given as (Carslaw et al., 1959, Appendix D):

$$S_r / S_0 = \frac{6}{\pi^2} \sum_{n=1}^{\infty} \frac{1}{n^2} \exp(-D_e n^2 \pi^2 t / r^2) \quad (4.2)$$

where n = an integer

D_e = effective diffusion coefficient of the compound in the material of the sphere (m^2/s)

Equation 4.2 above may be simplified using a quantity t_c defined as:

$$t_c = r^2 / \pi^2 D_e \quad (4.3)$$

where t_c = a characteristic time for the extraction (min)

As shown in Chapter 2, the curve for the above solution tends to become linear at longer times (generally after $t > 0.5t_c$), and $\ln(S_r/S_0)$ is given approximately by

$$\ln(S_r/S_0) = -0.4977 - t/t_c \quad (4.4)$$

In general, the value of the y-intercept is thought to depend on the particle shape and size distribution (for the former in particular the surface to volume ratio) and also the distribution of solute within the matrix particles (i.e. whether the solute is primarily located near the surface or in the interior of the particle).

A plot of $\ln(S_r/S_0)$ versus time of experimental data for the flow rate of 2 and 4ml/min was shown in Figure 4.8. As expected, shape of the curves are similar to the theoretical hot ball model, and the linearity was observed towards the longer time limit. The physical explanation of the form of the curve is that the initial portion is extraction, principally out of the outer parts of the sphere, which establishes a smooth concentration profile across each particle, peaking at the center and falling to zero at the surface. When this has happened, the extraction becomes an exponential decay. It should be noted that the experimental curve differs from the theoretical curve in two respects. Firstly, the curves are close to a straight line after 120 minutes and 65 minutes for the flow of 2 ml/min and 4 ml/min. This is later than that predicted by the theory which should be equivalent to $0.5t_c$ (63.30 and 46.30 minutes, respectively for the corresponding flow rates). Secondly, the intercept was lower than -0.4977. The values of t_c and I obtained by experiment were -1.57 and -1.66 for the flow rate of 2 and 4 ml/min, respectively. Westwood et al.,1959 reported that the I values of approximately 2 are common and the occurrence of an intercept below that of the theoretical value indicates either non-uniform distribution of extractable compound or irregular particle shape.

An alternative form of Equation 4.4 can be written for the ratio of mass of analyte removed after time t to initial mass S_0 as given by:

$$\frac{S_t}{S_0} = 1 - e^{-kt} \quad (4.5)$$

where S_t = mass of the analyte removed by the extraction fluid after time t (mg/g)

S_0 = total initial mass of analyte in the matrix (mg/g)

$\frac{S_t}{S_0}$ = fraction of the analyte extracted after time t

k = a first order rate constant describing the extraction

Note that the kinetic desorption model includes no factor describing extraction flow rate, but relies solely on time. Therefore, doubling the extractant flow rate should have little effect on the extraction efficiency per unit time if the extraction efficiency is controlled by the kinetics of the initial desorption step (assuming the other extraction parameters remain constant).

Microsoft EXCEL solver was used to determine the desorption rate constant, k , from the data for all flow rates. The values are shown in Table 4.2 and the plot of the calculated and experimental percent extract of damnacanthal, $S_t/S_0 \times 100$ (%) versus time are shown in Figure 4.9. As mentioned, the kinetic desorption model does not include a factor describing extraction flow rate, k should be the same value for all flow rates if the model is said to fit the experimental data. However, this is not the case (Table 4.2). The kinetic desorption rate increased for the flow rates of 2 to 3 and 4 ml/min. Nevertheless, the rate constant for higher flow rates of 4 and 5 are comparable. This indicated that the kinetic desorption model better describes the data at high flow rates rather than at low flow rates.

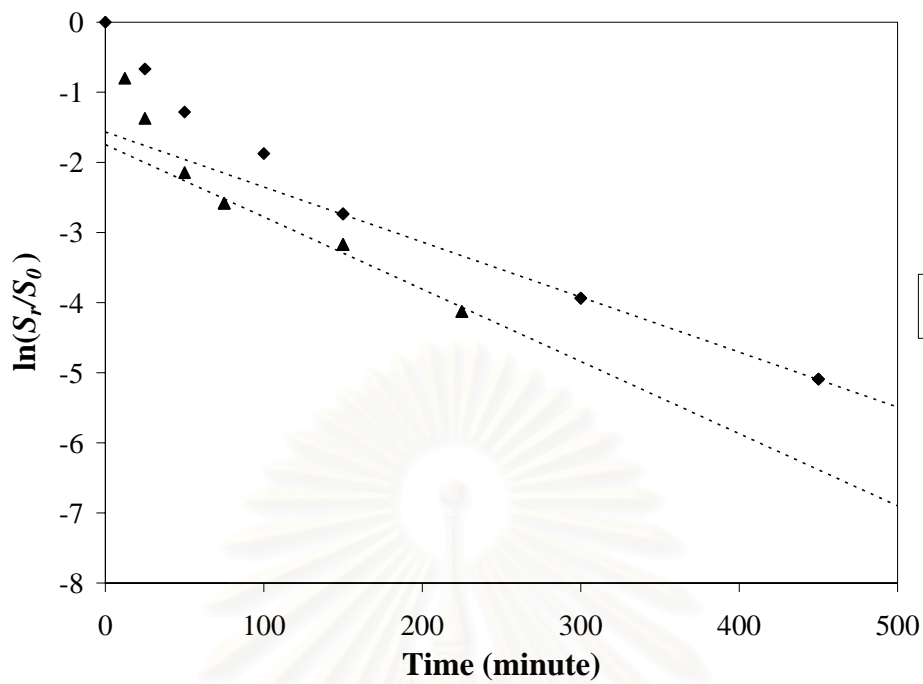


Figure 4.8 Damnacanthal extract with subcritical curve for the hot ball model at flow rate.

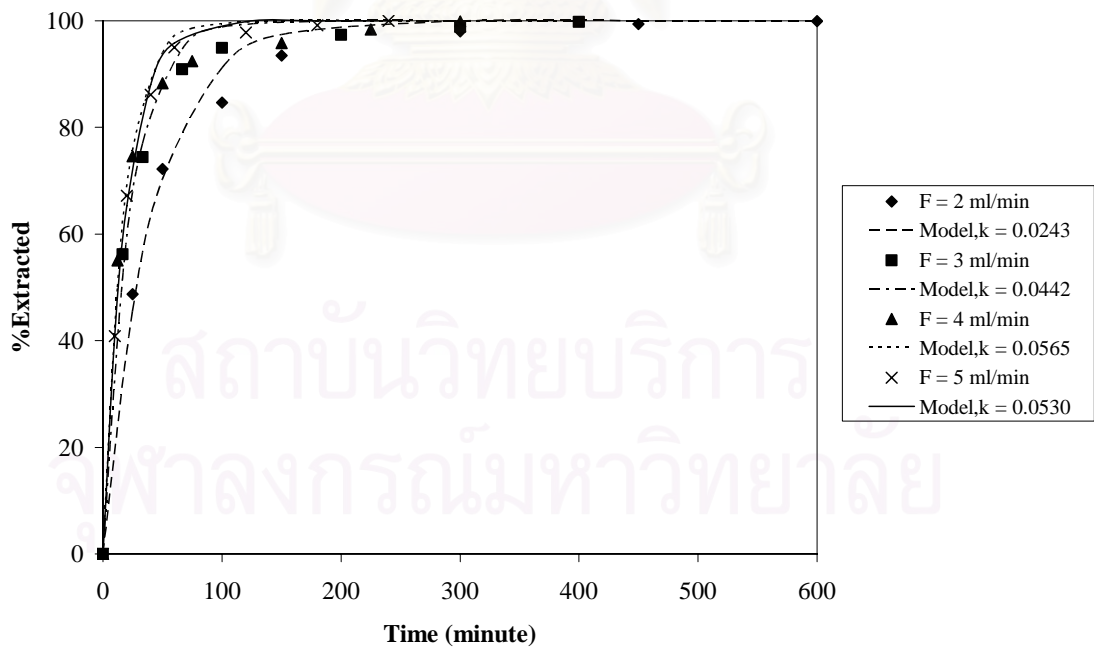


Figure 4.9 One-site kinetic desorption model fit of subcritical water extraction data (Symbols represent the experimental data, and the lines are based on curve fitting the experimental data).

Table 4.2: k values for one-site kinetic desorption model for different flow rate.

Parameter	Flow rate (ml/min)			
	2	3	4	5
k	0.0243	0.0442	0.0565	0.0530

4.4.3 Two-site kinetic desorption model

One site kinetic desorption model assumes initial uniform distribution of solute. A modification of this model describes extraction which occurs from the “fast” and “slow” part, and this model is called a two-site kinetic desorption model which was tested by curve fitting with the experimental data. In particular, this model requires two steps to define an extraction curve, i.e. a certain fraction (F) of the analyte desorbs at a fast rate defined by k_1 , and the remaining fraction ($1-F$) desorbs by a slower rate defined by k_2 . The simple two-site kinetic desorption model consists of two first order extractions described by the following equation:

$$\frac{S_t}{S_0} = 1 - [F e^{-k_1 t}] - [(1-F) e^{-k_2 t}] \quad (4.6)$$

where S_t = mass of the analyte removed by the extraction fluid after time t (mg/g)

S_0 = total initial mass of analyte in the matrix (mg/g)

$\frac{S_t}{S_0}$ = fraction of the analyte extracted after time t

F = fraction of the analyte released quickly

$1-F$ = fraction of the analyte released slowly

k_1 = first-order rate constant describing the quickly released fraction (min^{-1})

k_2 = first-order rate constant describing the slowly released fraction (min^{-1})

As in the one-site kinetic desorption model, doubling the extractant flow-rate should have little effect on the extraction efficiency per unit time if the extraction efficiency is controlled by the kinetics of the initial desorption step (assuming the other extraction parameters remain constant). The values of k_1 and k_2 were determined by fitting experimental data with the two-site kinetic desorption models by minimizing the errors between the data and the model results, using the value of 0.76 for F . Note that the value of F of 0.76 used was the average of the F values determined from the data obtained at different flow rates found using EXCEL solver. The k_1 and k_2 values for all flow rates are shown in Table 4.3. The results demonstrated that the extraction rates are not completely independent of flow rate particularly at lower flow rates. The comparison of the experimental data to various models described thus far led us to examine another model that describe the extraction whose rate is controlled by both thermodynamic partitioning and external mass transfer diffusion.

Table 4.3: k_1 and k_2 values for two-site kinetic desorption model for different flow rate ($F = 0.76$).

Parameter	Flow rate (ml/min)			
	2	3	4	5
k_1	0.0357	0.065	0.090	0.064
k_2	0.0078	0.0144	0.0143	0.029

4.4.4 External mass transfer model

This model describes extraction which is controlled by external mass transfer whose rate is described by resistance type model of the following form:

$$\frac{\partial c_s}{\partial t} = -k_e a_p [(c_s / K_D) - c] \quad (4.7)$$

where k_e is external mass transfer coefficient and a_p is specific surface area of particles. If the concentration of the solute in the bulk fluid is assumed small and the solute concentration in the liquid at the surface of solid matrix is described by partitioning equilibrium K_D , the solution of Equation 4.7 for the solute concentration in the solid matrix, c_s , becomes (see Appendix D for detailed derivation):

$$c_s = c_0 \exp(-k_e a_p t / K_D) \quad (4.8)$$

From this equation, the amount of solute extracted can be written as:

$$S_t = 1 - S_0 \exp(-k_e a_p t / K_D) \quad (4.9)$$

Because a_p is difficult to be measured accurately, a_p and k_e are usually determined together as $k_e a_p$, which is called overall volumetric mass transfer coefficient. The factors that influence the value of $k_e a_p$ include the velocity, u , of solvent through the extractor and the size and shape of plant sample.

The values for the model parameters, K_D and $k_e a_p$ determined by Microsoft EXCEL solver from experimental data obtained at 170°C are summarized in Table 4.4 for different flow rate (W). Linear regression of the plot between $\ln(k_e a_p)$ and $\ln W$ (Figure 4.10) gives the following correlation for $k_e a_p$ and W :

$$k_e a_p = 0.90W^{0.8995} \quad (4.10)$$

If the flow rate of water, W , is substituted by the superficial velocity of water, u , through extractor Equation 4.10 is replaced by

$$k_e a_p = 1.30 \times 10^{-4} u^{0.8995} \quad (4.11)$$

Figure 4.11 shows the experimental extraction efficiency of damnacanthal versus time, compared with the model prediction which suggested that predicted value agree reasonably with experimental data.

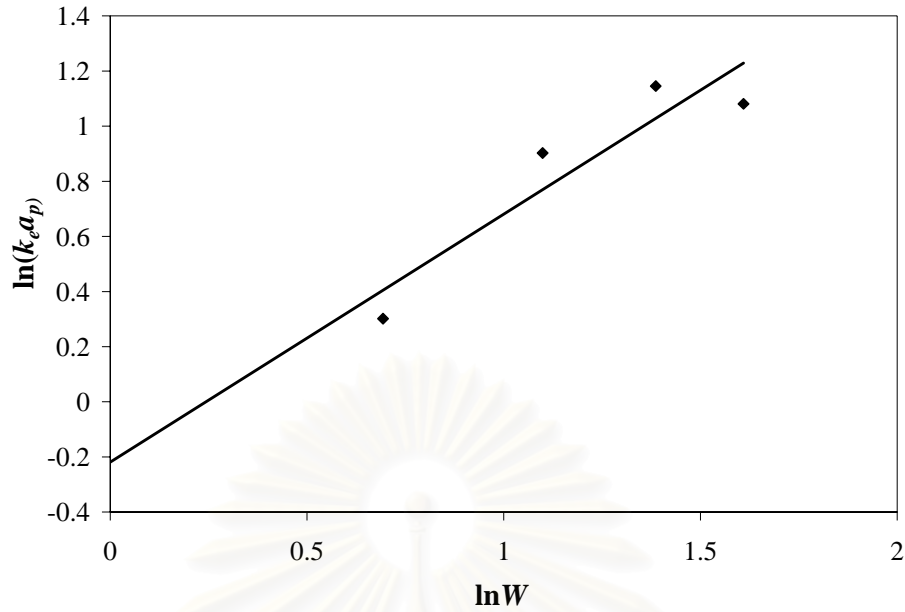


Figure 4.10 Volumetric mass transfer coefficient ($k_e a_p$) versus flow rate (W).

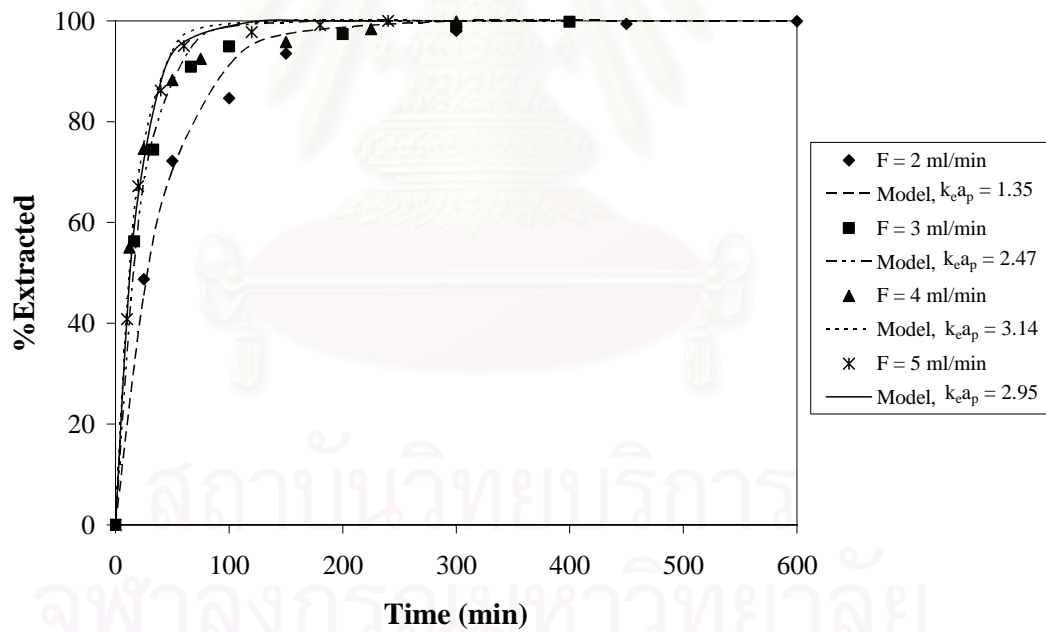


Figure 4.11 External mass transfer model fit of subcritical water extraction data (Symbols represent the experimental data, and the lines are based on curve fitting the experimental data).

Table 4.4: Parameters K_D and $k_e a_p$ for external mass transfer model.

Flow rate (ml/min)	Velocity (m/s)	Parameter	
		K_D	$k_e a_p$ (s^{-1})
2	1.08×10^{-4}	55.70	1.35
3	1.62×10^{-4}	55.83	2.47
4	2.16×10^{-4}	55.61	3.14
5	2.70×10^{-4}	55.65	2.95

4.5 Comparison of extraction models

To more quantitatively compare the extraction models, the mean percentage errors between the experimental data and the models were considered. For the K_D model, the value of K_D calculated from fitting the data at the flow rate of 2 ml/min was used to calculate model curves for the other flow rates. For the kinetic desorption model on the other hand, because the model more accurately describe the data at higher flow rates, the value of k 's determined from the data for the flow rate of 5 ml/min were used to represent the kinetic desorption models.

Based on the result in Table 4.5, K_D was quite suitable overall for the description of extraction at different flow rates tested. On the other hand, one-site and two-site kinetic desorption models describe the extraction data reasonably well at higher flow rates. Of all the models considered, the combined partitioning and external film transfer appeared to best fit the experimental data. The K_D were relatively equal and the dependence of mass transfer coefficient on flow velocity were resulted.

Table 4.5: Mean percent absolute errors between experimental data and extraction model results.

Model	Parameter model	%Mean absolute errors at difference flow rate (ml/min)			
		2	3	4	5
Partitioning coefficient model	K_D	2.27	2.69	3.44	2.26
One site kinetic desorption model	k	8.66	3.11	3.07	0.95
Two site kinetic desorption model	k_1, k_2	8.57	3.12	2.49	0.83
External mass transfer model	$K_D, k_e a_p$	2.27	2.35	2.97	0.95

CHAPTER V

CONCLUSIONS AND RECOMMENDATIONS

5.1 Conclusions

1. Subcritical water provides a promising alternative for extraction of the anti-cancer damnacanthal from roots of *Morinda citrifolia*.
2. The results of HPLC chromatogram show that both fractions (water soluble and precipitate dissolved into DMSO fraction) contained damnacanthal.
3. The solubility of damnacanthal in subcritical water increased when the temperature increased due to the decrease in water polarity.
4. The amount of damnacanthal in the extract increased as temperature increased up to 170°C.
5. At higher temperature than 170°C, the decomposition of damnacanthal occurred.
6. In this study, the most suitable condition for subcritical water extraction of damnacanthal was at the temperature of 170°C and the flow rate of 3-5 ml/min.
7. Overall, a mathematical model based on the combination of partition coefficient (K_D) and external mass transfer gave a good description of damnacanthal extraction by subcritical water, while the kinetic model described the extraction reasonably at higher flow rates.

5.2 Recommendations

1. Other factors affecting extraction efficiency such as particle sizes, solvent to sample ratio, and sample moisture content should be considered the further work.
2. It would be interesting to determine the degradation information regarding the mathematical model of damnacanthal in subcritical water as it is one of the factors that determine the success of the extraction process.
3. Development of standard procedure should be established for the purification of the compound, damnacanthal, for the subcritical water extracts of *Morinda citrifolia* roots.
4. The damnacanthal extracted with subcritical water was found to precipitate after a period of time when it was allowed to cool in the atmospheric condition. This precipitate is of particular interest for the future study and the detailed study would suggest the possibility of purifying the sample.
5. Other purification process which includes, for example, column chromatography using subcritical water as an eluent or the mobile phase, should be further studied.

REFERENCES

- Akgun, M., Akgun, N.A., and Dincer, S. Extraction and modeling of lavender flower essential using supercritical carbon dioxide. Industrial and Engineering Chemistry Research 39 (2000): 473-477.
- Asahina, A.Y., Ebesu, J.S., Ichinotsubo, D., Tongson, J., and Hokoma, Y. Effect of okadaic acid (OA) and noni fruit extraction in the synthesis of tumor necrosis factor- α (TNF- α) by peripheral blood mononuclear (PBN) cells *in vitro*. In Proceedings International Symposium of Ciguatera and Marine Natural Products (1994): 197-205.
- Ayala, R.S., and Luque de Castro, M.D. Continuous subcritical water extraction as a useful tool for isolation of edible essential oils. Food Chemistry 75 (2001): 109–113.
- Biomol Research Laboratory Inc. [Online] Available from <http://www.biomol.com>. [2005, August 30]
- Basile, A., Jiménez-Carmona, M.M., and Clifford, A.A. Extraction of rosemary by superheated water. Journal of Agricultural and Food Chemistry 46 (1998): 5205-5209.
- Carlslaw, H.S., and Jaeger, J.C. Conduction of heat in solids. 1st ed. Oxford: Clarendon, 1959
- Clifford, A.A., Basile, A., and Al Saidi, S.H.R. A comparison of the extraction of clove buds with supercritical carbon dioxide and superheated water. Journal of Analytical Chemistry 364 (1999): 635-637.
- Clifford, A.A., and Hawthorne, A.B. Processes in subcritical water. In Proceedings of Super Green 2002 (2002)
- Crank, J. The mathematics of diffusion. 1st ed. Oxford: Clarendon, 1975
- Critical Process Ltd. [Online] Available from <http://www.criticalprocesses.com/> SHW more.html. [2005, August 30]
- Dadkhah, A.A., and Akgerman, A. Hot water extraction with in situ wet oxidation: PAHs removal from soil. Journal of Hazardous Materials B. 93 (2002): 307–320.

- Dabiri, M., Salimi, S., Ghassempour, A., Rassouli, A., and Talebi, A. Optimization of microwave-assisted extraction for alizarin and purpurin in Rubiaceae plants and its comparison with conventional extraction methods. Journal of Separation Science 28 (2005): 387-396.
- Epstein, M., and Yariv, S. Visible-spectroscopy study of the adsorption of alizarinate by Al-montmorillonite in aqueous suspensions and in solid state. Journal of Colloid and Interface Science 263 (2003): 377–385.
- Fernández-Perez, V., Jiménez-Carmona, M. M., and Luque de Castro, M. D. An approach to the static-dynamic subcritical water extraction of laurel essential oil: comparison with conventional techniques. Journal of Analytical Chemistry 125 (2000): 481-485.
- Gámiz-Gracia, L., and Luque de Castro, M.D. Continuous subcritical water extraction of medicinal plant essential oil: comparison with conventional techniques. Talanta 51 (2000): 1179–1185.
- Goto, M., Roy, B.C. and Hirose, T. Shrinking-core leaching model for supercritical fluid extraction. The Journal of Supercritical Fluids 9 (1996): 128-133
- Greig, D; [Online] Available from: <http://www.anbg.gov.au.html>. [2005, August 30]
- Hashimoto, S., Watanabe, K., Nose, K., and Morita, M. Remediation of soil contaminated with dioxins by subcritical water extraction. Chemosphere 54 (2004): 89–96.
- Hawthorne, S.B., Grabanski, C.B., Martin, E., and Miller, D.J. Comparisons of Soxhlet extraction, pressurized liquid extraction, supercritical fluid extraction and subcritical water extraction for environmental solids: recovery, selectivity and effects on sample matrix. Journal of Chromatography A 892 (2000): 421–433.
- Hiramatsu, T., Imoto, M., Koyano, T., and Umezawa, K. Induction of normal phenotypes in ras-transormed cells by damnacanthol from *Morinda citrifolia*. Cancer Letters 73 (1993): 161-166.
- Jiménez-Carmona, M. M., Ubera, J. L., and Luque de Castro, M. D. Comparison of continous subcritical water extraction and hydrodistillation of majoram essential oil. Journal of Chromatography A 855 (1999): 625-632.
- King, M.B., and Bott, T.R. Extraction of natural products using near-critical solvents. 1st ed. London: Blackie Academic & Professional, 1993.

- Kiriamiti, H.K., Rascol, E., Marty, A., and Condoret, J.S. Extraction rates of oil from high oleic sunflower seeds with supercritical carbon dioxide. Chemical Engineering and Processing 41 (2001): 711–718.
- Krieger, M.S., Wynn, J.L., and Yoder, R.N. Extraction of cloransulam-methyl from soil with subcritical water and supercritical CO₂. Journal of Chromatography A 897 (2000): 405–413.
- Kubátová, A., Miller, D. J., and Hawthorne, S.B. Comparison of subcritical water and organic solvents for extracting kava lactones from kava root. Journal of Chromatography A 923 (2001): 187-194.
- Kubátová, A., Lagadec, A. J. M., Miller, J. D., and Hawthorne, S.B. Selective extraction of oxygenates from savory and peppermint using subcritical water. Flavour and Fragrance Journal 16 (2001): 64-73.
- Kubátová, A., Jansen, B., Vaudoisot, J.F., and Hawthorne, S.B. Thermodynamic and kinetic models for the extraction of essential oil from savory and polycyclic aromatic hydrocarbons from soil with hot (subcritical) water and supercritical CO₂. Journal of Chromatography A 975 (2002): 175-188.
- Mannila, M. H., Kim, H., and Wai, C.M. Supercritical carbon dioxide and high-pressure water extraction of bioactive compounds in St. John's wort. In Proceedings of Super Green 2002 (2002)
- Marrone, C., Poletto, M., Reverchon, E., and Stassi, A. Almond oil extraction by supercritical CO₂: Experiments and modelling. Chemical Engineering Science 53 (1998): 3711-3718.
- Mcgowin, A.E., Adom, K.K., and Obubuafo, A.K. Screening of compost for PAHs and pesticides using static subcritical water extraction. Chemosphere 45 (2001): 857-864.
- Miller, D.J., and Clifford, A.A Solubility of polycyclic aromatic hydrocarbons in subcritical water from 298 to 498 K. Journal of Chemical Engineering and Data 43 (1998): 1043-1047.
- Miller, D.J., and Hawthorne, S.B. Solubility of liquid organic flavor and fragrance compounds in subcritical (hot/liquid) water from 298 K to 473 K. Journal of Chemical Engineering and Data 45 (2000): 315-318.

- Ollanketo, M., Peltoketo, A., Hartonen, K., Hiltunen R., and Riekkola, M. L.; Extraction of sage (*Salvia officinalis* L.) by pressurized hot water and conventional methods: antioxidant activity of the extracts. European Food Research Technology 215 (2002): 158-163.
- Ong, E. S., and Len, S.M. Pressurized hot water extraction of berberine, baicalein, and glycyrrhizin in medicinal plants. Analytical Chemistry Acta 482 (2003): 81-89.
- Ozel, M.Z., Gogus, F., and Lewisc, A.C. Subcritical water extraction of essential oils from *Thymbra spicata*. Food Chemistry 82 (2003): 381–386.
- Pawlowski, T.M. Extraction of Thiabendazole and Carbendazim from foods using pressurized hot (subcritical) water for extraction: a feasibility study. Journal of Agricultural and Food Chemistry 46 (1998): 3124-3132.
- Perrut, M., Clavier, J. Y., Poletto, M., and Reverchon, E. Mathematical modeling of sunflower seed extraction by supercritical CO₂. Industrial and Engineering Chemistry Research 36 (1996): 430-435.
- Prausnitz, J.M., Lichtenthaler, R.N., and Azevedo, E.G. Molecular thermodynamics of fluid-phase equilibrium. 3 rd ed.: Englewood Cliffs, N.J, Prentice Hall PTR, 1999.
- Pongnaravane, B. Subcritical water extraction of anthraquinones from roots of *Morinda citrifolia*. Master's Thesis, Department of Chemical Engineering, Faculty of Engineering, Chulalongkorn University, 2004.
- Reverchon, E, and Marrone, C. Supercritical extraction of clove bud essential oil: isolation and mathematical modeling. Chemical Engineering Science 52 (1997): 3421-3428.
- Reverchon, E., Kaziunas, A., and Marrone C. Supercritical CO₂ extraction of hiprose seed oil: experiments and mathematical modeling. Chemical Engineering Science 55 (2000): 2195-2201.
- Richter, P., Sepúlveda, B., Oliva, R., Calderón, K., and Seguel, R. Screening and determination of pesticides in soil using continuous subcritical water extraction and gas chromatography–mass spectrometry. Journal of Chromatography A 994 (2003): 169–177.
- Rogalinski, T., Valle, J.M.D., Zetzl, C., and Brunner, G.; Extraction of Boldo (*Peumus boldus* M.) leaves with hot pressurized water and supercritical CO₂. In Proceedings of Super Green 2002 (2002).

- Roy, B.C., Goto M., and Hirose, T. Extraction of ginger oil with supercritical carbon dioxide: experiment and modeling. Industrial and Engineering Chemistry Research 35 (1996): 607-612.
- Shotipruk, A., Kiatsongserm, J., Pavasant, P., Goto, M., and Sasaki, M., Subcritical water extraction of anthraquinones from the roots of *Morinda citrifolia*. Biotechnology Progress 20 (2004): 1872-1876.
- Sovova, H. Rate of the vegetable oil extraction with supercritical CO₂ –I modeling of extraction curves Chemical Engineering Science 49 (1994): 409-414.
- Sovova, H. Mathematical model for supercritical fluid extraction of natural products and extraction curve evaluation. The Journal of Supercritical Fluids 33 (2005):35-52.
- Smith, R.M. Extraction with superheated water. Journal of Chromatography A 975 (2002): 31–46.
- Statova, J., Jez, J., Bartlova, M., and Sovova, H. Rate of the vegetable oil extraction with supercritical CO₂ –III extraction from sea buckthorn. Chemical Engineering Science 51 (1996): 4347-4352.
- Suomi, J., Sirén, H., Hartonen, K., and Riekkola, M. L. Extraction of iridoid glycosides and their determination by micellar electrokinetic capillary chromatography. Journal of Chromatography A 868 (2000): 73-83.
- Westwood, S.A. Supercritical fluid extraction and its use in chromatographic sample preparation. 1st ed. London: Blackie Academic & Professional, 1993.
- Yang, Y., Bowadt, S., Hawthorne, S.B., and Miller, D.J. Subcritical water extraction of polychlorinated biphenyls from soil and sediment. Journal of Analytical Chemistry 67 (1995): 4571-4576.
- Yang, M.Y., West, B.J., Jensen, C.J., Nowicki, D., SU, C., Palu, A.K., and Anderson, G. *Morinda citrifolia* (Noni): A literature review and recent advances in Noni research. Acta Pharmacologica Sinica 12 (2002):1127 -1141.
- Zin, Z.M., Abdul-Hamid, A., and Osman, A. Antioxidative activity of extracts from Mengkudu (*Morinda citrifolia* L.) root, fruit and leaf. Food Chemistry 78 (2002): 227–231.



APPENDICES

สถาบันวิทยบริการ
จุฬาลงกรณ์มหาวิทยาลัย

APPENDIX A

EXPERIMENTAL DATA

A-1 Standard calibration curve of damnacanthal

Table: A-1.1 Standard calibration curve data.

Concentration of damnacanthal (mmol/l)	UV detector at 250 nm.		
	No.1	No.2	Average
0.0177	7570163	6806342	7158253
0.0354	15842501	14377808	15110155
0.0708	33393714	30264195	31828955
0.1062	53623916	49598507	51611212
0.1416	69524712	63109147	66316930

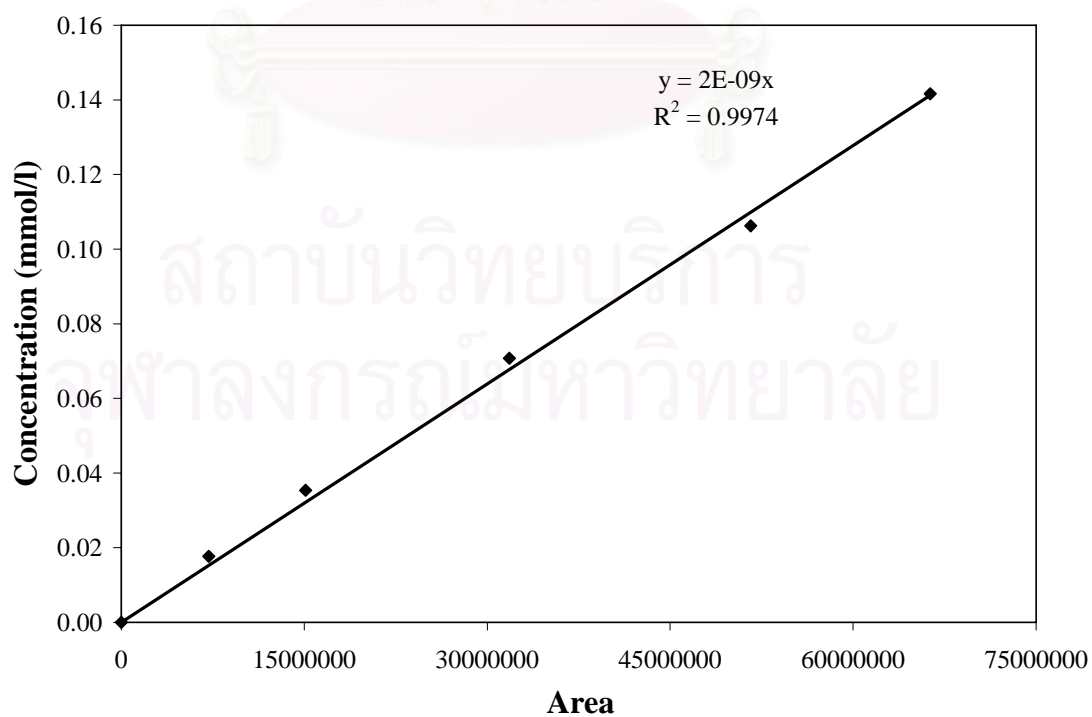


Figure A-1.2 Standard calibration curve of damnacanthal (average).

A-2 Property of *Morinda citrifolia* roots

A-2.1 Particle size analysis

Table: A.2.1 Particle size results of *Morinda citrifolia* roots.

No.	Diameter of roots (mm.)	Std.
1	0.3690	0.0019
2	0.3685	
3	0.3720	
Average	0.3698	

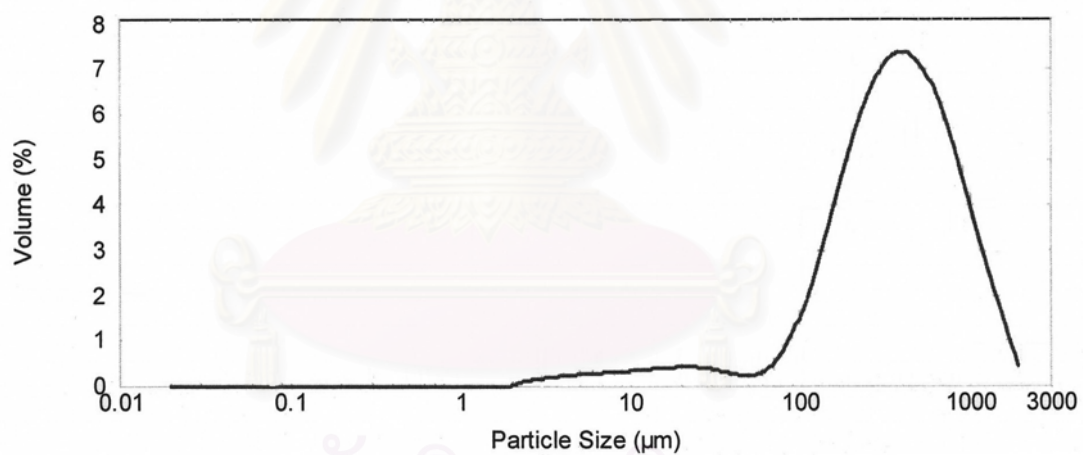


Figure A-2.1 Particle size distribution of powder of *Morinda citrifolia* roots.

A-2.2 Density of *Morinda citrifolia* roots

Table A.2.2: Density results of *Morinda citrifolia* roots.

Mass (g)	No.	Volume (ml)	Apparent density(g/ml)	Std.
1.0035	1	0.6925	1.4492	0.0024
	2	0.6881	1.4583	
	3	0.6940	1.4459	
	4	0.6912	1.4518	
	5	0.6938	1.4463	
	Average	0.6919	1.4503	

A-3 Experimental data of damnacanthal extract with subcritical water

Effect of subcritical water temperature

Table A-3.1: Subcritical water extraction of temperature 150°C and pressure 4 MPa for flow rate 5 ml/min.

Time (min)	Volume (ml)	Accumulate extracted (mg/g)			Std.
		No. 1	No. 2	Average	
0	0	0	0	0	0
10	50	0.2556	0.2863	0.2709	0.0217
20	100	0.4155	0.4986	0.4570	0.0588
40	200	0.4920	0.5881	0.5401	0.0680
60	300	0.5443	0.6192	0.5818	0.0530
120	600	0.5898	0.6481	0.6190	0.0413
180	900	0.6381	0.6561	0.6471	0.0128
240	1200	0.6583	0.6604	0.6593	0.0015

Table A-3.2: Subcritical water extraction of temperature 170°C and pressure 4 MPa for flow rate 5 ml/min.

Time (min)	Volume (ml)	Accumulate extracted (mg/g)			Std.
		No. 1	No. 2	Average	
0	0	0	0	0	0
10	50	0.2832	0.3073	0.2952	0.0170
20	100	0.4761	0.4949	0.4855	0.0133
40	200	0.6110	0.6331	0.6221	0.0156
60	300	0.6748	0.6982	0.6865	0.0166
120	600	0.6954	0.7168	0.7061	0.0152
180	900	0.7057	0.7271	0.7164	0.0151
240	1200	0.7106	0.7325	0.7216	0.0155

Table A-3.3: Subcritical water extraction of temperature 200°C and pressure 4 MPa for flow rate 5 ml/min.

Time (min)	Volume (ml)	Accumulate extracted (mg/g)			Std.
		No.1	No.2	Average	
0	0	0	0	0	0
10	50	0.1252	0.1282	0.1267	0.0021
20	100	0.1695	0.1698	0.1696	0.0002
40	200	0.1902	0.1852	0.1877	0.0035
60	300	0.2074	0.1982	0.2028	0.0065
120	600	0.2224	0.2130	0.2177	0.0067
180	900	0.2311	0.2200	0.2256	0.0078
240	1200	0.2349	0.2200	0.2275	0.0105

Table A-3.4: Subcritical water extraction of temperature 220°C and pressure 4 MPa for flow rate 5 ml/min.

Time (min)	Volume (ml)	Accumulate extracted (mg/g)			Std.
		No.1	No.2	Average	
0	0	0	0	0	0
10	50	0.1064	0.1183	0.1123	0.0084
20	100	0.1350	0.1397	0.1374	0.0033
40	200	0.1624	0.1639	0.1631	0.0011
60	300	0.1815	0.1756	0.1786	0.0042
120	600	0.1896	0.1864	0.1880	0.0022
180	900	0.1975	0.1900	0.1938	0.0053
240	1200	0.2021	0.1928	0.1975	0.0066

Effect of flow rate

Table A-3.5: Subcritical water extraction of temperature 170°C and pressure 4 MPa for flow rate 2 ml/min.

Time (min)	Volume (ml)	Accumulate extracted (mg/g)			Std.
		No. 1	No. 2	Average	
0	0	0	0	0	0
25	50	0.3114	0.3021	0.3068	0.0065
50	100	0.4591	0.4500	0.4545	0.0065
100	200	0.5344	0.5311	0.5327	0.0023
150	300	0.5964	0.5805	0.5885	0.0112
300	600	0.6277	0.6063	0.6170	0.0152
450	900	0.6329	0.6179	0.6254	0.0107
600	1200	0.6363	0.6213	0.6288	0.0106

Table A-3.6: Subcritical water extraction of temperature 170°C and pressure 4 MPa for flow rate 3 ml/min.

Time (min)	Volume (ml)	Accumulate extracted (mg/g)			Std.
		No. 1	No. 2	Average	
0	0	0	0	0	0
16.40	50	0.3613	0.3928	0.3770	0.0222
33.20	100	0.4797	0.5186	0.4991	0.0275
66.40	200	0.5860	0.6331	0.6096	0.0333
100	300	0.6187	0.6542	0.6365	0.0251
200	600	0.6369	0.6689	0.6529	0.0226
300	900	0.6472	0.6790	0.6631	0.0225
400	1200	0.6549	0.6836	0.6692	0.0203

Table A-3.7: Subcritical water extraction of temperature 170°C and pressure 4 MPa for flow rate 4 ml/min.

Time (min)	Volume (ml)	Accumulate extracted (mg/g)			Std.
		No. 1	No. 2	Average	
0	0	0	0	0	0
12.30	50	0.3795	0.3856	0.3826	0.0043
25	100	0.5184	0.5187	0.5186	0.0002
50	200	0.5904	0.6368	0.6136	0.0328
75	300	0.6294	0.6554	0.6424	0.0184
150	600	0.6634	0.6683	0.6658	0.0034
225	900	0.6906	0.6770	0.6838	0.0096
300	1200	0.7061	0.6826	0.6944	0.0166

Table A-3.8: Subcritical water extraction of temperature 170°C and pressure 4 MPa for flow rate 5 ml/min.

Time (min)	Volume (ml)	Accumulate extracted (mg/g)			Std.
		No. 1	No. 2	Average	
0	0	0	0	0	0
10	50	0.2832	0.3073	0.2952	0.0170
20	100	0.4761	0.4949	0.4855	0.0133
40	200	0.6110	0.6331	0.6221	0.0156
60	300	0.6748	0.6982	0.6865	0.0166
120	600	0.6954	0.7168	0.7061	0.0152
180	900	0.7057	0.7271	0.7164	0.0151
240	1200	0.7106	0.7325	0.7216	0.0155

APPENDIX B

MODELING DATA

B-1 Partitioning coefficient (K_D) model

$$\frac{S_b}{S_0} = \frac{\left(1 - \frac{S_a}{S_0}\right)}{\left(\frac{K_D m}{(V_b - V_a)\rho} + 1\right)} + \frac{S_a}{S_0} \quad (\text{B.1})$$

where S_a = cumulate mass of the analyte extracted after volume V_a (mg/g)

S_b = cumulate mass of the analyte extracted after volume V_b (mg/g)

S_0 = initial total mass of analyte in the matrix (mg/g)

$\frac{S_a}{S_0}$ = cumulative fractions of the analyte extracted by the extraction fluid
of the volume V_a

$\frac{S_b}{S_0}$ = cumulative fractions of the analyte extracted by the extraction fluid
of the volume V_b

K_D = thermodynamics partitioning coefficient

ρ = density of extraction fluid at temperature 170°C and at pressure 4 MPa
is 928.15 mg/ml

m = mass of the extracted sample (mg)

Table B-1.1: Value of %extracted ($\%S_d/S_0$) with flow rate 2 ml/min, at temperature 170°C and pressure 4 MPa.

Which $S_0 = 0.629$ mg damnacanthal/g dried roots

$$K_D = 55.60$$

Time (min)	%Extracted	
	Exp.	Model
0	0	0
25	48.7455	45.4928
50	72.2302	70.2897
100	84.6545	91.1730
150	93.5091	97.3775
300	98.0459	99.9312
450	99.3791	99.9982
600	99.9242	100

Table B-1.2: Value of %extracted ($\%S_d/S_0$) with flow rate 3 ml/min, at temperature 170°C and pressure 4 MPa.

Which $S_0 = 0.671$ mg damnacanthal/g dried roots

$$K_D = 43.27$$

Time (min)	% Extracted	
	Exp.	Model
0	0	0
16.40	56.2245	51.7514
33.20	74.4323	76.7207
66.40	90.8997	94.5808
100	94.9106	98.7384
200	97.3602	99.9841
300	98.8761	99.9998
400	99.7938	100

Table B-1.3: Value of %extracted ($\%S_d/S_0$) with flow rate 4 ml/min, at temperature 170°C and pressure 4 MPa.

Which $S_0 = 0.695$ mg damnacanthal/g dried roots

$$K_D = 45.68$$

Time (min)	% Extracted	
	Exp.	Model
0	0	0
12.30	55.0463	50.3948
25	74.6161	75.3932
50	88.2863	93.9451
75	92.4343	98.5101
150	95.8024	99.9778
225	98.3851	99.9997
300	99.9087	100

Table B-1.4: Value of %extracted ($\%S_d/S_0$) with flow rate 5 ml/min, at temperature 170°C and pressure 4 MPa.

Which $S_0 = 0.722$ mg damnacanthal/g dried roots

$$K_D = 66.46$$

Time (min)	% Extracted	
	Exp.	Model
0	0	0
10	40.8587	41.1174
20	67.1745	65.3284
40	86.1496	87.9788
60	95.0139	95.8321
120	97.7839	99.8263
180	99.1690	99.9928
240	100	99.9997

Table B-1.5: Value of %extracted ($\%S_d/S_0$) with flow rate 3 ml/min, at temperature 170°C and pressure 4 MPa.

Which $S_0 = 0.671$ mg damnacanthal/g dried roots

$$K_D = 55.60$$

Time (min)	% Extracted	
	Exp.	Model
0	0	0
12.30	55.0463	45.4928
25	74.6161	70.2897
50	88.2863	91.1730
75	92.4343	97.3775
150	95.8024	99.9312
225	98.3851	99.9982
300	99.9087	100

Table B-1.6: Value of %extracted ($\%S_d/S_0$) with flow rate 4 ml/min, at temperature 170°C and pressure 4 MPa.

Which $S_0 = 0.695$ mg damnacanthal/g dried roots

$$K_D = 55.60$$

Time (min)	% Extracted	
	Exp.	Model
0	0	0
16.40	56.2245	45.4928
33.20	74.4323	70.2897
66.40	90.8997	91.1730
100	94.9106	97.3775
200	97.3602	99.9312
300	98.8761	99.9982
400	99.7938	100

Table B-1.7: Value of %extracted ($\%S_t/S_0$) with flow rate 5 ml/min, at temperature 170°C and pressure 4 MPa.

Which $S_0 = 0.722$ mg damnacanthal/g dried roots

$$K_D = 55.60$$

Time (min)	% Extracted	
	Exp.	Model
0	0	0
10	40.8587	45.4928
20	67.1745	70.2897
40	86.1496	91.1730
60	95.0139	97.3775
120	97.7839	99.9312
180	99.1690	99.9982
240	100	100

B-2 One-site kinetic desorption models

$$\ln(S_r / S_0) = -0.4977 - t/t_c \quad (\text{B.2})$$

where S_r = mass remaining of analyte in the matrix after extraction for time, t
(mg/g)

S_0 = initial total mass of analyte in the matrix (mg/g)

t_c = a characteristic time for the extraction (min)

t = extraction time (min)

Table B-2.1: Value of $\ln(S_r/S_0)$ with flow rate 2 ml/min, at temperature 170°C and pressure 4 MPa.

Which $S_0 = 0.629$ mg damnacanthal/g dried roots

Time (min)	S_r (mg/g)	S_r/S_0	$\ln(S_r/S_0)$
0	0.6293	1	0
25	0.3225	0.5125	-0.6684
50	0.1747	0.2777	-1.2814
100	0.0965	0.1534	-1.8747
150	0.0408	0.0649	-2.7356
300	0.0123	0.0195	-3.9382
450	0.0039	0.0061	-5.0913

Table B-2.2: Value of $\ln(S_r/S_0)$ with flow rate 3 ml/min, at temperature 170°C and pressure 4 MPa.

Which $S_0 = 0.671$ mg damnacanthal/g dried roots

Time (min)	S_r (mg/g)	S_r/S_0	$\ln(S_r/S_0)$
0	0.6706	1	0
16.40	0.2936	0.5622	-0.5758
33.20	0.1715	0.1821	-1.7033
66.40	0.0610	0.1647	-1.8038
100	0.0341	0.0401	-3.2161
200	0.0177	0.0245	-3.7092
300	0.0075	0.0152	-4.1892
400	0.0014	0.0092	-4.6910

Table B-2.3: Value of $\ln(S_r/S_0)$ with flow rate 4 ml/min, at temperature 170°C and pressure 4 MPa.

Which $S_0 = 0.695$ mg damnacanthal/g dried roots

Time (min)	S_r (mg/g)	S_r/S_0	$\ln(S_r/S_0)$
0	0.6950	1	0
12.30	0.3124	0.4495	-0.7996
25	0.1764	0.2538	-1.3711
50	0.0814	0.1171	-2.1446
75	0.0526	0.0756	-2.5819
150	0.0292	0.0419	-3.1713
225	0.0112	0.0161	-4.1276

Table B-2.4: Value of $\ln(S_r/S_0)$ with flow rate 5 ml/min, at temperature 170°C and pressure 4 MPa.

Which $S_0 = 0.722$ mg damnacanthal/g dried roots

Time (min)	S (mg/g)	S_r/S_0	$\ln(S_r/S_0)$
0	0.7216	1	0
10	0.4263	0.4092	-0.8937
20	0.2361	0.2637	-1.3330
40	0.0995	0.1893	-1.6647
60	0.0351	0.0893	-2.4159
120	0.0154	0.0272	-3.6037
180	0.0052	0.0142	-4.2562

When written equation B-2 as the amount extracted at time t , becomes:

$$\frac{S_t}{S_0} = 1 - e^{-kt} \quad (\text{B.3})$$

where S_t = mass of the analyte removed by the extraction fluid after time t
(mg/g)

S_0 = total initial mass of analyte in the matrix. (mg/g)

k = first order rate constant describing the extraction

t = extraction time (min)

Table B-2.5: Value of %extracted ($\%S_t/S_0$) with flow rate 2 ml/min, at temperature 170°C and pressure 4 MPa.

Which $S_0 = 0.629$ mg damnacanthal/g dried roots

$$k = 0.0243$$

Time (min)	%Extracted	
	Exp.	Model
0	0	0
25	48.7455	45.4928
50	72.2302	70.2897
100	84.6545	91.1730
150	93.5091	97.3775
300	98.0459	99.9312
450	99.3791	99.9982
600	99.9242	100

Table B-2.6: Value of %extracted ($\%S_t/S_0$) with flow rate 3 ml/min, at temperature 170°C and pressure 4 MPa.

Which $S_0 = 0.671$ mg damnacanthal/g dried roots

$$k = 0.0442$$

Time (min)	%Extracted	
	Exp.	Model
0	0	0
16.40	56.2245	51.5402
33.20	74.4323	76.9278
66.40	90.8997	94.6767
100	94.9106	98.7933
200	97.3602	99.9854
300	98.8761	99.9998
400	99.7938	100

Table B-2.7: Value of %extracted ($\%S_t/S_0$) with flow rate 4 ml/min, at temperature 170°C and pressure 4 MPa.

Which $S_0 = 0.695$ mg damnacanthal/g dried roots

$$k = 0.0565$$

Time (min)	%Extracted	
	Exp.	Model
0	0	0
12.30	55.0463	50.1102
25	74.6161	75.6666
50	88.2863	94.0789
75	92.4343	98.5592
150	95.8024	99.9792
225	98.3851	99.9997
300	99.9087	100

Table B-2.8: Value of %extracted ($\%S_t/S_0$) with flow rate 5 ml/min, at temperature 170°C and pressure 4 MPa.

Which $S_0 = 0.722$ mg damnacanthal/g dried roots

$$k = 0.0530$$

Time (min)	%Extracted	
	Exp.	Model
0	0	0
10	40.8587	47.8705
20	67.1745	73.3947
40	86.1496	92.9216
60	95.0139	98.1168
120	97.7839	99.9645
180	99.1690	99.9993
240	100	100

Table B-2.9: Value of %extracted ($\%S_t/S_0$) with flow rate 2 ml/min, at temperature 170°C and pressure 4 MPa.

Which $S_0 = 0.629$ mg damnacanthal/g dried roots

$$k = 0.0530$$

Time (min)	%Extracted	
	Exp.	Model
0	0	0
25	48.7455	73.3947
50	72.2302	92.9216
100	84.6545	99.4990
150	93.5091	99.9645
300	98.0459	100
450	99.3791	100
600	99.9242	100

Table B-2.10: Value of %extracted ($\%S_t/S_0$) with flow rate 3 ml/min, at temperature 170°C and pressure 4 MPa.

Which $S_0 = 0.671$ mg damnacanthal/g dried roots

$$k = 0.0530$$

Time (min)	%Extracted	
	Exp.	Model
0	0	0
16.40	56.2245	58.0455
33.20	74.4323	82.7672
66.40	90.8997	97.0303
100	94.9106	99.4990
200	97.3602	99.9975
300	98.8761	100
400	99.7938	100

Table B-2.11: Value of %extracted ($\%S_t/S_0$) with flow rate 4 ml/min, at temperature 170°C and pressure 4 MPa.

Which $S_0 = 0.695$ mg damnacanthal/g dried roots

$$k = 0.0530$$

Tim (min)	%Extracted	
	Exp.	Model
0	0	0
12.30	55.0463	47.8705
25	74.6161	73.3947
50	88.2863	92.9216
75	92.4343	98.1168
150	95.8024	99.9645
225	98.3851	99.9993
300	99.9087	100

B-3 Two-site kinetic desorption model

$$\frac{S_t}{S_0} = 1 - [F e^{-k_1 t}] - [(1-F) e^{-k_2 t}] \quad (\text{B.4})$$

where S_t = mass of the analyte removed by the extraction fluid after time t (mg/g)

S_0 = total initial mass of analyte in the matrix. (mg/g)

$\frac{S_t}{S_0}$ = fraction of the analyte extracted after time t

F = fraction of the analyte released quickly.

$(1-F)$ = fraction of the analyte released slowly.

k_1 = first-order rate constant describing the quickly released fraction (min^{-1})

k_2 = first-order rate constant describing the slowly released fraction (min^{-1})

t = extraction time (min)

Table B-3.1: Value of %extracted ($\%S_t/S_0$) with flow rate 2 ml/min, at temperature 170°C and pressure 4 MPa.

Which $S_0 = 0.629$ mg damnacanthal/g dried roots, $F = 0.76$

$k_1 = 0.0357$ and $k_2 = 0.0078$

Time (min)	%Extracted	
	Exp.	Model
0	0	0
25	48.7455	49.1811
50	72.2302	71.0566
100	84.6545	86.8953
150	93.5091	92.2189
300	98.0459	97.7009
450	99.3791	99.2892
600	99.9242	99.7801

Table B-3.2: Value of %extracted ($\%S_t/S_0$) with flow rate 3 ml/min, at temperature 170°C and pressure 4 MPa.

Which $S_0 = 0.671$ mg damnacanthal/g dried roots, $F = 0.76$,
 $k_1 = 0.065$ and $k_2 = 0.0144$

Time (min)	%Extracted	
	Exp.	Model
0	0	0
16.40	56.2245	55.0425
33.20	74.4323	76.4599
66.40	90.8997	89.8026
100	94.9106	94.2199
200	97.3602	98.6603
300	98.8761	99.6835
400	99.7938	99.9252

Table B-3.3: Value of %extracted ($\%S_t/S_0$) with flow rate 4 ml/min, at temperature 170°C and pressure 4 MPa.

Which $S_0 = 0.695$ mg damnacanthal/g dried roots, $F = 0.76$
 $k_1 = 0.090$ and $k_2 = 0.0143$

Time (min)	%Extracted	
	Exp.	Model
0	0	0
12.30	55.0463	54.7711
25	74.6161	75.2376
50	88.2863	87.4604
75	92.4343	91.7465
150	95.8024	97.2224
225	98.3851	99.0551
300	99.9087	99.6786

Table B-3.4: Value of %extracted ($\%S_t/S_0$) with flow rate 5 ml/min, at temperature 170°C and pressure 4 MPa.

Which $S_0 = 0.722$ mg damnacanthal/g dried roots, $F = 0.76$,
 $k_1 = 0.064$ and $k_2 = 0.0029$

Time (min)	%Extracted	
	Exp.	Model
0	0	0
10	40.8587	42.9899
20	67.1745	66.6859
40	86.1496	87.6320
60	95.0139	94.8595
120	97.7839	99.4163
180	99.1690	99.9152
240	100	99.9872

Table B-3.5: Value of % extracted ($\% S_t/S_0$) with flow rate 2 ml/min, at temperature 170°C and at pressure 4 MPa.

Which $S_0 = 0.629$ mg damnacanthal/g dried roots, $F = 0.76$,
 $k_1 = 0.064$ and $k_2 = 0.0029$

Time (min)	%Extracted	
	Exp.	Model
0	0	0
25	48.7455	74.2737
50	72.2302	92.1328
100	84.6545	98.8525
150	93.5091	99.7798
300	98.0459	99.9981
450	99.3791	100
600	99.9242	100

Table B-3.6: Value of %extracted ($\%S_t/S_0$) with flow rate 3 ml/min, at temperature 170°C and pressure 4 MPa.

Which $S_0 = 0.671$ mg damnacanthal/g dried roots, $F = 0.76$,
 $k_1 = 0.064$ and $k_2 = 0.0029$

Time (min)	%Extracted	
	Exp.	Model
0	0	0
16.40	56.2245	59.7000
33.20	74.4323	82.9004
66.40	90.8997	96.0348
100	94.9106	98.8525
200	97.3602	99.9549
300	98.8761	99.9981
400	99.7938	99.9999

Table B-3.7: Value of % extracted ($\%S_t/S_0$) with flow rate 4 ml/min, at temperature 170°C and at pressure 4 MPa.

Which $S_0 = 0.695$ mg damnacanthal/g dried roots, $F = 0.76$,
 $k_1 = 0.064$ and $k_2 = 0.0029$

Time (min)	%Extracted	
	Exp.	Model
0	0	0
12.30	55.0463	49.7325
25	74.6161	74.2737
50	88.2863	92.1328
75	92.4343	97.1636
150	95.8024	99.7798
225	98.3851	99.9795
300	99.9087	99.9981

B-4 External mass transfer model

$$S_t = 1 - S_0 \exp(-k_e a_p t / K_D) \quad (\text{B.5})$$

where S_t = mass of the analyte removed by the extraction fluid after time t (mg/g)

S_0 = total initial mass of analyte in the matrix (mg/g)

k_e = external mass transfer coefficient (m/s)

a_p = specific surface area of particles (m^2/m^3)

K_D = thermodynamics partitioning coefficient

t = extraction time (min)

Table B-4.1: Value of %extracted ($\%S_t/S_0$) with flow rate 2 ml/min, at temperature 170°C and pressure 4 MPa.

Which $S_0 = 0.629$ mg damnacanthal/g dried roots

$$K_D = 55.70, k_e a_p = 1.35$$

Time (min)	%Extracted	
	Exp.	Model
0	0	0
25	48.7455	45.4928
50	72.2302	70.2897
100	84.6545	91.1730
150	93.5091	97.3775
300	98.0459	99.9312
450	99.3791	99.9982
600	99.9242	100

Table B-4.2: Value of %extracted ($\%S_t/S_0$) with flow rate 3 ml/min, at temperature 170°C and pressure 4 MPa.

Which $S_0 = 0.671$ mg damnacanthal/g dried roots

$$K_D = 55.83, k_e a_p = 2.47$$

Time (min)	% Extracted	
	Exp.	Model
0	0	0
16.40	56.2245	51.5402
33.20	74.4323	76.9278
66.40	90.8997	94.6767
100	94.9106	98.7933
200	97.3602	99.9854
300	98.8761	99.9998
400	99.7938	100

Table B-4.3: Value of %extracted ($\%S_t/S_0$) with flow rate 4 ml/min, at temperature 170°C and pressure 4 MPa.

Which $S_0 = 0.695$ mg damnacanthal/g dried roots

$$K_D = 55.61, k_e a_p = 3.1440$$

Time (min)	% Extracted	
	Exp.	Model
0	0	0
12.30	55.0463	50.1102
25	74.6161	75.6666
50	88.2863	94.0789
75	92.4343	98.5592
150	95.8024	99.9792
225	98.3851	99.9997
300	99.9087	100

Table B-4.4: Value of %extracted ($\%S_t/S_0$) with flow rate 5 ml/min, at temperature 170°C and pressure 4 MPa.

Which $S_0 = 0.722$ mg damnacanthal/g dried roots

$$K_D = 55.65, k_{ea_p} = 2.95$$

Time (min)	% Extracted	
	Exp.	Model
0	0	0
10	40.8587	41.1176
20	67.1745	65.3286
40	86.1496	87.9790
60	95.0139	95.8321
120	97.7839	99.8263
180	99.1690	99.9928
240	100	99.9997

APPENDIX C

SOLUBILITY PREDICTION

In general, the solute solubility depends on the interaction between the molecules of the solute and the solvent (the activity coefficient). However, factors other than intermolecular forces between solvent and solute also play a large role in determining the solubility of a solid. To illustrate, consider the solubility of two isomers, phenanthrene and anthracene in benzene at 25°C are 20.7 and 0.81 mol%, respectively. This example showed that the solubility is not depended on the activity coefficient of the solute but also on the standard state fugacity to which that activity coefficient refer and on the fugacity of pure solid, according to the following equation.

$$Z = \frac{f_{\text{pure-solid}}}{\gamma f_{\text{subcooled-liquid}}^0} \quad (\text{C.1})$$

Where $f_{\text{pure-solid}}$ is fugacity of solid at equilibrium and $f_{\text{subcooled-liquid}}^0$ is standard state fugacity taken to be that of subcooled liquid.

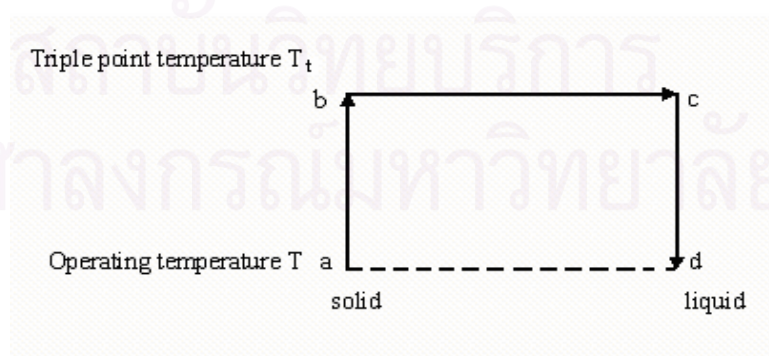


Figure C.1 Path independence thermodynamic properties

$$\Delta M_{a \rightarrow d} = \Delta M_{a \rightarrow b} + \Delta M_{b \rightarrow c} + \Delta M_{c \rightarrow d} \quad (\text{where } M \text{ means any state property})$$

The ratio of the two fugacities are relate to the change of Gibbs energy in going from the state of solid (denoted as state a) to subcooled liquid (denoted as state d) following form equation:

$$\Delta G = \kappa T \ln \left(\frac{f_{\text{subcooled-liquid}}}{f_{\text{pure-solid}}} \right) \quad (\text{C.2})$$

The change of Gibbs energy is related to the change of enthalpy and the change of entropy by the following equation:

$$\Delta G_{a \rightarrow d} = \Delta H_{a \rightarrow d} - T \Delta S_{a \rightarrow d} \quad (\text{C.3})$$

To calculate $\Delta H_{a \rightarrow d}$ and $\Delta S_{a \rightarrow d}$, it is more convenient to employ thermodynamic cycle as shown in Figure C.1. Because the enthalpy and entropy are not dependent of the path, the $\Delta H_{a \rightarrow d}$ and $\Delta S_{a \rightarrow d}$ can be calculated from $a \rightarrow b$, $b \rightarrow c$ and $c \rightarrow d$.

$$\Delta H_{a \rightarrow d} = \Delta H_{a \rightarrow b} + \Delta H_{b \rightarrow c} + \Delta H_{c \rightarrow d} \quad (\text{C.4})$$

The above equation becomes

$$\Delta H_{a \rightarrow d} = \Delta_{\text{fus}} H_{\text{at } T_t} + \int_{T_t}^T \Delta C_P dT \quad (\text{C.5})$$

Where $\Delta_{\text{fus}} H$ is the enthalpy of fusion, $\Delta C_P = C_{P \text{ liquid}} - C_{P \text{ solid}}$, the difference between the heat capacity of liquid and the heat capacity of solid, and T_t is the triple point temperature of the solute.

Similarly, the entropy change from a to d can be determined from the following equation

$$\Delta S_{a \rightarrow d} = \Delta S_{a \rightarrow b} + \Delta S_{b \rightarrow c} + \Delta S_{c \rightarrow d} \quad (\text{C.6})$$

Which can be written as follows

$$\Delta S_{a \rightarrow d} = \Delta_{fus} S_{at T_t} + \int_{T_t}^T \Delta C_p dT \quad (C.7)$$

Where $\Delta_{fus} S$ is entropy of fusion which is related to $\Delta_{fus} H$ by the following equation:

$$\Delta_{fus} S = \frac{\Delta_{fus} H}{T_t} \quad (C.8)$$

Substituting Equations C.7, C.5 and C.3 into Equation C.2, and assuming that ΔC_p is constant over the temperature range $T_t \rightarrow T$, we obtain the following equation.

$$\ln \left(\frac{f_{subcooled-liquid}}{f_{pure-solid}} \right) = \frac{\Delta_{fus} H}{\kappa T_t} \left(\frac{T_t}{T} - 1 \right) - \Delta C_p \left(\frac{T_t}{T} - 1 \right) + \Delta C_p \ln \left(\frac{T_t}{T} \right) \quad (C.9)$$

This equation gives an expression for the ratio of the fugacities, which can be substituted Equation C.8 in Equation C.9 to give the expression for the solubility as follows.

$$\ln Z = -\frac{\Delta_{fus} S}{\kappa} \left(\frac{T_t}{T} - 1 \right) + \Delta C_p \left(\frac{T_t}{T} - 1 \right) - \Delta C_p \ln \left(\frac{T_t}{T} \right) - \ln \gamma \quad (C.10)$$

As an approximation, the term of ΔC_p can be neglected and it is permissible to substitute melting temperature for triple point temperature. Then, Equation C.10 becomes:

$$\ln Z = -\frac{\Delta_{fus} S}{\kappa} \left(\frac{T_m}{T} - 1 \right) - \ln \gamma \quad (C.11)$$

To represent the values at equilibrium or saturation, the superscript, *SAT*, is used and the equation becomes:

$$\ln Z^{SAT} = \frac{\Delta_{fus} S}{\kappa} \left(1 - \frac{T_m}{T} \right) - \ln \gamma^{SAT} \quad (C.12)$$

This equation shows that the solute solubility depends on temperature and intermolecular forces between solute and solvent as represented by the activity coefficient. For an ideal solution, the activity coefficient is equal to 1. For non-ideal solution, activities coefficient is not equal to 1. Many solubility estimation methods such as Robbins chart, UNIFAC model, Hansen solubility parameter, and Margules equation can be used to estimate of the value of activity coefficient, and thus solubility. The knowledge of solute solubility in extraction solvents at various conditions is useful for the design of the process (Prausnitz et al., 1993).



สถาบันวิทยบริการ
จุฬาลงกรณ์มหาวิทยาลัย

APPENDIX D

DERIVATION OF SIMPLE EQUILIBRIUM AND DIFFUSION MODELS

D-1 Equilibrium model (controlled by partitioning of solute between matrix and solvent)

This model describes the extraction process that is controlled by partitioning of solute between matrix and solvent. The model assumes the kinetics of the initial desorption step and the subsequent fluid-matrix partitioning is rapid, and thus do not significantly affect the extraction rate. Here the thermodynamics partitioning coefficient, K_D is defined as:

$$K_D = \frac{\text{Concentration of analyte in the matrix}}{\text{Concentration of analyte in the extraction fluid}}; \text{at equilibrium} \quad (\text{D.1})$$

If it is also assumed that the matrix has a uniform size, essentially, the mass of analyte in each unit mass of extraction fluid and the mass of analyte remaining in the matrix at that period in the extraction time can be calculated for the entire extraction time based on the K_D value determined for a plant compound of interest.

Let S_a be the cumulate mass of the analyte extracted after volume V_a (mg solute/g sample) passed the extraction vessel, then the cumulate mass of the analyte extracted in the next time period after volume V_b (mg solute/g sample) pass ($V_b > V_a$), or S_b , can be found from the following equation:

$$S_b = S_a + f(S_0 - S_a) \quad (\text{D.2})$$

Where $f(S_0 - S_a)$ = function of solute mass extracted (into fluid of the volume $V_b - V_a$)

After the amount S_a was extracted, the total mass remained to be extracted will be partition into two parts as follows:

$$S_0 - S_a = \text{Mass of solute on the matrix} + \text{Mass of solute in the fluid} \quad (\text{D.3})$$

where $S_0 - S_a =$ mass of the remaining solute of the volume $V_b - V_a$.

Rewriting Equation D.1, we obtain:

$$K_D = \frac{\text{Mass of solute on the matrix/ Volume of matrix}}{\text{Mass of solute in the fluid/ Volume of fluid}} \quad (\text{D.4})$$

Thus, from Equation D.4, we have

$$\text{Mass of solute on the matrix} = K_D \times \frac{\text{Mass of solute in the fluid}}{\text{Volume of fluid}} \times \text{Volume of matrix} \quad (\text{D.5})$$

Substituting Equation D.5 into Equation D.3 gives:

$$S_0 - S_a = K_D \times \frac{\text{Mass of solute in the fluid}}{\text{Volume of fluid}} \times \text{Volume of matrix} + \text{Mass of solute in the fluid} \quad (\text{D.6})$$

or

$$S_0 - S_a = \text{Mass of solute in the fluid} \left(\frac{K_D \times \text{Volume of matrix}}{\text{Volume of fluid}} + 1 \right) \quad (\text{D.7})$$

or

$$\text{Mass of solute in the fluid} = \frac{S_0 - S_a}{\left(\frac{K_D \times \text{Volume of matrix}}{\text{Volume of fluid}} + 1 \right)} \quad (\text{D.8})$$

Mass of solute in the fluid substitute into $f(S_0-S_a)$ in equation D.2, we obtain:

$$S_b = S_a + \frac{S_0 - S_a}{\left(\frac{K_D \text{Volume of matrix}}{\text{Volume of fluid}} + 1 \right)} \quad (\text{D.9})$$

This is equivalent to

$$S_b = S_a + \frac{S_0 - S_a}{\left(\frac{K_D m}{\text{Volume of fluid} \rho} + 1 \right)} \quad (\text{D.10})$$

where m = mass of the extraction fluid at given conditions (g)

ρ = density of extraction fluid at given conditions (mg/ml) volume of fluid = $V_b - V_a$

Thus, the expression for cumulative fraction of the solute in the plant matrix extracted by extraction fluid of volume V_b would be defined by:

$$\frac{S_b}{S_0} = \frac{S_a}{S_0} + \frac{1 - \frac{S_a}{S_0}}{\left(\frac{K_D m}{(V_b - V_a) \rho} + 1 \right)} \quad (\text{D.11})$$

D-2 Equilibrium model with external mass transfer resistance

In the equilibrium model, it was assumed that the kinetics of the initial desorption step and the fluid-matrix partitioning is rapid. In this model, rapid partitioning is not assumed. In other words, there exists an external mass transfer resistance in the liquid film around the solid matrix. The solution of the extraction profile could be solved based on the differential equation presented in Chapter 2, Equation 2.2, written as follows:

$$\frac{\partial c_s}{\partial t} = -j(c_s, c) \quad (\text{D.12})$$

where the function $j(c_s, c)$ takes into account the external mass transfer phenomena and can be written as.

$$j(c_s, c) = k_e a_p (c^* - c) \quad (\text{D.13})$$

where $k_e a_p$ is the external mass transfer coefficient, a_p is the specific solid-solvent interfacial area, c^* is the solute concentration in the liquid that is in equilibrium with that in the solid matrix, described by K_D , $c^* = c_s / K_D$, and c_0 is the initial concentration of solute on the matrix.

Substituting Equation D.13 into Equation D.12, the following equation results:

$$\frac{\partial c_s}{\partial t} = -k_e a_p [(c_s / K_D) - c] \quad (\text{D.14})$$

Assuming that the fluid concentration, c is small, then $c = 0$, then integration of Equation D.14 gives

$$\int_{c_0}^{c_s} \frac{1}{c_s} dc_s = \frac{-k_e a_p}{K_D} \int_0^t dt \quad (\text{D.15})$$

and the solution becomes:

$$\ln \frac{c_s}{c_0} = \frac{-k_e a_p}{K_D} t \quad (\text{D.16})$$

or

$$c_s = c_0 \exp(-k_e a_p t / K_D) \quad (\text{D.17})$$

Because the interfacial area, a_p , is difficult to be measured accurately, it can be put together with k_e , where $k_e a_p$ is called overall volumetric mass transfer coefficient.

The factors that influence the value of $k_e a_p$ are the velocity of solvent through the extractor and the size and shape of root.

The amount of remaining solute concentration in matrix is given as a fraction of the mass of solute in the matrix

$$S_r = S_0 \exp(-k_e a_p t / K_D) \quad (\text{D.18})$$

where S_r = mass of extractable compound that remains in the matrix sphere after extraction for time, t , (mg/g)

S_0 = initial total mass of analyte in the matrix (mg/g)

From Equation D.18, the ratio of the mass of diffusing substance leaving the sample to the initial mass of solute in the sample, S_t/S_0 is given by

$$S_t = 1 - S_0 \exp(-k_e a_p t / K_D) \quad (\text{D.19})$$

D-3 Diffusion model

For diffusion in a sphere in a radial direction, the equation a constant diffusion coefficient takes the form:

$$\frac{\partial c}{\partial t} = D_e \left(\frac{\partial^2 c}{\partial r^2} + \frac{2}{r} \frac{\partial c}{\partial r} \right) \quad (\text{D.20})$$

where c = fluid concentration (mol/m³)

D_e = effective diffusion coefficient of the compound in the material of sphere (m²/s).

On putting

$$u = cr \quad (\text{D.21})$$

Equation D.20 becomes

$$\frac{\partial u}{\partial t} = D_e \frac{\partial^2 u}{\partial r^2} \quad (\text{D.22})$$

The boundary and initial conditions are as follows:

$$\begin{aligned} u &= 0 & r &= 0 & t &> 0 \\ u &= Rc_0 & r &= R & t &> 0 \\ u &= rf(r) & t &= 0 & 0 < r < R \end{aligned}$$

where c_0 is the constant concentration at the surface of the sphere and $f(r)$ is the concentration profile as a function of the sphere radius.

The solution in the form of a trigonometrical series is

$$\begin{aligned} c &= c_1 + (c_0 - c_1) \frac{r}{R} + \frac{2}{\pi} \sum_1^{\infty} \frac{S_2 \cos n\pi - S_1}{n} \sin \frac{n\pi r}{R} \exp(-D_e n^2 \pi^2 t / R^2) \\ &+ \frac{2}{R} \sum_1^{\infty} \sin \frac{n\pi r}{\pi} \exp(-D_e \pi^2 n^2 t / R^2) \int_0^1 f(r') \sin \frac{n\pi r'}{R} dr' \end{aligned} \quad (\text{D.23})$$

In the case of most common occurrence $f(r)$ is either zero or constant or that is the sphere is initially at a uniform concentration c_1 , the integral in equation D.23 is readily evaluated. The solution becomes:

$$\frac{c - c_1}{c_0 - c_1} = 1 + \frac{2R}{\pi r} \sum_{n=1}^{\infty} \frac{(-1)^n}{n} \sin \frac{n\pi r}{R} \exp(-D_e n^2 \pi^2 t / R^2) \quad (\text{D.24})$$

The concentration at the center is given by the limit as $r \rightarrow 0$, that is by

$$\frac{c - c_1}{c_0 - c_1} = 1 + 2 \sum_{n=1}^{\infty} (-1)^n \exp(-D_e n^2 \pi^2 t / R^2) \quad (\text{D.25})$$

The total amount of diffusing substance leaving the sphere, $S_t = c \times V$, is given as a fraction of the initial mass of solute in the sample, S_0 , by

$$\frac{S_t}{S_0} = 1 - \frac{6}{\pi^2} \sum_{n=1}^{\infty} \frac{1}{n^2} \exp(-D_e n^2 \pi^2 t / R^2) \quad (\text{D.26})$$

The corresponding solutions for small times are

$$\frac{c - c_1}{c_0 - c_1} = \frac{R}{r} \sum_{n=0}^{\infty} \left\{ \operatorname{erfc} \frac{(2n+1)R - r}{2\sqrt{(D_e t)}} - \operatorname{erfc} \frac{(2n+1)R + r}{2\sqrt{(D_e t)}} \right\} \quad (\text{D.27})$$

and

$$\frac{S_t}{S_0} = 6 \left(\frac{D_e t}{R^2} \right)^{\frac{1}{2}} \left\{ \pi^{-\frac{1}{2}} + 2 \sum_{n=1}^{\infty} \operatorname{ierfc} \frac{nR}{\sqrt{(D_e t)}} \right\} - 3 \frac{D_e t}{R^2} \quad (\text{D.28})$$

สถาบันวิทยบริการ
จุฬาลงกรณ์มหาวิทยาลัย

APPENDIX E

Technology and Innovation for Sustainable Development Conference

(TISD2006)

25-26 January 2006, Sofitel Raja Orchid Hotel, Khon Kaen, Thailand

Subcritical Water Extraction of Anticancer Damnacanthal from Roots of *Morinda citrifolia*

Thitiporn Anekpankul¹, Motonobu Goto², Mitsuru Sasaki², Artiwan Shotipruk^{1,*}

1. Department of Chemical Engineering, Faculty of Engineering

Chulalongkorn University, Patumwan, Payathai, Bangkok, 10330, Thailand

Email: neloony@hotmail.com, artiwan.s@chula.ac.th (* corresponding author)

2. Department of Applied Chemistry and Biochemistry, Kumamoto University,

Kumamoto 850-8555, Japan

Email: mgoto@kumamoto-u.ac.jp, msasaki@kumamoto-u.ac.jp

1. Abstract

Roots of *Morinda citrifolia* (Noni or Ton Yor in Thai) are the source of important compounds, anthraquinones, which have been proven to have anti-viral, anti-bacterial, anti-cancer activities.

The most medicinally valuable anthraquinones in the root of this plant is damnacanthal, an anthraquinone compound which has been used for treatment of chronic diseases such as cancer and heart disease. In this study, subcritical water extraction was

investigated as a benign alternative for solvent extraction of damnacanthal from the dried root of *Morinda citrifolia*. The objective of this study is to find the suitable conditions for subcritical water extraction of this compound. The experiments were conducted in continuous a flow system at a pressure of 4 MPa at different temperature between 150 and 220°C and at water flow rates of 5 ml/min. Reversed-phase high-performance liquid chromatography was used for the analysis of damnacanthal with the UV detection at 250 nm. The temperature of 170°C was found to give the highest amount of damnacanthal extracted with subcritical water. The amount extracted at this condition was 610 $\mu\text{g g}^{-1}$ dry weight which was comparable to that extracted with dimethyl sulfoxide (DMSO) which was 650 $\mu\text{g g}^{-1}$ dry weight.

Keywords: subcritical water extraction, *Morinda citrifolia*, damnacanthal, anthraquinones

2. Introduction

Morinda citrifolia, sometimes called Noni, Indian Mulberry, or in Thai, Ton Yor or Yor, refers to a kind of plants belonging to the Rubiaceae family. The plants are grown widely in tropical

areas, including parts of Asia. They are small evergreen shrubs or trees that grow from three to six metres. The plants have straight trunks, large elliptical leaves, white tubular flowers and ovoid yellow fruits of up to 12 cm in diameter. The roots, stems, bark, leaves, flowers, and fruits of noni plants are all involved in various combinations of almost 40 known and recorded herbal remedies. For example, ripe noni fruits are reported to have a broad range of health benefits such as prevention and suppression of cancer, infection, arthritis, diabetes, asthma, hypertension, and pain. The leaves are used to treat eye problems; heated leaves are used to relieve coughs, nausea, colic; juice of the leaves can be taken for treatment of arthritis; and the roots are used to produce a yellow dye and to relieve chronic diseases such as cancer, diabetes, and cardiovascular diseases, and etc [1]. One of the most important constituents responsible for these therapeutic properties is anthraquinones. The compounds can be found in the leaves, barks, and roots, but the highest amount of anthraquinones is found in the roots of *M. citrifolia*. Examples of these compounds are damnacanthal, alizarin, and lucidin. Of all the anthraquinones, damnacanthal is the most important in terms of medicinal

values. It has been shown to be more effective than over 500 other botanical isolates in changing cancer cells back into normal cells. It is thus effective for fighting cancer, preventing the growth of pre-cancerous cells, and stimulating T cell [2].

Conventionally, anthraquinone is extracted with organic solvents, for example in ethanol or DMSO, followed by evaporation to separate from the product. This process is simple but it may leave toxic organic solvent residual in the product. Nowadays, the desire to reduce the use of organic solvent in environment has led to new extraction methods. In our previous study, subcritical water extraction has been shown to be suitable for extraction of slightly polar compound such as anthraquinones from *Morinda citrifolia* [3]. In this study, the compound was analyzed by spectrophotometry which gave qualitative determination of the total anthraquinones in the extract. In the present study, damnacanthal is of particular interest due to its high activity in fighting against cancer. The objective of this study is therefore to determine the suitable conditions for subcritical water extraction of this target compound.

3. Experimental

3.1 Plant material and chemicals

The roots of *Morinda citrifolia* were obtained in Thailand. The plant roots were harvested, washed, oven dried overnight at 40°C to almost complete dryness, and then ground in a mortar to small size in liquid N₂. This preparation gives small spherical particles whose average diameter was 2 mm, measured by a particle size analyzer (Beckman Coulter Model LS230, USA). Damnacanthal standard used in the experiments were obtained from Merck, Germany.

3.2 Subcritical water extraction

Subcritical water extraction was performed using an apparatus shown in Figure 1. The extraction system consisted of two HPLC pumps (PU 980, JASCO, Japan) used for delivering water and solvent, a degassing instrument (ERC 3215, CE, Japan), an oven (HARAEUS D63450), in which the extraction vessel (10 ml, Thar Design, USA) was mounted, a pressure gauge, and a back pressure regulator (AKICO, Japan). All connections are made with stainless steel capillaries (1/16 inch inside diameter).

Distilled water was passed through a degassing equipment to remove dissolved oxygen. The degassed water was then delivered, at a constant flow rate with the first HPLC pump, to a 3-m preheating section installed in the oven to heat it to the required temperature, which then passed through the extraction vessel, preloaded with 0.5 g of ground noni roots. The pressure of the system was adjusted to the desired condition (40 bar) by using the back-pressure regulator at the outlet coil to ensure that water was in liquid state at the temperatures tested. Before heating the extraction system, all connections were checked for possible leakage. The oven was turned on, and when the temperature reached the set point, the extraction started. The second pump was then turned on to deliver ethanol at constant flow rate to wash off any residual product in the outlet line behind the extractor. The extract was cooled in a coil immersed in a water bath to prevent possible product degradation, and was then collected in fractions.

The extraction experiments were carried out for 2 hours to determine the effect of temperature, and water flow rates. The temperatures studied were 150, 170, 200 and 220 °C respectively. The flow rate was set at 5 ml/min. All samples were analyzed by RP-HPLC.

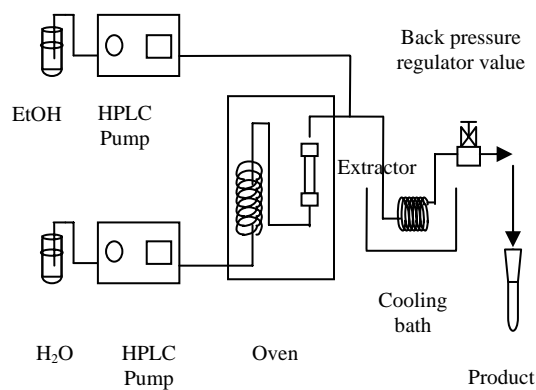


Figure1. Schematic diagram of the subcritical water extraction apparatus

3.3 Solvent extraction with DMSO

To determine the amount of damnacanthol recovered by solvent extraction, 0.1 g of ground roots was extracted in 2 ml DMSO at 60 °C in an ultrasonic bath (275DAE, Crest Ultrasonics, USA), with a power setting of 9 for 15 minutes. The solution was then replaced repeatedly with 2 ml of fresh DMSO and the root was extracted until the extract was clear. The extract concentration was then measured by RP-HPLC.

3.4 Sample preparation for RP-HPLC

Subcritical water extracts were evaporated under vacuum to dryness, and re-dissolved in distilled water. This resulted in two parts: solid precipitate and water soluble part which were

centrifuged at 3000 rpm for 15 minutes to separate the supernatant from the precipitate. DMSO was added to the precipitate from the previous step, and the mixture was then sonicated for 15 minutes. Both supernatant and precipitate-DMSO fractions contain the active compound of interest. The supernatant was directly analyzed while the precipitate- DMSO fraction was filtered through a membrane filter (0.45 μ m, Millipore, USA) before being subjected to HPLC analysis.

3.5 Analysis RP-HPLC procedure

The HPLC apparatus consisted of pump (LC-3A, Shimadzu, Japan), equipped with photodiode array detector (spectro monitor 4198, LDC Analytical USA). The analysis was carried out at room temperature on a phenomenex Luna C18, 100 A pore size, 5 μ m particle size, 250mm \times 4.60 mm I.D. column. The mobile phase used were modified from that described by Dabiri et al., 2004 [4], which consisted of a mixture of (70:30) acidic methanol (50 mM TFA)-buffer (50 mM KH₂PO₄, pH=3). The flow rate of the mobile phase was 1 ml/min and an injection volume of 100 μ L was used. The UV detection wavelength was 250 nm.

4. Results and discussion

4.1 Preliminary result

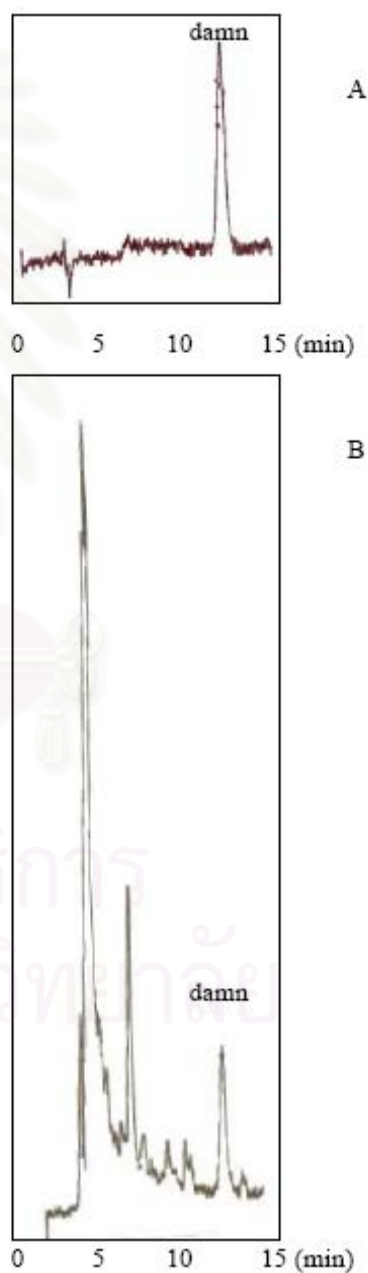
The release of anthraquinones from the roots can be seen readily by observing the yellow color of the extracts. Subcritical water shows a positive result as the extract appears yellow compares to the ambient water extraction. In previous studies [3], the amount of total anthraquinones was measured by a spectrophotometer with alizarin, a type of anthraquinones as a reference. Although the method was simple, the components of different anthraquinones could not be determined. There are varieties of different anthraquinones compounds in the roots of *Morinda citrifolia*. Alizarin and damnacanthal are two examples of this type of compound. Compared with damnacanthal, alizarin has much lower biological activity, and is commonly used in dying industry. Damnacanthal on the other hand has been proven for the anti-cancer activity and is therefore the target compound for investigation of subcritical extraction in this study. In this study, RP-HPLC was used for quantitative analysis of damnacanthal.

4.2 Evaluation of extraction protocols

Although RP-HPLC was able to more quantitatively determine the amount of damnacanthal target compound than spectrophotometry. The concentration of the compound of interest in the subcritical water is typically too diluted to be directly measured. A few steps are required to concentrate the extract and to purify it prior to proper HPLC analysis.

First, the extract was evaporated under vacuum to dryness and re-dissolved in water at ambient temperature. In this step, two parts were obtained, the water soluble part, and the water insoluble precipitate. These were separated by centrifugation and the two fractions were analyzed by HPLC. The water soluble part could be directly injected while the water insoluble part must be re-dissolved in DMSO before an injection into an HPLC. These steps were necessary for preparation of the sample for HPLC analysis. Re-dissolving the dried extract with DMSO alone resulted in unresolved HPLC peaks due to the interference of other impurities. Water added to the dried extract seemed to have removed polar impurities leaving the precipitate which contained fewer interfering peaks. The Chromatograms of damnacanthal

standard and those of the two fractions of the extract are shown in Figure 2. The results show that both fractions contain damnacanthal. The sum of the amounts of damnacanthal in the two fractions accounted for the total amount in the extract.



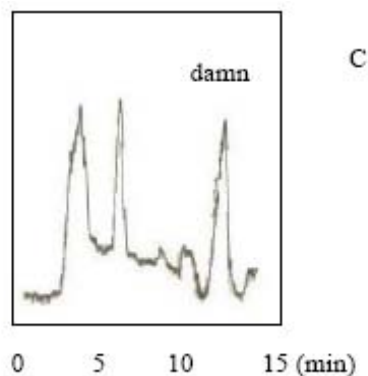


Figure2. HPLC chromatogram of damnacanthal (retention time, $t_R = 12.81$ min) in (A) standard, (B-C) noni roots extracts obtained from subcritical water extraction (B = supernatant, C = precipitate dissolve into the DMSO)

4.3 Effect of subcritical water temperature

The effect of the temperature of subcritical water on the extraction yield was determined. The product yield was found to be the highest at 170 °C as can be seen from Figure 3. As the temperature increased, the product solubility increased due to the decreasing dielectric constant. However, at 200 and 220 °C, the yield was low due to the degradation of the product at high temperatures. These results indicated that when the specific compound, damnacanthal, was considered with HPLC analysis, the results differed from those suggested by previous study in which total

anthraquinones was found to be the highest at the temperature of 220 °C [3].

The total amounts of damnacanthal extracted at different temperatures were plotted in Figure 4, which shows the fractions of the product in the precipitate and in the supernatant. The results indicated that the target compound was present in both fractions. This means that although the compound is known to be highly soluble in DMSO it is slightly soluble in water at ambient condition. Subcritical water extract of such compound tends to precipitate when water returned to ambient condition. This suggests a possible means for product purification by precipitation.

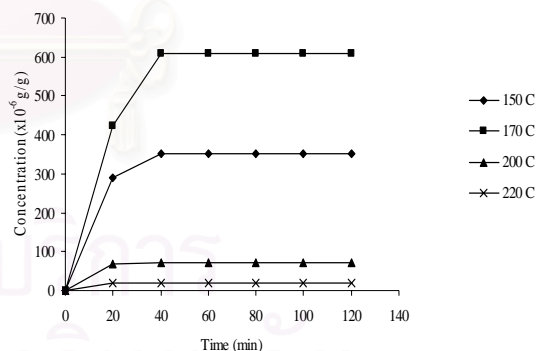


Figure3. Effect of temperature on yield of damnacanthal (Flow rate 5 ml/min at 4 MPa)

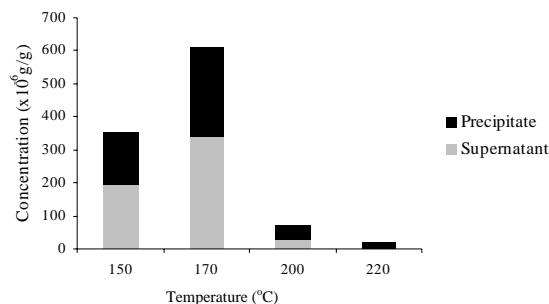


Figure 4. The fraction of damnacanthol concentration in supernatant and precipitate in DMSO

5. Conclusions

In summary, subcritical water provides a promising alternative for extraction of the anticancer damnacanthol from roots of *Morinda citrifolia*. At the temperature of 170 °C the yield was the highest. At temperatures of 200 and 220 °C, the decomposition of damnacanthol occurred. In the future study, development of standard procedure for purification of the compound would be conducted for the subcritical water extracts of *Morinda citrifolia*.

Acknowledgements

The authors thank Thailand Japan Technology Transfer Program, Thailand

Research Fund, and The Commission of Higher Education for financial support.

References

- [1] Wang M.Y., West B.J., Jensen C.J. and Nowicki D. 2002. *Morinda citrifolia* (Noni): A literature review and recent advances in Noni research. *Acta Pharmacologica Sinica*, 23: 1127-1141.
- [2] Hiramatsu T., Imoto M., Koyano T., and Umezawa K. 1993. Induction of normal phenotypes in ras-transformed cells by damnacanthol from *Morinda citrifolia*, *Cancer Letter*, 73: 161-166
- [3] Shotipruk A., Kiatsongserm J., Pavasant P., Goto M., and Sasaki M. 2004. Subcritical Water Extraction of anthraquinones from the Roots of *Morinda citrifolia*. *Biotechnol Progress*, 20: 1872-1876.
- [4] Dabiri M., Salimi S., Ghassempour A., Rassouli A. and Talebi A 2005. Optimization of microwave-assisted extraction for alizarin and purpurin in Rubiaceae plants and its comparison with conventional extraction methods. *Journal of Separation Science*, 28: 387-396.

VITA

Miss Thitiporn Anekpankul was born on 25 January, 1982 in Bangkok, Thailand. She received a Bachelor's Degree of Chemical Engineering from the Faculty of Engineering, Mahidol University in 2004. After then she subsequently completed the requirements for a Master's Degree in Chemical Engineering at the Department of Chemical Engineering, Faculty of Engineering, Chulalongkorn University in 2006.



สถาบันวิทยบริการ
จุฬาลงกรณ์มหาวิทยาลัย